Optimizing Planting Dates for Agricultural Decision-Making under Climate Change over Burkina Faso/West Africa

Dissertation zur Erlangung des Doktorgrades an der Fakultät für Angewandte Informatik der Universität Augsburg

vorgelegt von

Moussa Waongo

Master Physik und Ing. Agrarmeteorologie

2015

Erstes Gutachten: Prof. Dr. Harald Kunstmann
Zweites Gutachten: Prof. Dr. Peter Fiener
Tag der mündlichen Prüfung: 27.03. 2015

Acknowledgements

I remember that, during the 2008's forum on seasonal climate outlook in West Africa (PRESAO), a farmers' spokesman said *"you guys [scientists] provide a real support to us [farmers] with your JAS [July-August-September] rainfall but now, tell us when to plant our crops"*. Although this talk wasn't the first that farmers expressed their concern about this topic, it has the merit to highlight that the problem is still on the table. Since we cannot solve it by magic, so we (scientists) were embarrassed for this recurrent request. Two years later, when Prof. Dr. Harald Kunstmann offers me the opportunity to work on this "hot" topic, I had a feeling of a glimmer of hope for this issue of planting time. So, I would like here to express my heartfelt gratitude to Prof. Dr. Harald Kunstmann for offering me the opportunity to work on this topic. Prof. Dr. Kunstmann, I will always admire your total commitment to see the best out of your students and I feel extremely privileged to have been your student.

I am deeply indebted to my advisor Dr. Patrick Laux for his fundamental role in my doctoral work. You were the pioneer on this novel direction to deal with my topic and you provided me with every bit of guidance, assistance, and expertise that I needed to carry out my research. You have been a tremendous mentor for me and I hope you will be proud of this final product. I quite simply cannot imagine a better advisor. For everything you have done for me, Patrick, I thank you.

I would also like to thank Dr. Ing Jan Bliefernicht for his assistance. I am very grateful for your advise and administrative support throughout my research period.

During my time as a PhD student (and still) I have met many nice and inspiring scientists and their support has been invaluable. So, my sincere thanks to all senior and post-doc scientists who formed part of the Regional Climate and Hydrology group at IMK-IFU (KIT) and the Chair for Regional Climate and Hydrology group at the Institute of Geography, University of Augsburg. Among them are Benjamin Fersch, Christian Chwala, Christof Lorenz, Dominikus Heinzeller, Gerhard Smiatek, Hans-Richard Knoche, Johannes Werhahn, Joël Arnault, Michael Warscher, Seyni Salack, Sven Wagner, Andreas Wagner, Florian Marshall, and Thomas Rummler. Thanks to all of you for your support and the friendly and pleasant environment you have created.

I would also like to thank colleagues who have walked the path with me. These include Ganquan Mao, Jianhui Wei, Cornelia Klein, Luitpold Hingel, Manuel Lorenz, Noah Misati Kerandi and Thinh Dang. I will never forget the time we spent together.

I also owe this work to Karlsruhe Institute of Technology (KIT) who provide me all facilities and technical support I needed to carry out my research. For the staff of IMK-IFU "my research work place", your support is highly acknowledged. A special thanks to Dr. Elija Bleher for her great support, particularly during my first year in Germany.

I would like to thank University of Augsburg, particularly the Institute of Geography at the Faculty of Applied Computer Science for all facilities and support I benefit. I am particularly thankful to Prof. Dr. Peter Fiener, who accepted to be the second referee.

This research would not have carried out without the financial support of West African Science service center on Climate change and Adapted Land use (WASCAL), a project funded by the German Federal Ministry of Education and Research (BMBF). So, thanks to WASCAL's financial support.

I would like to acknowledge the morale and social support provided by all colleagues at various circles back home. The list is endless but I will always treasure every moment of support.

Lastly, a special thanks to my beloved wife, Jeanne and my daughter, Selene. I promise to spend more time with you after this.

Contents

List of Figures

List of Tables

Abbreviations

AEZ	**A**gro-**E**cological **Z**ones
AGB	**A**bove **G**round **B**iomass
APSIM	**A**gricultural **P**roduction system **SIM**ulator
AR5	IPCC fifth **A**ssessment **R**eport
BF	**B**urkina **F**aso
CAADP	**C**omprehensive **A**frica **A**griculture **D**evelopment **P**rogramme
CERES	**C**rop **E**nvironment **RE**source **S**ynthesis
CGS	**C**essation of the **G**rowing **S**eason
CORDEX	**CO**ordinated **R**egional climate **D**ownscaling **EX**periment
CropSyst	**Crop**ping **Syst**ems simulation model
CTRL	RCM control runs
CV	**C**oefficient of **V**ariation
CWR	**C**rop **W**ater **R**equirements
DGM	**D**irectorate **G**eneral of **M**eteorology
DSSAT	**D**ecision **S**upport **S**ystem for **A**grotechnology **T**ransfer
ET	**E**vapo**T**ranspiration
ETo	reference **E**vapo**T**ranspiration
FAO	**F**ood and **A**griculture **O**rganization
GDD	**G**rowing **D**egree **D**ays
GA	**G**enetic **A**lgorithm
GDAL	**G**eospatial **D**ata **A**bstraction **L**ibrary
GLAM	**G**eneral **L**arge **A**rea **M**odel for annual crops
HDI	**H**uman **D**evelopment **I**ndex
HWSD	**H**armonized **W**orld **S**oil **D**ata

IPCC	**I**ntergovernmental **P**anel on **C**limate **C**hange
ITCZ	**I**nter-**T**ropical **C**onvergence **Z**one
LAI	**L**eaf **A**rea **I**ndex
LGS	**L**ength of the **G**rowing **S**eason
MDG	**M**illennium **D**evelopment **G**oal
NEPAD	**NE**w **P**artnership for **A**frica's **D**evelopment
OGS	**O**nset of the **G**rowing **S**eason
OK	**O**rdinary **K**riging
OPD	**O**ptimized **P**lanting **D**ate
RCM	**R**egional **C**limate **M**odel
RCP	**R**epresentative **C**oncentration **P**athway
RMSD	**R**oot **M**ean **S**quare **D**ifference
RMSE	**R**oot **M**ean **S**quare **E**rror
ORS	**O**nset of the **R**ainy **S**eason
SAP	**S**tructural **A**djustment **P**rogrammes
SMHI	**S**wedish **M**eteorological and **H**ydrological **I**nstitute
SOYGRO	**SOY**bean crop **GRO**wth simulation model
SSA	**S**ub-**S**aharan **A**frica
SST	**S**ea **S**urface **T**emperature
SRES	**S**pecial **R**eport on **E**mission **S**cenarios
USDA	**U**nited **S**tates **D**epartment of **A**griculture
WA	**W**est **A**frica
YGP	**Y**ield **G**ap **P**arameter

Variables and Symbols

R_n	Net solar radiation ($MJ\ m^{-2}\ day^{-1}$)
G	Soil heat flux density ($MJ\ m^{-2}\ day^{-1}$)
$\gamma =$	Psychometric constant ($KPa\ {}^{\circ}C^{-1}$)
T	Air temperature (${}^{\circ}C$)
T_b	Crop base temperature (${}^{\circ}C$)
T_o	Crop optimum temperature (${}^{\circ}C$)
T_m	Crop maximum temperature (${}^{\circ}C$)
T_{eff}	Effective temperature (${}^{\circ}C$)
T_T	Actual rate of transpiration ($cm\ day^{-1}$)
E_T	Normalized transpiration efficiency ($g\ kg^{-1}\ Pa^{-1}$)
$E_{TN,max}$	Maximum transpiration efficiency ($g\ kg^{-1}$)
u_2	Wind speed at 2 m height ($m\ s^{-1}$)
e_s	Saturated vapor pressure (KPa)
e_a	Actual vapor pressure (KPa)
Δ	Slope vapor pressure curve ($KPa\ {}^{\circ}C^{-1}$)
$R_a =$	Extra atmosphere global solar radiation ($MJ\ m^{-2}\ day^{-1}$)
R_s	Shortwave solar radiation ($MJ\ m^{-2}\ day^{-1}$)
h	Measured sunshine duration ($hour$)
H	Maximum possible duration of sunshine ($hour$)
a	Angström parameters ($-$)
b	Angström parameters ($-$)
t	Time (day)
$x(t)$	Vector of crop and soil state variables

$\frac{dx}{dt}$	Vector of rate of changes of state variables
f	Non-linear set of equations
p_1	Vector of crop cultivar-specific parameters
p_2	Vector of soil physical and chemical parameters
$w(t)$	Time-varying weather inputs
$m(t)$	Time-varying management inputs
$\frac{dH}{dt}$	Harvest index rate parameter
$m_A(x)$	Classical or fuzzy logic set
$\mu_i(x)$	Fuzzy logic membership function
$F(x)$	Fitness function
$g_i(x)$	Constraint function
p_i	Probability of selecting the ith string for mating
p_m	Mutation probability
Y	Yield ($kg\ ha^{-1}$)
w_i	Fraction of cropping land $(-)$
a_1	Fuzzy logic membership parameter for rainfall (mm)
a_2	Fuzzy logic membership parameter for rainfall (mm)
b_1	Fuzzy logic membership parameter for number of wet-day (day)
b_2	Fuzzy logic membership parameter for number of wet-day (day)
c_1	Fuzzy logic membership parameter for number of dry-day (day)
c_2	Fuzzy logic membership parameter for number of dry-day (day)
k	Fuzzy logic defuzzification parameter $(-)$
γ_1	Fuzzy logic membership representing 5-day rainfall amount $(-)$
γ_2	Fuzzy logic membership representing the number of wet-day $(-)$
γ_3	Fuzzy logic membership representing the number of dry-day $(-)$

Abstract

Rainfed agriculture is the main source of income for population and the main driver of the economy in Africa, particularly in West Africa (WA). The agricultural system is characterized by smallholder and subsistence farming in a context of farmers' low capacity. In water-limited regions of WA, most of the crop management decisions are made based on the perceived risk of climate and the socio-economic conditions of the farmers. Therefore, technologies and approaches in the field of agricultural water management are likely to make a difference for agricultural development and thus food security. However, only those strategies which require little resources in terms of labor and money have a chance to engage a large number of farmers. As a farming strategic decision, the planting time has the potential to sustain crop production as well as to be adopted by farmers.

With regards to the high intra-seasonal rainfall variability in WA, early planting dates can lead to crop failure due to long dry spells which occur shortly after planting. In contrast, late planting dates have the chance to avoid crop failure but they correspond to short growing seasons which can potentially reduce crop production.

In this thesis, an approach to derive an optimal planting time has been developed. Based on the crop water requirements throughout the crop growing cycle, this planting date approach uses a process-based crop model in conjunction with a fuzzy rule-based planting date definition to derive optimized planting dates (OPDs).

First, by taking into account the inherent uncertainties of rainfall measurements and computations issues, three fuzzy logic memberships, which are fully determined by two fuzzy parameters each, have been developed to represent the three main criterions used to define planting date. Then, the General Large-Area Model for annual crops (GLAM) and the fuzzy rule-based planting date have been coupled with a genetic algorithm optimization technique. Finally, this has been applied to calibrate GLAM for maize cropping and subsequently to derive OPDs for maize cropping. To allow a time window for crop planting, an ensemble member principle has been applied to derive a 10-member ensemble of optimized fuzzy parameters.

Burkina Faso (BF) has been selected as a case study area to derive OPDs. The performance of the OPDs approach have been evaluated by comparing maize yield derived from the OPDs method and two state-of-the-art methods which are currently in use in WA. The analysis comprises both present climate and future climate projections. Present climate data encompassed observed data and European Centre for Medium-Range Weather Forecasts (ECMWF) Interim Re-Analysis (ERA-Interim) data over BF for the period 1961-2010 and 1980-2010, respectively. Future climate encompassed eight regional climate models outputs based on the greenhouse gas emission scenarios RCP4.5 and RCP8.5 covering the period 2011-2050. Beside the climate data, soil and observed maize yield data have been involved in this study.

The results show that, on average, OPDs ranged from 1 May (South-West) to 11 July (North) across the country under present climate. In comparison to selected state-of-the art methods, the results suggest earlier planting dates across BF, ranging from 10-20 days for the northern and central BF, and less than 10 days for the southern BF. With respect to the potential yields, the OPD approach indicates that an increase of maize potential mean yield of around 20% could be achieved in water limited regions in BF. However, the potential yield surpluses strongly decrease from the North to the South. For future climate projections, the OPDs approach achieves approximately +15% higher potential maize yield regardless of the Regional Climate Model (RCM) and the time horizons. When the OPD approach is used as adaptation strategy, the change in maize mean yield varies between -23% and 34% from the baseline period (1989-2008) for the majority of locations. The regional mean yield deviations strongly depend on the location and RCM, particularly for the RCP8.5 scenario. On average, negative changes of mean yield is observed. Considering the period 2011-2050, RCMs ensemble mean of yield change is -3.4% for RCP4.5 and -8.3% for RCP8.5. Mean yield decreases are more pronounced for RCP8.5 during the period 2031-2050.

These findings highlight the potential of OPDs as a crop management strategy. The implementation of the presented approach in agricultural decision support is expected to improve agricultural water-related risk management in WA. The OPD

approach can be used in combination with seasonal climate forecasts to provide planting date information to farmers. However, the predictability of OPDs has to be investigated and further in-field validation of OPDs is required before being implemented as short-term tactical decision by farmers. It is apparent however, that farmers need to combine OPDs with others suited farming practices to adequately respond to climate change. Moreover, in order to efficiently support agricultural long-term strategic decision-making in WA, it is worth to perform further multi-model ensemble simulations by using additional multiple RCMs driven by multiple Global Circulation Models (GCMs) and emissions scenarios. Such investigations might contribute to better capture the magnitude of climate change impacts on crop production, thereby enhancing the development of climate chance adaptation strategies.

Zusammenfassung

Regenfeldbau stellt die Haupteinnahme für die Bevölkerung in Afrika dar und ist zugleich Haupteinflußfaktor für die Wirtschaft, insbesondere in Westafrika. Die Landwirtschaft is charakterisiert durch Familien -und Subsistenzlandwirtschaft und ist limitiert durch eine geringen Anpassungsfähigkeit der Farmer. In den wasserknappen Gebieten Westafrikas werden die meisten landwirt-schaftlichen Entscheidungen basierend auf dem Klimarisiko und den sozio-ökonomischen Bedingungen der Farmer getroffen. Darum bieten Methoden und Technologien im landwirtschaftlichen Wassermanagement erhebliches Potential zur Steigerung der Ernährungssicherheit in Westafrika. Jedoch werden nur Strategien mit geringen Ansprüchen an Ressourcen im Hinblick auf Arbeitskraft und Geld von der überwiegend armen und durch Familienlandwirtschaftgeprägten Bevölkerung akzeptiert und angenommen. Die Anpassung des Anpflanzzeitpunktes hat das Potential von den Farmern akzeptiert zu werden und kann gleichzeitig die Produktivität erhalten.

Durch die hohe intrasaisonale Niederschlagsvariabilität in Westafrika kann ein frühzeitiges Anpflanzen zu Ernteausfällen führen, insbesondere wenn lange Trockenperioden nach dem Anpflanzen auftreten. Im Gegensatz dazu geht ein spätes Anpflanzen mit einem verringertem Risiko des Totalverlusts einher, jedoch ist aufgrund der verkürzten Vegetationsperiode mit teilweise erheblichen Ertragseinbußsen zu rechnen. In der vorliegenden Arbeit wird ein Ansatz zur Ableitung optimierter Anpflanztermine für Mais vorgestellt. Basierend auf dem Wasserbedarf während der gesamten Vegetationsperiode benutzt dieser Ansatz ein prozessbasierten Pflanzenwachstumsmodell in Kombination mit einem Fuzzy Logik Algorithmus zur Bestimmung des Anpflanzzeitpunktes. Erstens, unter Berücksichtigung der Messunsicherheiten von Niederschlag wurden drei verschiedene unscharfe Zugehörigkeitsfunktionen (beschrieben durch jeweils zwei Unschärfeparameter) zur Berechnung des Anpflanztermins entwickelt. Danach wurde das prozessorientierte regionale Ernteertragsmodell GLAM (General Large Area Modell) mit den Zugehörigkeitsfunktionen über einen genetischen Algorithmus gekoppelt. Dies wurde schließlich angewandt um GLAM für den Maisanbau zu

kalibrieren und ferner, um optimale Anpflanzzeitpunkte (OPDs) für die Region abzuleiten. Um die Ableitung eines Zeitfensters zur Aussaat zu ermöglichen - anstatt eines einzelnen Termins, wurde ein Ensemble aus zehn Mitgliedern von optimierten Unschärfeparametern verwendet.

In der vorliegenden Arbeit wurde Burkina Faso als Fallstudie für den Maisanbau in Westafrika ausgewählt. Die Güte des neuen OPDs Ansatzes wurde durch den Vergleich mit zwei in Westafrika etablierten Ansätzen unter gegenwärtigem als auch zukünftigem Klima bewertet. Die Klimadaten der Jetztzeit umfassten sowohl Beobachtungsdaten (1981-2010) und ERA-Interim Reanalysen (1980-2010, bereitgestellt von ECMWF). Für das Zukunftsklima wurden acht regionale Klimasmodelle mit jeweils zwei Emissionsszenarien (RCP4.5, RCP8.5) für den Zeitraum 2011 bis 2050 verwendet. Neben den Klimadaten, wurden v.a. edaphische Daten als auch Maisertragsdaten für diese Studie benötigt.

Die Studie hat gezeigt, dass das optimale Anpflanzdatum für Burkina Faso im Durchschnitt zwischen dem 1. Mai im Südwesten, und dem 11. Juli im Norden für das gegenwärtige Klima liegt. Im Gegensatz zu den beiden anderen Methoden führt die neue Methode zu früheren Anpflanzterminen in Burkina Faso, ca. 10-20 Tage früher für Nord- und Zentral Burkina Faso, und weniger als 10 Tage für den Süden. Bezüglich der potenziellen Erträge führt der OPD Ansatz zu einer Zunahme des Maisertrags von ca. +20% in den wasserknappen Gebieten von Burkina Faso. Für das zukünftige Klima liefert der OPDs Ansatz etwa +15% höhere Maiserträge unabhängig von den betrachteten regionalen Klimaszenarien und Zeitscheiben. Allerdings nehmen die simulierten Ertragsüberschüsse stark von Norden nach Süden hin ab.

Wird der OPD Ansatz als landwirtschaftliche Anpassungsstrategie verwendet, werden mittlere Änderungen des potentiellen Maisertrags in der Größenordnung von -23% bis +34%, verglichen mit der Referenzperiode (1989-2008) für die Mehrheit der Gitterzellen, prognostiziert. Die regionalen Ertragsänderungen hängen stark von der räumlichen Lage als auch dem regionalen Klimamodell (RCM) ab, insbesondere wenn man das RCP8.5 Szenario betrachtet. Im Durchschnitt ist mit einer Abnahme der Erträge zu rechnen. Für die Periode 2011-2050 beträgt das

Änderungssignal der Ensemble-RCMs -3,4% für das RCP4.5 Szenario, und -8,3% für das RCP8.5 Szenario.

Die Ergebnisse unterstreichen das Potenzial des OPD Ansatzes als landwirtschaftliche Managementstrategie. Die Umsetzung des vorgestellten Ansatzes in der landwirtschaftlichen Entscheidungsunterstützung führt möglicherweise zu einem verbesserten Risikomanagement unter Regenfeldbau für diese Region.

Der Ansatz kann potentiell mit saisonalen Klimavorhersagen benutzt werden. Jedoch muss zuvor die Vorhersagbarkeit der OPDs weiter analysiert werden und der Nutzen der OPDs muss vor deren Implementierung in Feldversuchen validiert werden. In Anbetracht des Klimawandels ist es offensichtlich, dass die Farmer die optimalen Anpflanzzeitpunkte mit weiteren geeigneten Anbaumethoden kombinieren müssen. Weitere Ensemble Simulationen, bestehend aus zusätzlichen RCMs, angetrieben durch mehrere Globale Zirkulationsmodelle (GCMs) und Emissionsszenarien sind notwendig, um die Unsicherheiten des Klimawandels besser zu quantifizieren zu können, und um somit zur Entwicklung verbesserter Klimaanpassungsstrategien beizutragen.

Chapter 1

Introduction

1.1 Food security and agriculture challenges in Africa

Most of the regions in the world have witnessed significant increases in per capita food production over the last 30 years. However, the opposite occurred in Sub-Saharan Africa (SSA) region in West Africa (WA). This region is faced with food deficits almost on an annual basis due to crop failure or low crop productivity. Food production per capita in SSA is still at the same level as it was in 1961 (Godfray et al., 2010). In contrast to Asia, which experienced impressive increase in crop yields, known as the Green Revolution, most of the increase in crop production in the past 30 years in SSA has been due to increase in area of farm lands (Figure 1.1) and much less due to increase in yield (Henao and Baanante, 2006). For instance, during 1998 the average yield of cereals in SSA was 15% lower than the world average (World Bank, 2000). This situation has been exacerbated by land degradation as well as extreme poverty. The major biophysical reason for low crop yields is the extreme depletion of soil nutrients in Africa. In addition to this, SSA experiences erratic climatic conditions which damper the efforts to sustain crop productivity under the low level of soil fertility. As a consequence, this has seen millions of people surviving on food relief measures to avert starvation disasters. Moreover, with a population growth rate of about 2.4, one of the

highest in the world (UNFPA, 2011), it is likely that food security in SSA represents a problem which will not be overcome in the near future and thereby failing to meet the Millennium Development Goals (MDGs) (UN, 2000). Therefore, the inability of Africa and particularly SSA to feed its growing population adequately has increasingly become the focus of national and international attention.

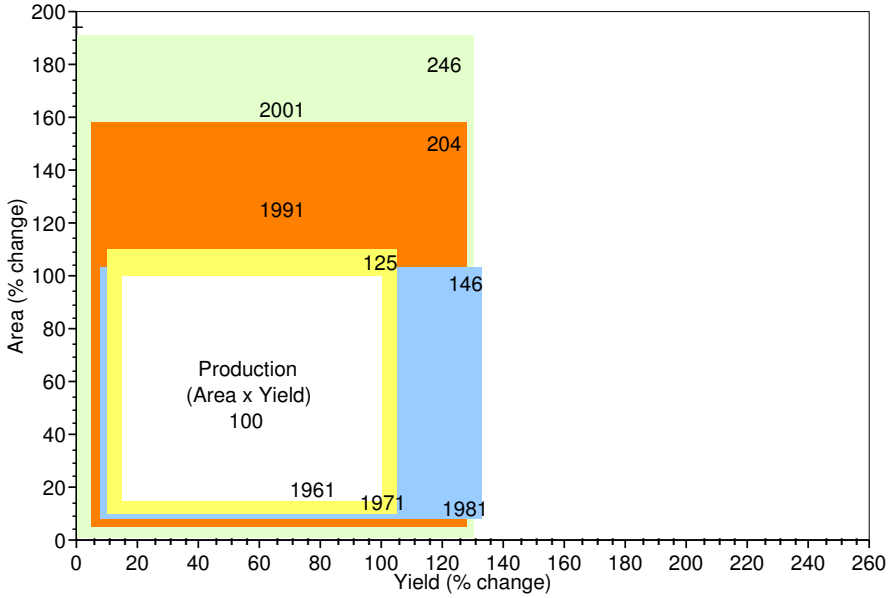

FIGURE 1.1: Changes in cereal production in SSA, referenced to the production level in 1961 (Adapted from Henao and Baanante, 2006).

To cope with hunger and the failure of the economies due to the 1980s Structural Adjustment Programmes (SAP), there is a growing national and regional commitment to investment in agriculture in Africa. It has been recognized that Africa's future relies not only on being able to export high-value crops, but also on strengthening its production of food crops (Holmén and Hudén, 2011). For international and national policy makers, it is time to drastically increase crops productivity and to improve human nutrition in Africa. To this end, a new and highly focused action plan, called the Double Green Revolution in Africa, that is increasing productivity in environmentally sustainable ways began (Conway, 2006). For instance, in the development of a plan to attain the Millennium Development Goal of reducing hunger in 2015 by 50%, agriculture has received more attention now. Likewise, in 2004, the initiative of New Partnership for Africa's Development (NEPAD) and Ministers of Agriculture of African Union member countries leaded

to the adoption of the Comprehensive Africa Agriculture Development Programme (CAADP) and the commitment made by the African presidents to set aside 10% of the national budget for the agricultural sector (Holmén and Hudén, 2011). This arising vision for agriculture promotion can be seen as a step in the right direction to make agriculture growing in ways that serve the triple purposes of ending hunger, reducing poverty and enabling a national development. However, in spite of these political engagements, policy makers will face a set of agricultural issues as they try to put promise into practice.

In addition to the aforementioned soil fertility problematic, climate-related risk and the vulnerability of smallholder farming systems associated with farmers' low adaptive capacity are the most crucial issues in SSA. Crop environment is composed of climatic and soil factors that exert a great influence on plant growth, and consequently, yield. Climatic factors such as temperature, solar radiation, and rainfall strongly impact on crop production. Weather influences the processes in the soil, such as nutrient availability, which is affected by both soil moisture and temperatures. Solar radiation and temperature also influence processes in plants, such as photosynthesis, the process that is essential for the biomass production and crop maintenance (Wallach et al., 2006). There is increasing evidence that both climate variability and climate change will strongly affect rainfed agriculture and therefore food security in SSA (e.g. Cooper et al., 2008, Müller et al., 2011a,b, Roudier et al., 2011, IPCC, 2014). In fact, rainfed agriculture provides about 90% of the region's food (Rosegrant et al., 2002) and it is the principal source of livelihood for more than 80% of the population (Hellmuth et al., 2007). Rainfed agriculture currently constitutes about 90% of SSA's staple food crop production, making it highly vulnerable to reduced quantity, distribution, and timing of rainfall. In addition, growing season length will likely decrease due to higher temperatures (Conway, 2008). Besides that, SSA is characterized by a high intra-seasonal and inter-annual rainfall variabilty (Nicholson and Grist, 2003, Laux et al., 2009). Hence, rainfall is both a critical input and a primary source of risk and uncertainties for rainfed agriculture production in SSA (Nelson et al., 2009).

1.2 Climate change impacts on agriculture in Africa

By using the longest period (1901 to 2012) to calculate regional trends of climate variables, IPCC (2013) warns that almost the entire globe has experienced surface warming. Global surface temperature changes for the end of the 21st century is likely to exceed 1.5°C compared to the period 1850-1900 for the majority of newly developed emission scenarios, the representative concentration pathways (RCPs). In fact, the projected temperature is likely to exceed 2°C for RCP6.0 and RCP8.5. However, changes in the global water cycle in response to the warming over the 21st century will not be uniform. For instance, in many mid-latitude and subtropical dry regions, mean precipitation will likely decrease, while in many mid-latitude wet regions, mean precipitation will likely increase by the end of this century under the RCP8.5 (IPCC, 2013).

The analysis of observed climate data in Africa has shown an increasing trend in surface mean temperature while rainfall changes have shown a strong spatial dependence. The IPCC (2013) has shown a clear increase of temperature in WA, particularly over the SSA where annual temperature increase is greater than 0.5° for the period 1901-2012 (Figure 1.2a). For precipitation, both positive and negative changes are observed over Africa with a great spatial variability. Nevertheless, in general, no change or a decrease in the annual precipitation is observed over WA (Figure 1.2b). More significantly, in that region, the Sahel belt have shown a clear decrease in the annual precipitation of greater than 5 mm/year/decade during the period 1951-2012.

Studies on the impact of climate change on crop yields worldwide, mostly using climate model projections to drive process-based or statistical crop models. Crop simulation models based on this complex interaction between soil, plants, and climate have been served to assess climate impacts on global and regional crop productivity. It is found that for the major crops (i.e. wheat, rice, and maize) in temperate and tropical regions, climate change without adaptation is projected to negatively impact production for local temperature increases of

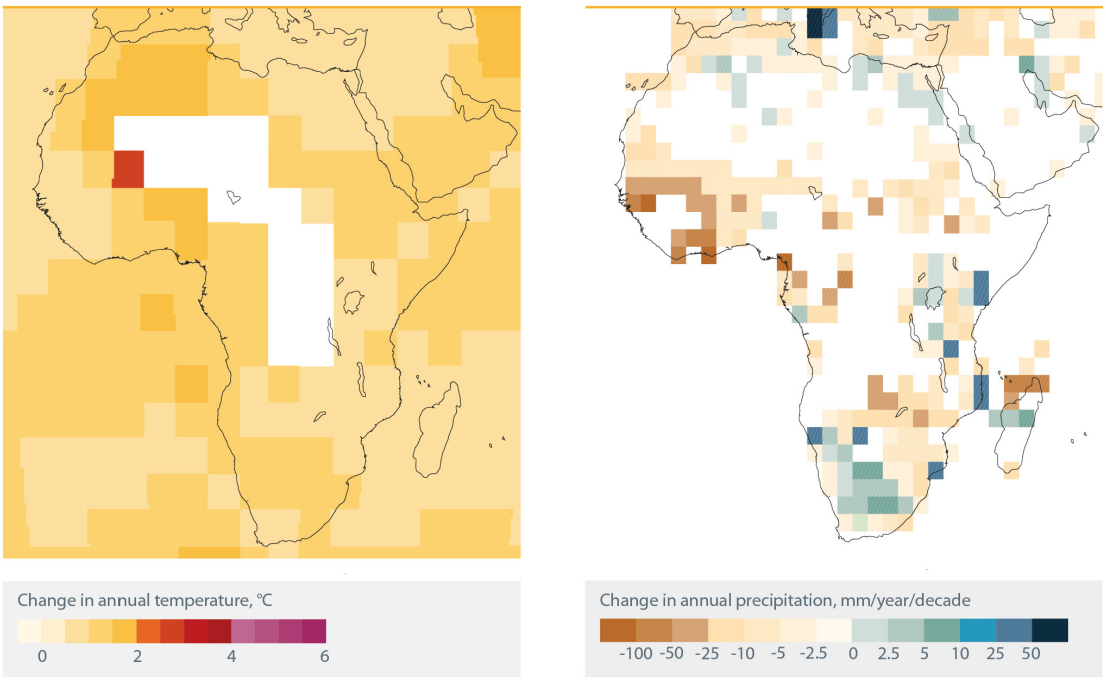

(a) (b)

FIGURE 1.2: Change in annual average temperature (a) and precipitation (b) over Africa for the period 1901-2012 and 1951-2012, respectively. White grid cells denote missing data.
(Source: http://cdkn.org/resource/observed-temperature-rainfall-africa/)

2°C or more above late-20th-century levels, although individual locations may benefit medium confidence (IPCC, 2014). Scientists argued that in low-latitude regions, where most of the developing countries are located, crop yields are likely to be strongly reduced by climate change. Even if projected changes in rainfall are much less clear, there is a global trend for increased frequencies of droughts, as well as heavy precipitation events over most land areas, which is therefore harmful for food production (Padgham, 2009). For illustration, several studies have demonstrated that the predicted rising temperature and changes in rainfall patterns may drastically affect the productivity of food crops in SSA (e.g. Long et al., 2007, Lobell et al., 2008, Nelson et al., 2009, Waha et al., 2013). On average, decreased crop yields of 18% for southern Africa to 22% across SSA are expected by mid-Century (IPCC, 2014). Roudier et al. (2011) conducted a meta-analysis of 16 studies over WA and shows that, over all climate scenarios and models, countries and crops, projected impacts are most frequently slightly

negative (-10%). Likewise, from a systematic review and meta-analysis of data in 52 original publications, Knox et al. (2012) found that across Africa, projected mean change in yield of -5% (maize), -15% (sorghum) and -10% (millet) are expected by 2050s. Moreover, climate change is projected to progressively increase inter-annual variability of crop yields in water-limited regions. Although a general decrease in yield is predicted for major crops across Africa, projected impacts vary across crops, regions and adaptation scenarios. This situation represents an alarming food security issue, which increases challenges that WA faces to feed its population in the coming decades. Thus, decreasing the vulnerability of agriculture to climate variability through a more informed choice of policies, practices and technologies will, in many cases, reduce its long-term vulnerability to climate change and thereby enhancing the resilience of farmers productivity to climate change.

1.3 Agricultural adaptation strategies in West Africa

Adaptations help to mitigate climate change effects. Agricultural adaptations can be made in planting and harvest dates, crop choice, crop rotations, crop varieties, irrigation, fertilization, and tillage practices. However, the capacity of people to adapt to global changes is correlated with poverty level, support mechanisms and governance. For instance, where farmers perceive weak support for adaptation interventions they are less likely to try what they perceive to be riskier technologies (Pedzisa et al., 2010). It is increasingly recognized that many small farmers have not benefitted from technologies todays, due to failure either of the technology or more commonly of the delivery mechanism (Cooper et al., 2009, Renkow and Byerlee, 2010). In WA, technologies or approaches that have the potential to support farmers in the fields of soil conservation and water management are likely to make a difference for food security and agricultural development. But, since farmers' options for coping and adaptation

are particularly limited in that region (Antwi-Agyei et al., 2013), it is necessary to carefully select crop management strategies that account for capacity constraints and therefore, can efficiently help farmers adapting to climate change. Many studies have stressed farmers' coping and adaptation strategies in WA (e.g. Roncoli et al., 2001, Kaboré and Reij, 2004, Barbier et al., 2009, Zampaligré et al., 2014, Webber et al., 2014). Among the broad range of crop management strategies, those fitting in the pool of low-cost strategies have been adopted by farmers (Kaboré and Reij, 2004, Sawadogo, 2011). For instance, low-cost strategies such as stone bunds, micro-water harvesting (*Zai*) and water harvesting (*Demi-Lune*) have been largely uptaken by farmers. In fact, the high level of poverty in WA leads farmers to abandon some crop management technologies and approaches, even though they are proven to be efficient. Thereby, only those strategies which require little resources in terms of labor and money have a change to engage a large number of farmers.

1.4 Planting dates: background and state-of-the-art

Several studies addressing the specific agricultural problems have shown that SSA, particularly West Africa (WA) is a water scarce region (Challinor et al., 2007, Roudier et al., 2011, Biazin et al., 2012), where farmers have to cope with high rainfall variability. In addition, the growing season in WA only lasts for few month and is therefore limiting the time within which crop must be planted for best results. According to Sivakumar (1988), there is a strong relation between the growing season and the onset of the rainy season and the time slot within which farmers must plant decreases southwards in WA. However, early planting dates can lead to crop failure due to long dry spells which can occur shortly after planting (Stern et al., 1982, Sivakumar, 1988). In contrast, late planting dates are likely to avoid crop failure but they correspond to short growing seasons, which can reduce the crops productivity (Laux et al., 2008). The crops to plant is a

result of the length of the growing season and the capacity of the farmer to find labor (i.e. for farm land preparation and sowing) and crop seeds (Barbara et al., 1986). In light of farmers' economic constraintes and the underlined agricultural climate-related risks, the decision to plant is influenced by the input costs and perceived risks of economic losses due to climate hazards. Therefore, the decision to plant at a specific time period is a challenging task for farmers.

The question of how to determine a suitable time for planting has been for a long time a concern for the scientific community. Various studies have suggested different approaches to estimate the planting dates, which is is often interchanged with the onset of the rainy season (e.g. Cochemé and Franquin, 1967, Benoît, 1977, Stern et al., 1982, Sivakumar, 1988, Omotosho, 1992, Omotosho et al., 2000, Diallo, 2001, Dodd and Jolliffe, 2001, Chamberlin and Diop, 2003, Laux et al., 2008, Laux, 2009, Laux et al., 2010). Most of these approaches are rainfall-based methods and more commonly used in SSA to estimate the date where suitable agronomical conditions are fulfilled for planting. The simplicity of the methods and the low demand of computer resources are among the main reasons for the success of rainfall-based methods in SSA. These methods seek adequate soil moisture for planting as well as favorable rainfall conditions during the early stage (a period of 30 days after the planting date is often considered) in order to eliminate crop failure. For computation purposes, a rainfall threshold is often used to relate soil moisture with planting time. For each method, a rainfall threshold is defined accordingly. In general, the value of the rainfall threshold corresponds to a certain amount of rainfall cumulated over a few days. The assumption made is that planting may take place when rainfall is sufficient to provide soil moisture equivalent to crop water requirements for germination. In addition, a long dry spell immediately after planting have to be avoided since it may dry out the top soil and produce a crop failure after germination. Based on these assumptions, different algorithms have been proposed to compute planting dates. Although these methods can be easily implemented and used for operational agricultural decision support, they are not crop specific since information about crop type and phenology are not explicitly involved.

With the increasing use of process-based crop models in agricultural impact studies, new crop specific approaches have been developed to estimate crop planting dates either at plot or regional scale. These methods can be subdivided into two groups:

The first group consists of methods using only crop models to derive suitable planting dates. In this group, a crop yield optimization method is required (e.g. Stehfest et al., 2007). Depending on the crop model and the optimization method, this approach can be computationally time demanding. To overcome this issue, specific assumptions are usually made. For instance, Folberth et al. (2012) estimated crop planting dates by employing a crop model at a monthly or weekly time step. According to the region, they limited the planting date computation period by using a reported earliest and latest planting date. Although a time window of one month for crop planting is valuable in general, it is not favorable for SSA's regions where the growing season lasts only three months. In this first group, in addition to the high demand in computing time, crop models require a lot of input data. Therefore, this is a limitation for crop simulation, particularly in the data scarce region of SSA.

The second group consists of a combination of crop models and rainfall distribution characteristics (e.g. Laux et al., 2010). In this approach, the first step is to derive planting dates which fulfill specific agronomical criterions using rainfall information only. Then, the resulting planting dates are used as input to a crop model to derive optimized planting rules by applying a suitable objective function and an optimization algorithm. This approach reduces significantly the required computation time and can be used to improve rainfall based methods. This latter approach may open a new avenue in planting date estimates, since it can be used to derive crop and location specific planting dates. However, determining the appropriate agrometeorological criteria to derive planting dates and the application of optimization methods to support agricultural decision-making under increasing climate variability and climate change, remains challenges.

With regards to the underlined challenge, any efforts towards improved planting

date estimation techniques can contribute to enhance farmers strategic decision-making support and therefore can be a valuable strategy to alleviate the impact of climate variability on agriculture. Apart from coping with climate variability, a strategy that farmers can use to maintain or increase crop yields in the face of the changing climate is to adjust planting dates (Lauer et al., 1999, Sacks et al., 2010).

The research reported in this thesis entitled "*Optimizing Planting Dates for agricultural decision-making under climate change over Burkina Faso/West Africa*" presents a new method to optimized crop planting date in water-limited regions in WA and its benefit as an agricultural management strategy.

1.5 Objectives of the thesis

The main objective of this research is to contribute to the support of decision-making in rainfed agriculture through an improved agricultural management strategy. This research focus on how to estimate a suitable planting time in water limited regions in WA in a context of climate variability and climate change, and smallholder farming systems. Specifically, this study aims at:

1. Developing a technique to optimize crop planting date for water-limited regions in WA, and

2. Evaluating the performance of the developed technique for maize cropping in the context of present climate and projected future climate in Burkina Faso, WA.

1.6 Innovations of the thesis

In comparison to the established planting date methods which are currently in use in West Africa, the Optimized Planting Date (OPD) approach has the following innovations:

1. The OPD approach is a fully objective method to derive location-specific planting dates which take into account crop types or cultivars. Instead of

relying exclusively on rainfall amount and distribution around planting, the OPD approach does not only account for plant water requirements and availability throughout the whole growing period, but also for radiation and temperature. This information is inherently included by coupling the planting rules to a process-based crop model.

2. In light of uncertainties in precipitation measurements, the use of fuzzy-logic memberships to define planting rules instead of binary logic gives further flexibility to estimate reliable planting dates where strict thresholds may fail.

3. The OPD approach is not elaborating a single specific planting date, but rather suggesting a set of reasonable planting rules, leading to a time window for planting of a few weeks. This can help to increase the adoptability of this approach for smallholders, because their decision about planting also depends on other external factors such as availability of seeds, labour, machines, etc.

1.7 Outline of thesis

The thesis is structured in five chapters. The first two chapters address the issues of food security and climate change in West Africa and introduce climate-based planting date strategies as a potential crop management option to alleviate crop failure and to enhance crop productivity. Based on climate observation data, an analysis of climate and agrometeorological factors has been performed for the study area, in order to describe climate-related risks in agriculture. The forth and fifth chapters deal with a new approach to optimize the planting dates and analyses the performance of this approach for maize cropping under present and projected future climate in the study area. The methods and results presented in chapter three and four are based on the two publications:

1. Waongo, M., P. Laux, S. B. Traore, M. Sanon, and H. Kunstmann, 2014: A crop model and fuzzy rule based approach for optimizing maize planting

dates in Burkina Faso, West Africa. Journal of Applied Meteorology and Climatology, 53, 598-613, doi:http://dx.doi.org/10.1175/JAMC-D-13-0116.1.

2. Waongo, M., P. Laux, and H. Kunstmann: Adaptation to climate change: the impacts of optimized planting dates on attainable maize yields under rainfed conditions in Burkina Faso. Journal of Agricultural and Forest Meteorology (submitted, under revision).

The last chapter summarizes the key findings of the thesis and gives an outlook to suggested further future research that can open new avenues towards an operational use of the optimized planting date approach.

Chapter 2

Climate and agro-climatological analysis of Burkina Faso

2.1 Introduction

An overview and the climate of the study area are presented in this chapter. Temperature and rainfall variability are considered in the analysis of the climate. This chapter address also the question of the climate-related risks, particularly rainfall probability and dry spell frequency in the study area. In addition, the analysis of the growing season characteristics (i.e. onset, cessation and length of the growing season) has been carried out based on state-of-the-art methods. Observed daily temperature and precipitation data have been used for the analysis. Since crop water demand is a key factor in crop management, the analysis of a simplified crop water balance has been performed using rainfall summary and the potential crop evapotranspiration, which is computed using climate variables.

2.2 Overview of the study area

Burkina Faso (BF) is a a land-locked West African country located in the mid-west SSA region (Figure 2.1). It covers an area of about 274200 km^2 and lies between 9 and 15.5°N and between 6°W and 3°E. It is bounded on the North and the West by Mali, on the East by Niger and on the South by Ivory Cost, Ghana, Togo and

Benin. The country is mainly flat, with a mean altitude of about 300 m a.s.l. (Azoumah et al., 2010). With a population about 17.3 millions in 2007, BF ranges among the poorest countries in the world with a very low Human Development Index HDI (e.g. HDI was 0.34 in 2012) (UNDP, 2014). Approximately 90% of its population lives in rural areas (Badini et al., 1987). The human pressure on natural resources is increasing because of the persistent population growth (e.g. population growth rate was 3.1 in 2006).

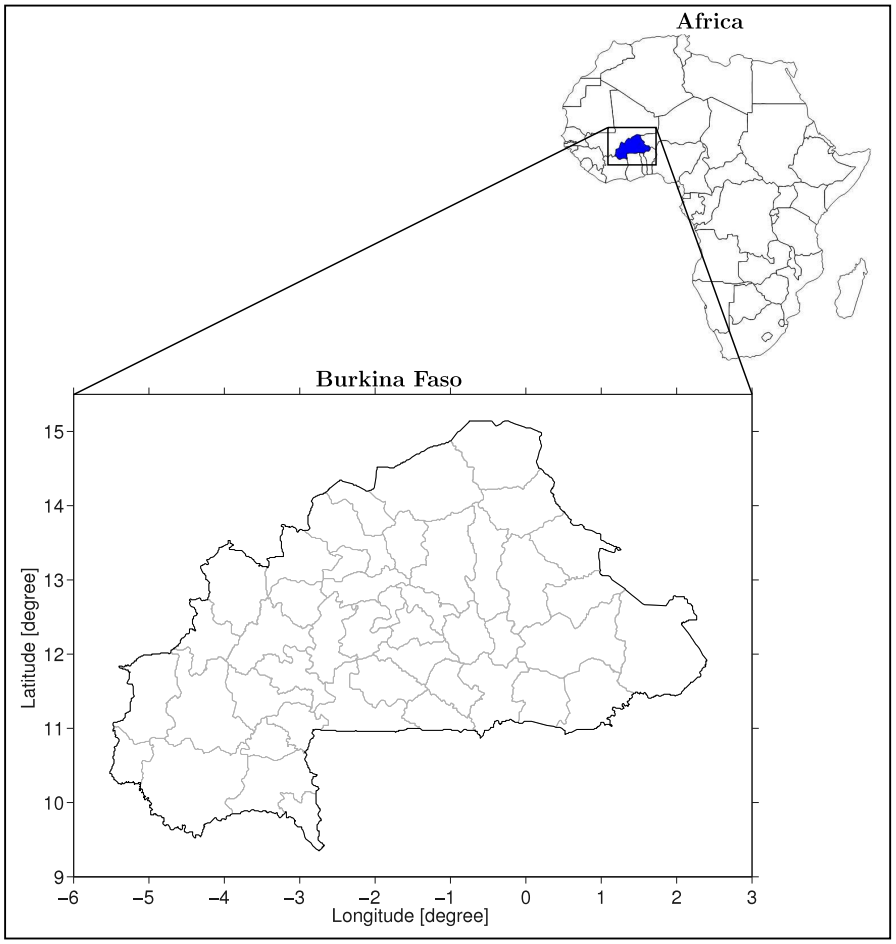

FIGURE 2.1: Study area and its location in Africa
(Data source: DGM Burkina Faso).

The climate over BF is characterized by two distinct seasons: a rainy season and a dry season. The dry season ranges from November to April while the rainy season ranges from May to October. During the dry season, the country is influenced by the Saharan anticyclone which causes a flux of dry and cool air, the so called 'Harmattan', over the country. At large scale, the rainy season is driven by the anomalies of the sea surface temperature (SST) in the tropical pacific

and atlantic oceans (Janicot et al., 1998, Ward, 1998). At regional scale, rainfall variability across the country is influenced by the North-South fluctuation of the Inter-Tropical Convergence Zone (ITCZ) associated to the West African Monsoon (WAM) (Sultan and Janicot, 2000). The ITCZ is a zone of rising turbulence. Its passage above various regions of inter-tropical Africa brings rain. Rainfall often follows, rather than accompanies, the passage of the ITCZ. The lag between the ITCZ and the release of heavy showers can be 200 to 300 km. The characteristic movement of the ITCZ and the disturbances associated with this phenomenon bring summer rainfall in WA. With a unimodal rainfall regime, the mean annual rainfall decreases from more than 1100 mm in the Southern BF to less than 300 mm in the Northern BF (Figure 2.2a). The North-South rainfall gradient is more pronounced if compared to the East-West rainfall gradient. On different time scales, a southward shifting of isohyets can be observed (Figure 2.2b).

The mean temperature of the wet season has been estimated to range between 20 and 36°C and decreases from the North to the South across the country (Sivakumar and Gnoumou, 1987). The highest temperatures occur mainly in April-May while the coolest temperatures occur mainly in December-January (Sivakumar and Gnoumou, 1987). The agro-ecological zones match with the north-south distribution of the rainfall. The inter-annual and intra-seasonal variability of rainfall are the main drivers of rainfed production in Burkina Faso. Traditional land use in BF is comprised of shifting cultivation, smallholder agriculture and nomadic pastoralism. Agricultural activities mainly take place during the rainy season with varying growing season of three to six months from the North to the South (Sivakumar and Gnoumou, 1987). BF's economy relies strongly on agricultural products and about 80% of the population is involved in rainfed agriculture (Brooks et al., 2013). In addition, agricultural production contributes more than 30% to the GDP and is the main source of income for the rural population (Diao et al., 2007).

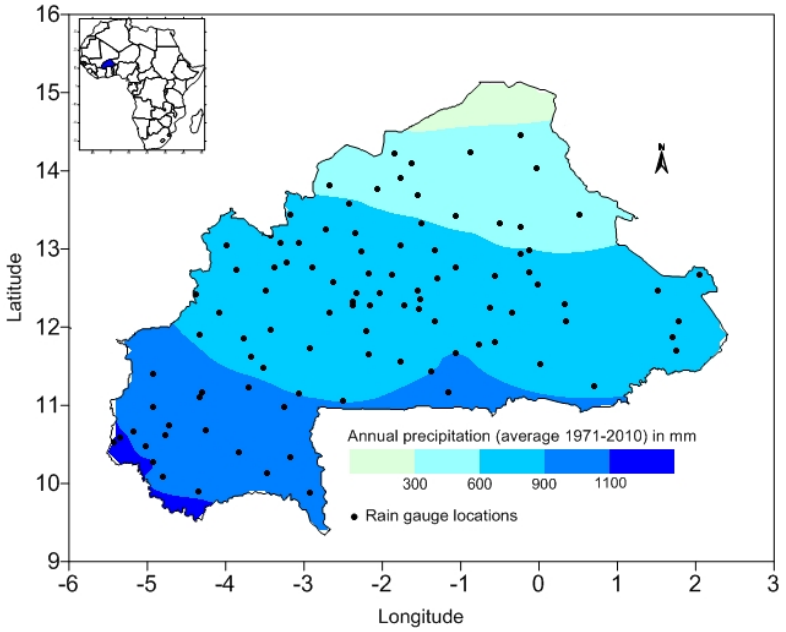

(a)

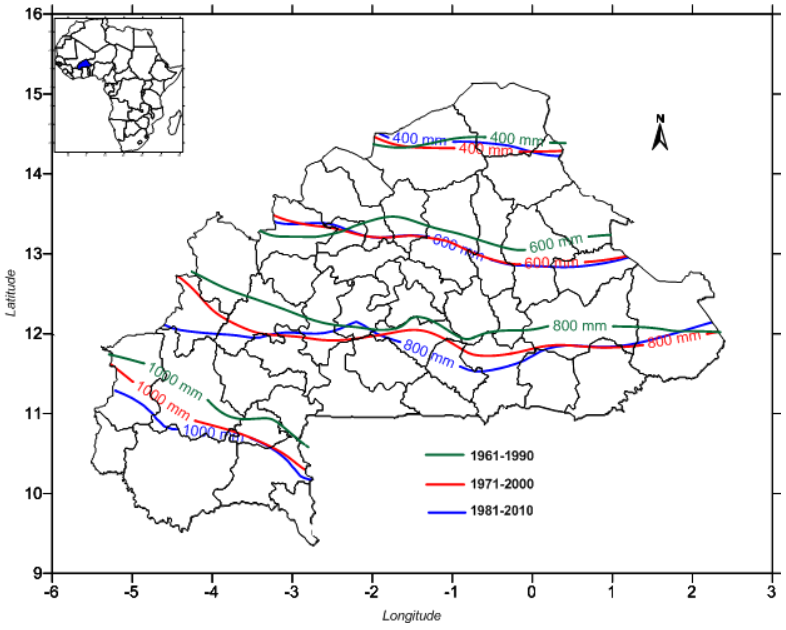

(b)

FIGURE 2.2: Annual precipitation (mean 1971-2010) (a) and position of the running 30-year mean isohyets (b), in the study area (Data source: DGM Burkina Faso).

Cereal crop production is predominantly subsistence-oriented. Sorghum (*Sorghum bicolor*), millet (*Panicum sp.*) and maize (*Zea mays L.*) are the main pillars for food security in BF. The annual production of these three staple crops have shown a rapid increase since 1984 with highest increase rate for maize (Figure 2.3). Based on the annual production, sorghum is the most important, followed by millet and

then maize. However, since 2000, maize is ranked as the second cereal crop after sorghum in terms of annual production. In general, the spatial distribution of these staple crops follows the rainfall distribution. Indeed, millet, which is more resistant to water stress, is grown widely in the North and maize, which less resistant to water stress is grown in the South. Sorghum, a slight resistant crop is grown over a large area between the North and the South. Other subsistence crops are rice, which is grown as a flooded or irrigated crop, and groundnut. Cotton, which is intensively grown in the South-West, is the main cash crop in BF.

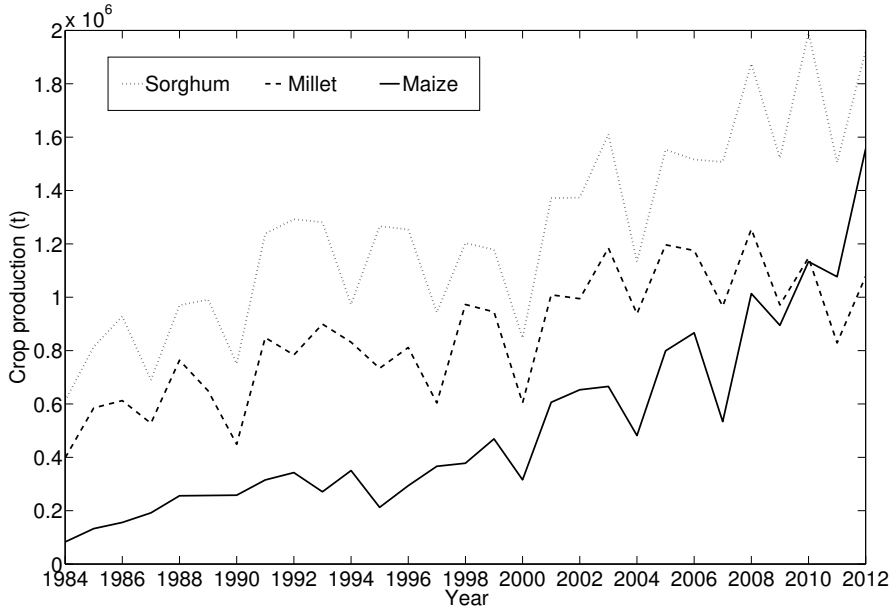

FIGURE 2.3: Evolution of three staple crops production in Burkina Faso. Data have been retrieved from CountrySTAT, FAO database (https://countrystat.org/home.aspx?c=BFA).

2.2.1 Climate data availability

The Directorate General of Meteorology (DGM) is the BF's governmental service which is in charge of climate observation network and weather watching across BF. DGM's climate observation network is composed of synoptic, climatic agrometeorologic and rain gauges stations. Synoptic stations are operated by meteorologists from DGM while the rest of the network is operated by skilled staff hired by the DGM in cooperation with others governmental services. A broad range of climate

variables measured at measured at synoptic stations including rainfall, temperature, solar radiation and sunshine, relative humidity, wind speed and direction and pan evaporation. Beside rainfall, climatic and agrometeorologic stations measure temperature, relative humidity and specific variables related to the type of stations. Climate data involved in this study have been collected from the DGM. The database included daily minimum and maximum temperature, daily rainfall, daily mean of wind speed, daily global solar radiation and sunshine duration. The time series of data for involved climate variables varies from location and type of station (i.e. rain gauge station or synoptic station). Rainfall and temperature from the period 1960-2010 have been used for this climatic analysis. Precipitation data are from 122 locations (Figure 2.4) comprising rain gauge and synoptic stations in BF (Appendix A). Temperature data are from the ten synoptics stations operated by the DGM across BF (Figure 2.4).

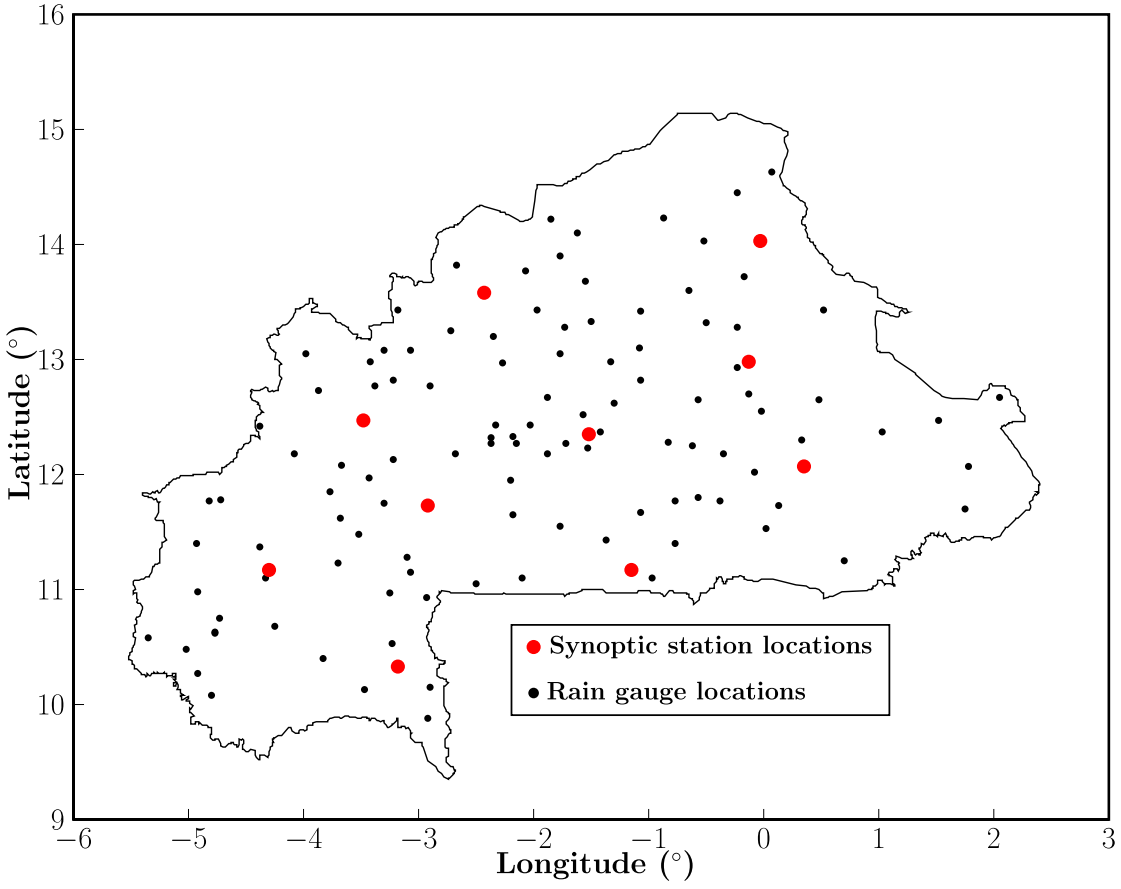

FIGURE 2.4: Climate observation network in Burkina Faso (Data source: DGM Burkina Faso).

2.3 Climate variability in Burkina Faso

2.3.1 Rainfall

Season-based climate information has considerable implications for impact studies, especially in agriculture. For instance, seasonal rainfall distribution helps in making useful comparisons of agricultural potential. In WA, seasonal and intra-seasonal distribution of rainfall are crucial for smallholder farming. The characteristics of seasonal (May-October) rainfall in BF have been examined. The analysis is carried out using the statistics (i.e. mean and standards deviation) of the spatial distribution of seasonal and intra-seasonal rainfall amount. From rainfall amount statistics, the ordinary kriging (OK) method is used to perform a spatial interpolation. The analysis of the spatial distribution of seasonal rainfall centers on the 50-year period mean (1961-2010) and the 30-year period means from 1961 to 2010 with a 10-year "sliding-window" (i.e. 1961-1990, 1971-2000, 1981-2010).

The analysis showed considerable variability in estimates of the 30-year mean and standard deviation of seasonal rainfall. As shown in Figure 2.5, the seasonal rainfall in BF decreases northward from 1200 mm in the extreme South-West to 300 mm in the North regardless the time period in consideration. The standard deviation varies between 100 mm to 180 mm and decreases northward. A relatively low variance is observed for the period 1971-2000. By comparing the different time periods a slight southward shift of seasonal rainfall between the period 1961-1990 and 1971-2000 is depicted whereas a northward shifting is observed between the period 1971-2000 and 1981-2010.

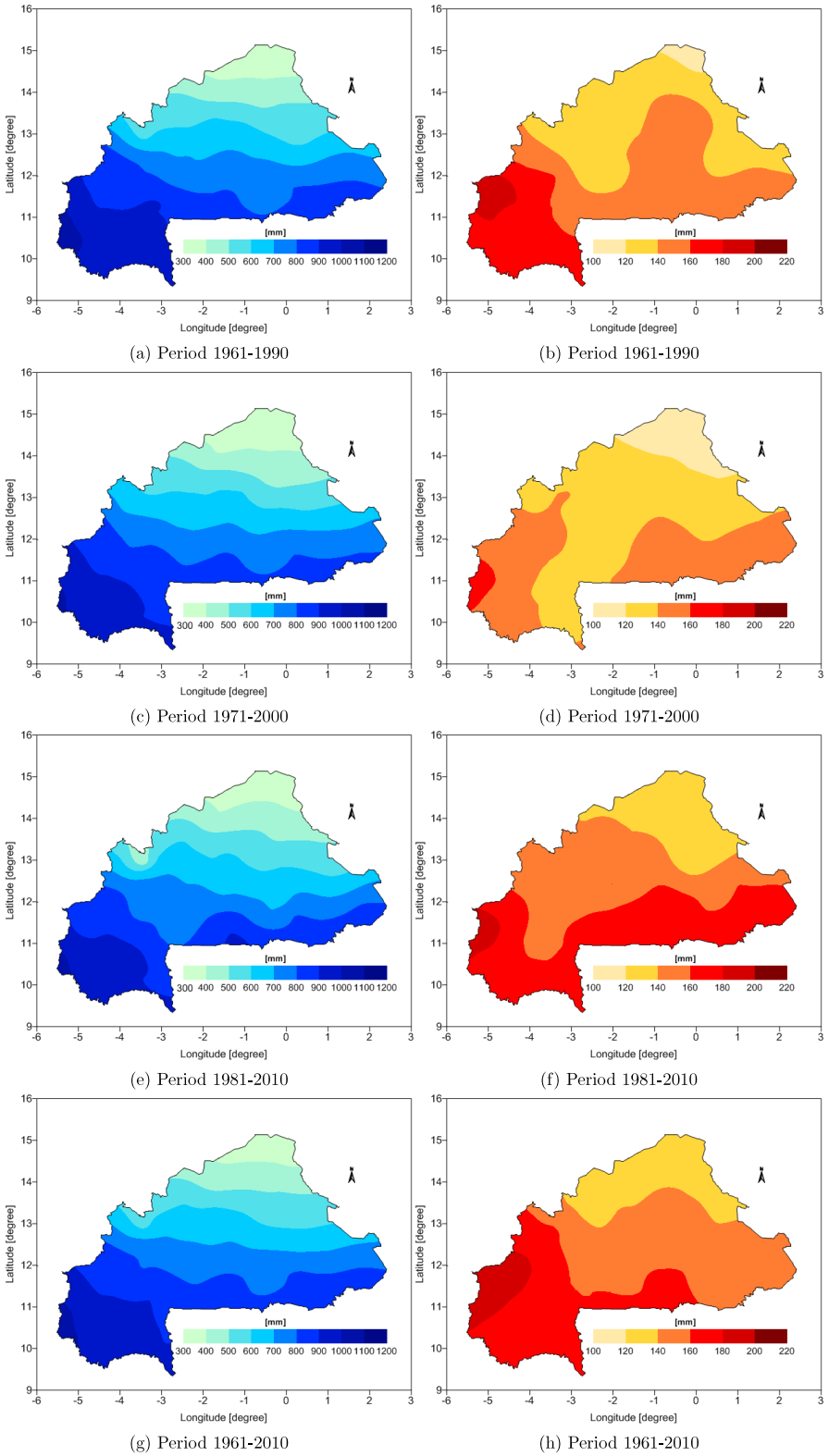

(a) Period 1961-1990 (b) Period 1961-1990

(c) Period 1971-2000 (d) Period 1971-2000

(e) Period 1981-2010 (f) Period 1981-2010

(g) Period 1961-2010 (h) Period 1961-2010

FIGURE 2.5: Spatial variability of the mean (left) and standard deviation (right) of seasonal (May-October) rainfall amount. The Ordinary Kriging (OK) method is used to interpolate the estimates for three time windows through a 10-year "sliding-window" from 1961 to 2010. The bottom figures represent the mean and standard deviation for the whole period (1961-2010).

To capture the annual cycle of monthly rainfall, three synoptic stations have been selected to carry out this analysis. The distribution of rainfall at the selected stations characterizes roughly the three agroecological zones (AEZs) in BF, that is the Sahelian zone with Dori as reference synoptic station, the Soudano-sahelian with Ouagadougou as reference synoptic station and the Soudanian zone with Bobo-Dioulasso as reference synoptic station. The analysis confirms the unimodal distribution of rainfall with a negative skew for all AEZs (Figure 2.6). The magnitude of monthly rainfall amount increases from the North (Dori) to the South (Bobo-Dioulasso) (Figure 2.6). The month of August is the wettest month across the three AEZs. The maximum monthly rainfall amount is about 170 mm at Dori, 220 mm at Ouagadougou and 280 mm at Bobo-Dioulasso. Rainfall amount for the period July-August-September represents about 80% and 60% of the annual rainfall in the North and the South, respectively. By considering only months with 50 mm as cumulative rainfall, the length of the wet season decreases from six months in the South to four months in the North (Figure 2.6).

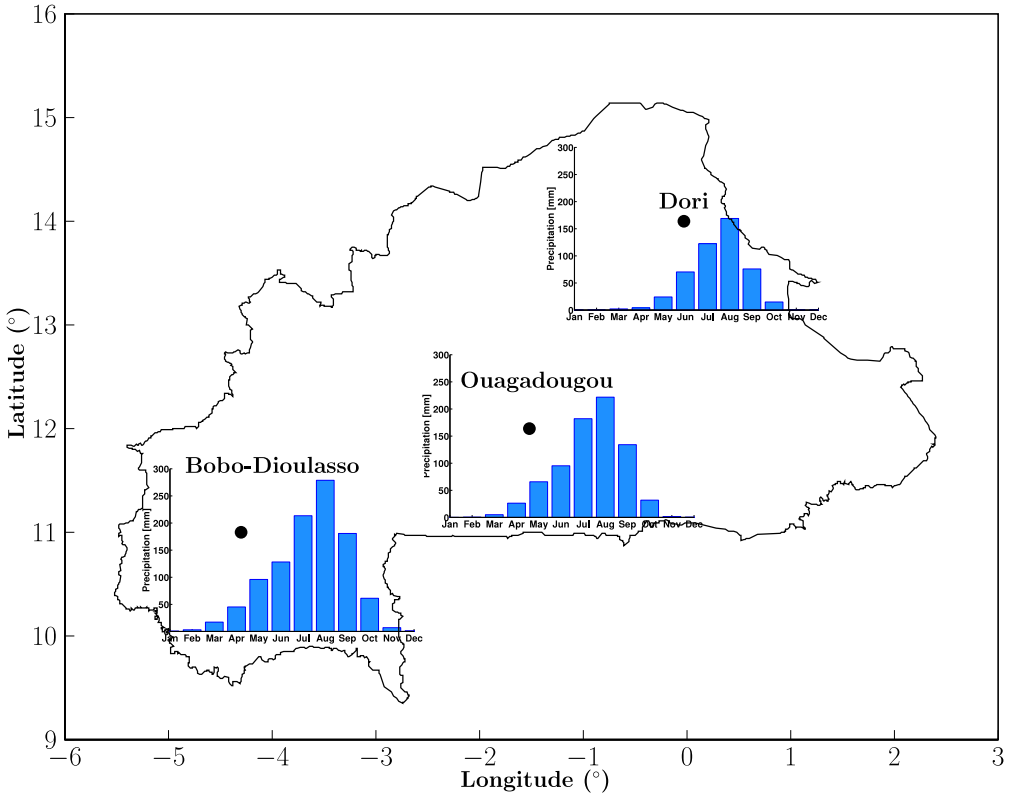

FIGURE 2.6: Annual cycle of mean monthly rainfall for three synoptic stations. The mean rainfall amounts are computed based on the period 1961-2010. The Black dots represent the locations of the selected stations.

2.3.2 Temperature

Monthly and annual temperature were calculated using daily temperature data from 1961 to 2010. Figure 2.7a depicts the annual cycle of the daily mean temperature over BF. In general, the daily mean temperature decreases from the North to the South and varies between 17 and 40°C for the three AEZs represented here by the three synoptic stations (see box and whisker plots in Figure 2.7a). However, the monthly mean temperature varies between 23°C and 35°C. The highest temperatures are observed during April-May (global maximum) and October (local maximum), while the lowest temperatures are observed during December-January (global minimum) and August (local minimum). On monthly basis, the spread of the variation of the daily mean temperature over the period 1961-2010 increase from the South (Bobo-Dioulasso) to the North (Dori). The analysis of the temperature annual cycle revealed also a clear discrimination of temperature between the three AEZs during April-October with a difference of 2°C between two consecutive synoptic stations southward.

An analysis of the temporal distribution of daily temperature at the selected station locations showed that the probability of exceeding a mean temperature of 25°C is about 90% for all AEZs. However, there is less than 1% probability of getting a daily mean temperature greater than 33°C, 35°C and 37°C at Dori, Ouagadougou and Bobo-Dioulasso, respectively (Figure 2.7b).

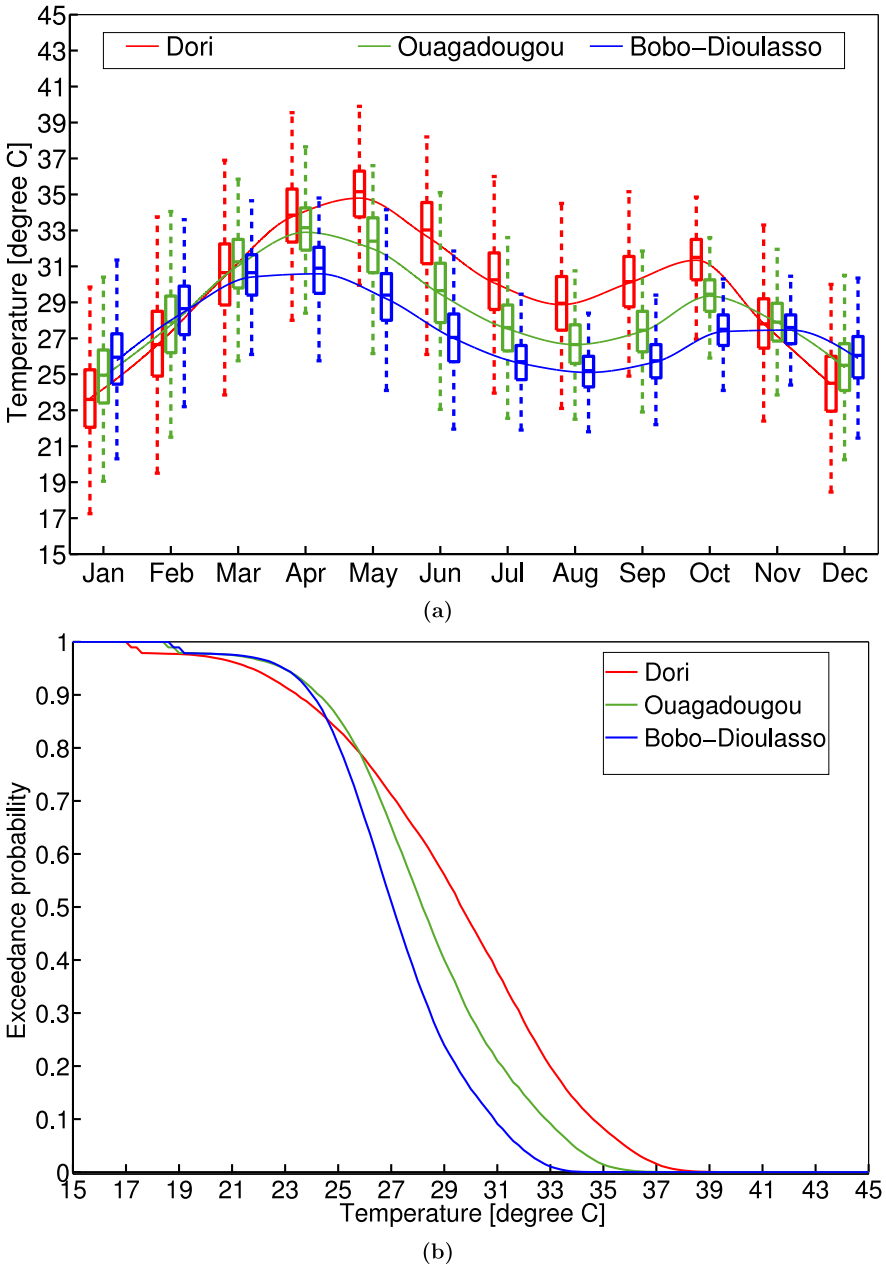

FIGURE 2.7: Annual cycle of monthly mean temperature (a) and exceedance probability of daily mean temperature (b) for three reference synoptic stations. Given a station and a month, the box and whisker plots (a) represent the distribution of daily mean temperature during the period 1961-2010. Solid lines (a) represent the annual cycle of monthly mean (period 1961-2010) temperature.

In order to capture the long term changes in annual temperature, an analysis of the minimum and maximum temperature is performed for the selected stations. Figure 2.8 shows that the long term evolution of minimum and maximum temperature depicts a statistically significant ($p < 0.05$) positive linear trend. The trend is on average 0.31°C/decade and 0.17°C/decade for the minimum and

maximum temperature, respectively. The trend of the minimum temperature slightly decreases from the North to the South whereas the maximum temperature shows similar trend for the three synoptic stations.

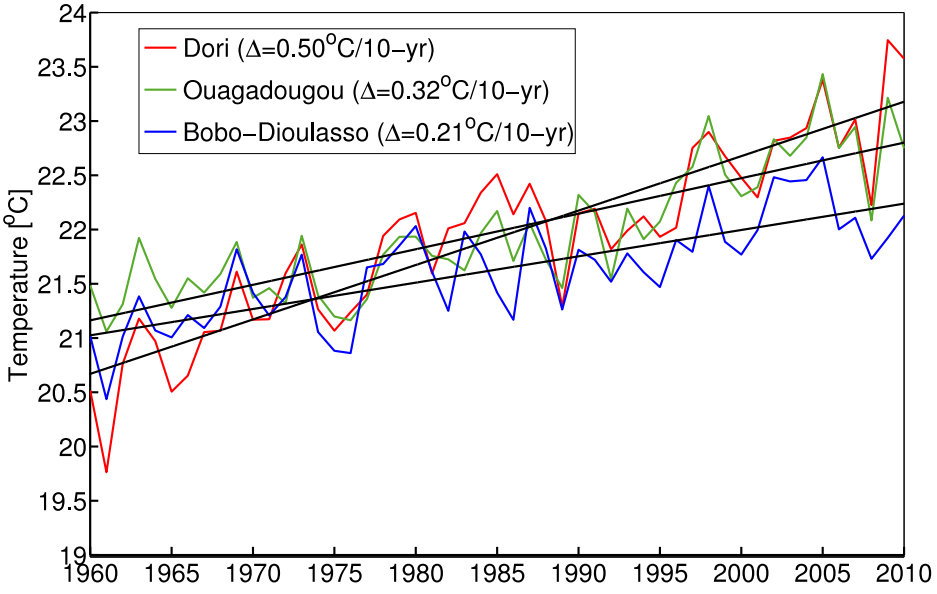

(a) Minimum temperature

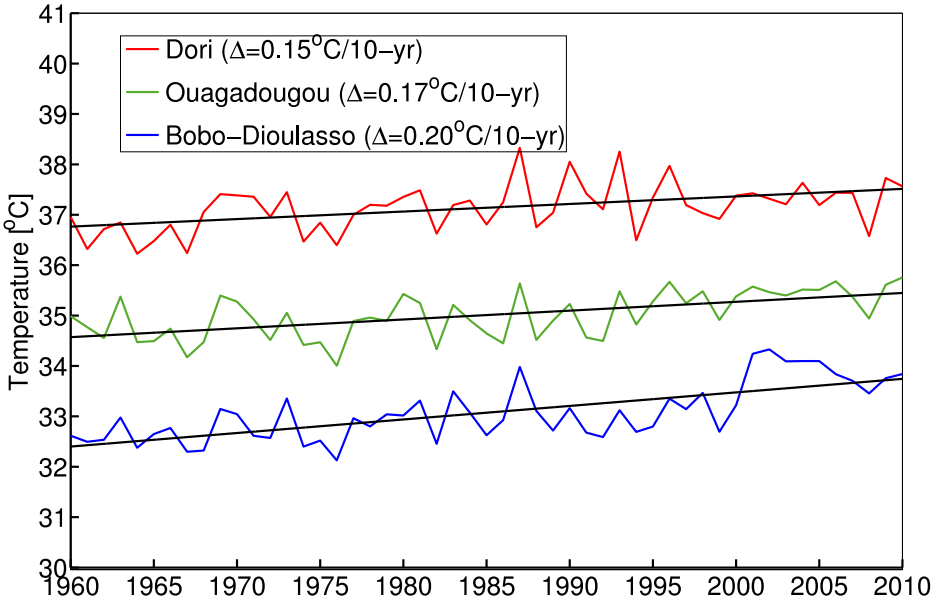

(b) Maximum temperature

FIGURE 2.8: Inter-annual variability of (a) minimum temperature and (b) maximum temperature for three synoptic stations. Solid lines (b) represent statistically significant ($p < 0.05$) linear trends of the annual mean of minimum and maximum temperature.

2.4 Analysis of agrometeorological factors

2.4.1 Introduction

The analysis of intra-seasonal precipitation patterns has a high practical value for planning agricultural activities. It is crucial to know the beginning of the rainy season in order to make strategic decisions for the upcoming growing season and to trigger field operations. Thus, the climatology or, even better, the prediction of the period of the rainy season during which crops are likely to suffer from dry spells are crucial for agricultural decision-making. For instance, short-term lasting dry spells or extreme events such as floods and droughts could lead to crop failures and thereby food insecurity. Therefore, the choice of agricultural strategies to stabilize crops yields depends on seasonal rainfall characteristics. For agricultural purposes, an analysis of the climatology of various descriptors which characterized seasonal rainfall is carried out. Among them, rainfall probability, dry spells occurrence and water availably for crop through crop water requirement are selected for this analysis. There is increasing evidence from crop experiments that short-term weather events of only a few days duration can severely impact crop productivity if they coincide with a sensitive phase of crop growth such as the first development stage (i.e. from crop emergence to a couple of weeks after crop emergence) and the time of crop flowering (Wheeler et al., 2000). Thus, when these crop climate-related stressors occur, the nature of crop response will be a vital part of the impact of climate on crop productivity.

2.4.2 Rainfall probability

For agricultural planning and implementation in a given geographical region, it is important to have reliable estimates of rainfall amounts. For this purpose, an analysis of the probability of receiving 5-days cumulative rainfall greater than 10 mm and 20 mm is carried out. These threshold values have been chosen to enable field operations such as soil preparation and crop planting. The period May-July is used for the computation of rainfall probability in BF on a monthly basis. Daily rainfall data from 123 climate stations for the period 1961-2010 have been

used. Figure 2.9 shows the spatial pattern of rainfall probability on a monthly basis. As expected, it follows similar patterns as the seasonal rainfall patterns. The patterns highlight that the chance of receiving 10 mm or 20 mm in 5 days decreases northward. In general, the wet conditions are increasing from May to July. It is only in July that the chance of receiving 10 mm within 5 days across the whole BF is greater than 50% (Figure 2.9e). However for the same month (July) there is more than 20% risk of receiving less than 20 mm (Figure 2.9f). Regarding May and June, the chance of receiving 20 mm is less than 40% (Figure 2.9b) and 60% (Figure 2.9d), respectively. Statistically, this findings show that every two years farmers cope with at least one year of adverse rainfall conditions on May, which might lead to crop failure after planting. With respect to the spatial distribution of 10 and 20 mm rainfall probability, farmers in the North have very limited chance to do fields operations on May and, to a lesser degree on June. In fact, receiving at less 20 mm of rainfall within 5 days is likely to happen one year out of 5 years on May and June in the North.

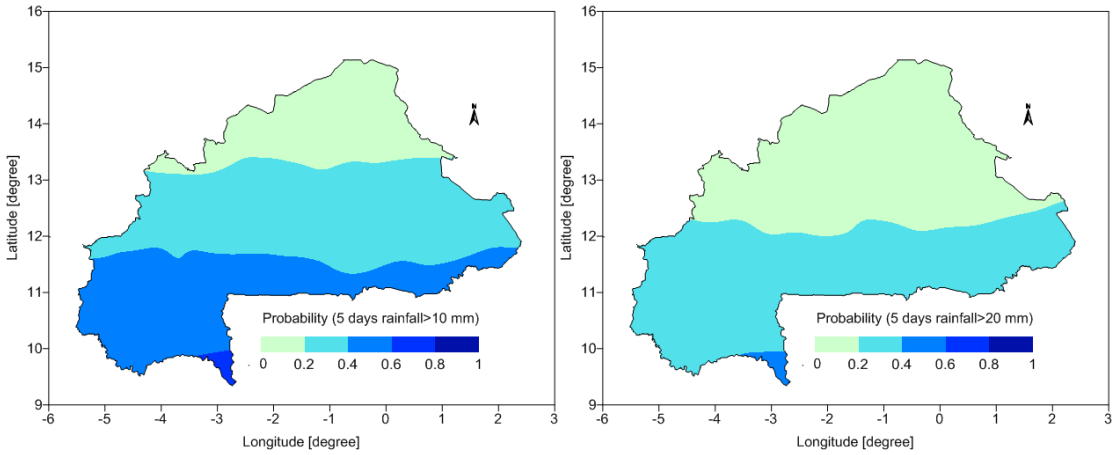

(a) May

(b) May

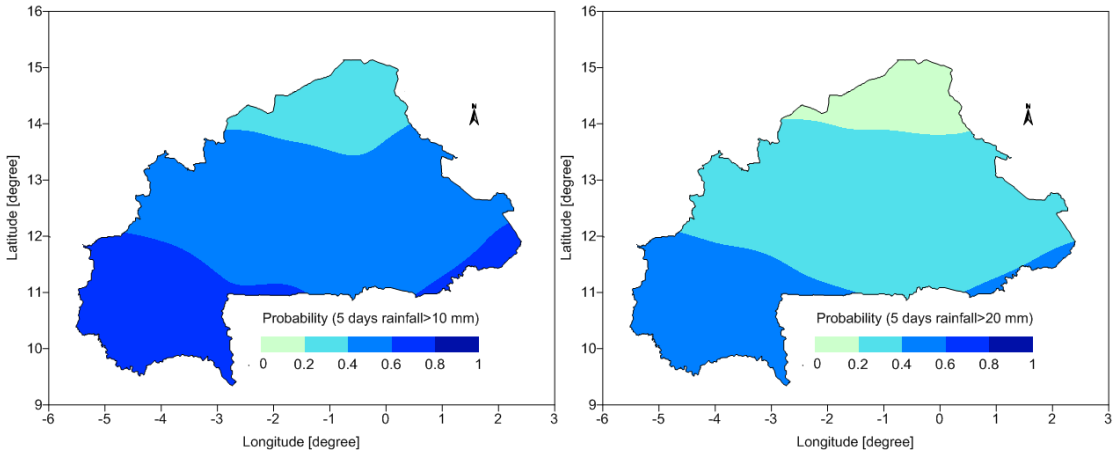

(c) June

(d) June

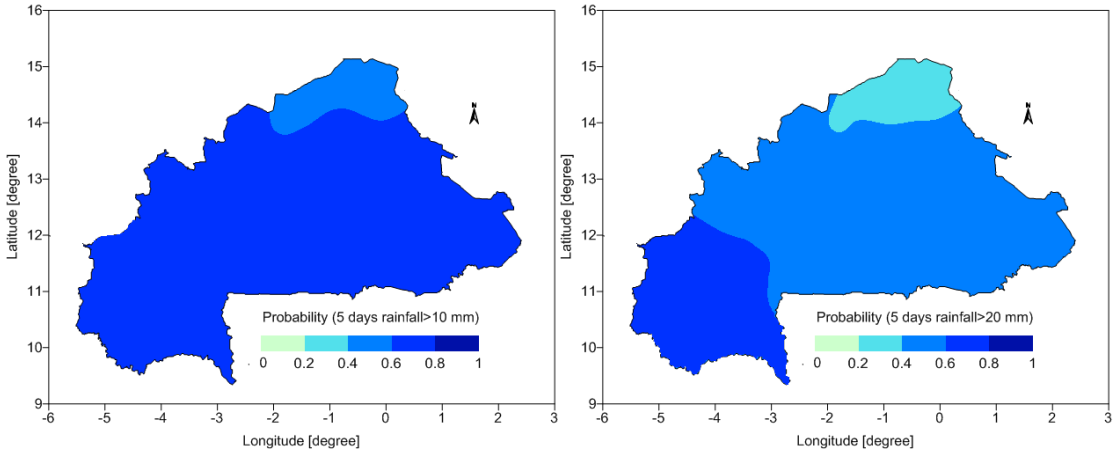

(e) July

(f) July

FIGURE 2.9: Spatial variability of the probability of receiving 5-days cumulative rainfall amount greater than 10 mm (left) and 20 mm (right) on May (top), June (middle) and July (bottom).

2.4.3 Dry spell frequency

Dry spells occurring after crop planting time is an important climatic information for agricultural management. For rainfed agriculture, dry spells can be useful (dry spells can be used by farmer to conduct field operations such as sowing, weeding, applying fertilizer, harvesting) as well as harmful (e.g. in water-limited regions, crops can suffer from water stress due to a relatively long period of dry-day). In this section, the scenario where dry spell becomes harmful for crops is of interested. Thus, a "long dry spell" will be simply named "dry spell". For computation, a dry spell is defined as the maximum number of consecutive dry days occurring during a given period, which is set to a month in our case. A dry day is defined as a day with less than 0.1 mm as recorded rainfall amount. In WA, dry spells greater than 7 days are the most damageable for the major food crops. In order to capture the climatology of dry spell lengths , an analysis of dry spells greater than 7 days and 10 days occurring on May, June and July have been performed. The analysis focused on these three months because, as already mentioned in previous sections, rainfall distribution during the considered three months is critical for field operations in SSA. Moreover, apart from the time of crop flowering, crop vulnerability is higher during this considered period.

Likewise rainfall probability, the southward distribution pattern of dry spells (Figure 2.10) are similar to the seasonal rainfall pattern in BF. Highest risks of observing dry spells (>7 or >10 days) is found in the North while lowest risks of dry spell is found in the South. Also, dry spells risk decreases with time from May to July. May is the most critical month with 60% (Figure 2.10a) and 40% (Figure 2.10b) risk for a dry spells greater than 7 days and 10 days, respectively (Figure 2.10a,b). Although the risk is decreasing with time, it remains greater than 80% (40%) on May (June) in the North. On July, the risk of dry spells greater than 10 days is found to be low (< 20%) for the whole BF (Figure 2.10f). However, across the country, the risk of dry spells greater than 7 days remains greater than 20% from May till July (Figure 2.10a,c,e). Based on this analysis, it is likely that field operations in BF such as sowing face a risk of failure whose magnitude decreases from May to July.

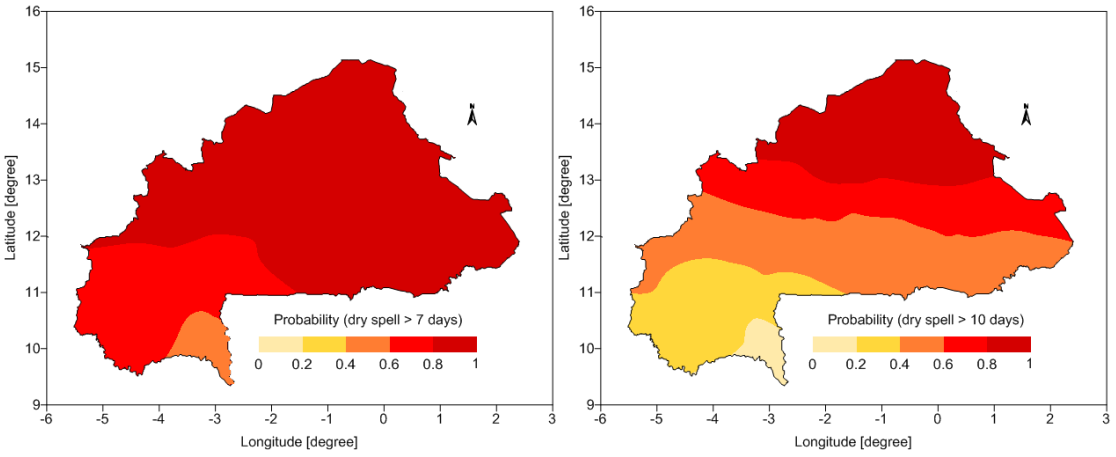

(a) May

(b) May

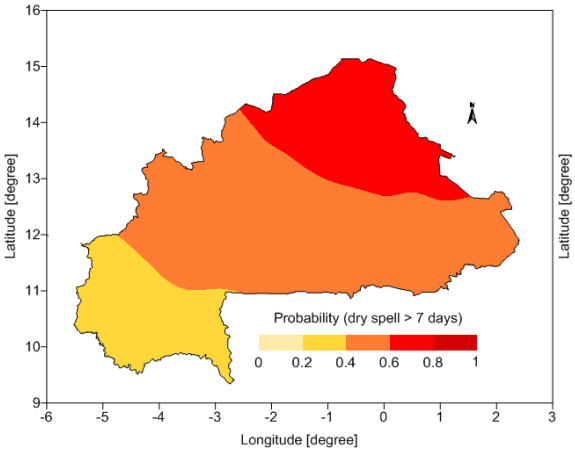

(c) June

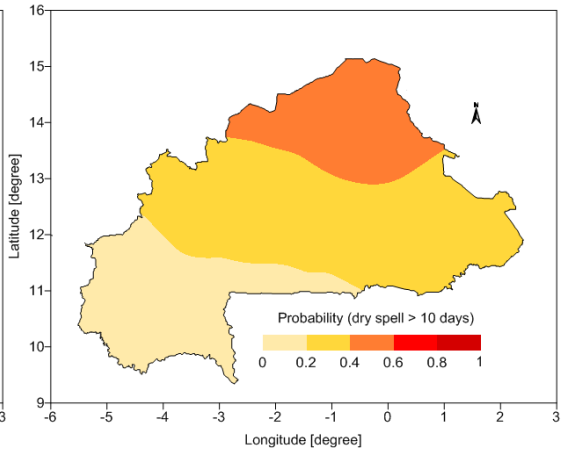

(d) June

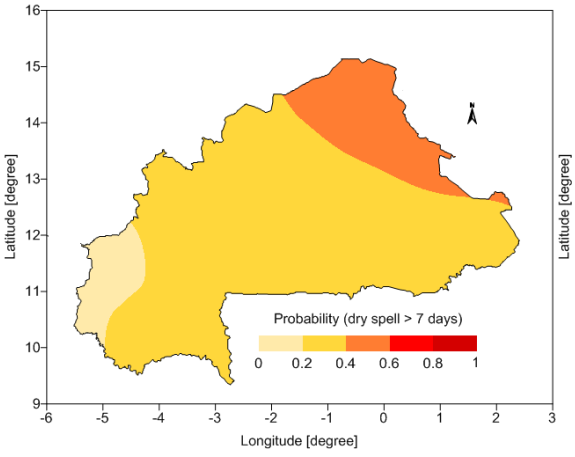

(e) July

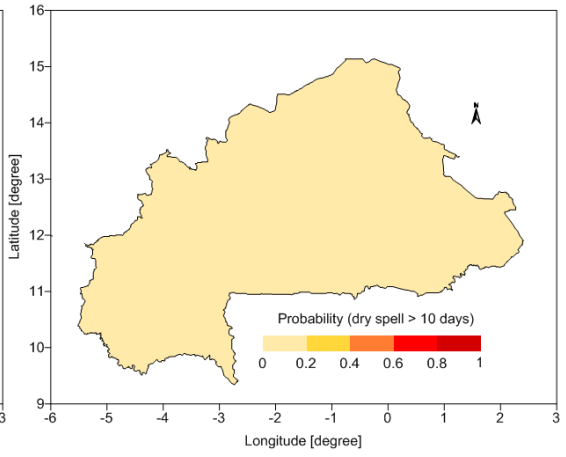

(f) July

FIGURE 2.10: Spatial variability of the risk of dry spells greater than 7 days (left) and 10 days (right) on May (top), June (middle) and July (bottom).

2.4.4 Crop water requirements

The agricultural practice requires a careful management of water resources, especially in the areas where water is naturally scarce. The knowledge about crop water requirements (CWR) is crucial for the optimization of the water consumptions and the irrigation techniques. For rainfed agriculture, the estimates of CWR allows for instance a zoning of crops based on water availability across different climatic zones. The main component of determining crop water requirements is the evapotranspiration (ET). ET represents the combined loss of soil water from the earth's surface to the atmosphere through evaporation of water from the soil or plant surfaces and transpiration via the stomata of the plant. In fact, in agricultural production systems, these two losses of water represent a major component of the water balance of the crop. The morphological and physiological characteristics of the crop and, to a limited degree, the effect of management practices are used in combination with ET to estimate CWR.

It is well known that ET is a very complicated function of climate variables. This complexity has led a number of investigators to attempt to estimate ET by direct measurements or on the basis of empirical functions of climate variables. Direct measurements of ET can be performed using techniques such as lysimeters, eddy covariance and soil water balances. However, the use of direct measurement techniques is limited, mainly due to their high cost and the need for skilled personnel to install and maintain equipment and to interpret the resulting data (Allen et al., 1998). To overcome these limitations, indirect measurement methods based on climate variables have been proposed as alternatives to estimate ET (e.g. Penman, 1948, Priestley and Taylor, 1972, Doorenbos and Pruit, 1977, Hargreaves and Samani, 1982, Allen et al., 1998). Since observational data are not often available for some of the climate variables such as radiation, vapor pressure deficit and wind speed at appropriate levels, most of the aforementioned methods used temperature, humidity and precipitation to estimate ET. When data are available, the FAO-56 Penman-Monteith method (Allen et al., 1998) is recommended by the Food and Agriculture Organization of the United Nations (FAO) since this method

is tested in different parts of the world and has been proven to have a higher performance compared to other methods (Allen et al., 1998, Adeboye et al., 2009). ET computed by the FAO-56 Penman-Monteith method (Eq.2.1) is known as reference evapotranspiration (ETo) or alfalfa reference evapotranspiration (ETr). As shown in Eq.2.1, ETo computation requires solar radiation, temperature, relative humidity and wind speed. In tropical regions, ETo is relatively higher and is considered as the maximum value of CWR during stages of crop growth. However, during crop reproductive stage, CWR is lightly higher than ETo.

$$ETo = \frac{0.408 \times \Delta \times (R_n - G) + \gamma \times (\frac{900}{T+273}) \times u_2 \times (e_s - e_a)}{\Delta + \gamma \times (1 + 0.34 \times u_2)} \tag{2.1}$$

where

ETo = reference evapotranspiration ($mm\ day^{-1}$),

R_n = net solar radiation at the crop surface ($MJ\ m^{-2}\ day^{-1}$),

G = soil heat flux density ($MJ\ m^{-2}\ day^{-1}$),

γ = psychometric constant ($KPa\ °C^{-1}$),

T = daily mean air temperature at 2 m ($°C$),

u_2 = wind speed at 2 m height ($m\ s^{-1}$),

e_s = saturated vapor pressure (KPa),

e_a = actual vapor pressure (KPa),

Δ = slope vapor pressure curve ($KPa\ °C^{-1}$).

In order to compute ETo, daily climate data emcompassing minimum and maximum temperature, minimum and maximum relative humidity, wind speed at 10 m and solar sunshine duration from the ten synoptic stations in BF have been used. Wind speeds at 10 m have been converted to the speed at a height of 2m. An algorithm has been designed to compute ETo on daily basis for the period 1971-2010. The algorithm folows the computation steps suggested in the FAO-56 Penman-Monteith method. Daily mean air temperature is calculated based on the daily maximum and minimum air temperatures. Relative humidity is used in combination with temperature and saturation vapor pressure curve to compute e_a and e_s . Δ is computed based on the relationship between saturation vapor

pressure and temperature. γ is calculated based on atmospheric pressure, which is a function of the altitude of the station. Details of the formulas can be found in Allen et al. (1998).

Because of the huge number of missing data in measured solar radiation and the availability of measured sunshine duration, Angström's formula which relates solar radiation to extraterrestrial radiation and relative sunshine duration (Eq.2.2) , is used to compute shortwave radiation (R_s) and therefore R_n.

$$R_s = R_a \times \left(a + b \times (\frac{h}{H})\right) \tag{2.2}$$

where

R_a = extra atmosphere global solar radiation ($MJ\ m^{-2}\ day^{-1}$)

R_s = shortwave solar radiation ($MJ\ m^{-2}\ day^{-1}$),

h = measured sunshine duration ($hour$),

H = maximum possible duration of sunshine or daylight hours ($hour$),

a and b are unitless location specific Angström parameters.

In Eq.2.2, the value of the parameter a and b is location-specific. Based on climatic zones, standard values for a and b have been proposed for the tropical regions (Allen et al., 1998). In this study, instead of using the stanadard values for a and b, optimized a and b have been derived for the synoptics stations by minimizing the Root Mean Square Error (RMSE) between computed solar radiation and available measured solar radiation for a given location (Table 2.1). Then, the optimized a and b have been used in combination with sunshine duration to compute R_n. Finally, ETo has been computed for the period 1971-2010 on a daily basis.

TABLE 2.1: Angström's parameters for tropical regions and optimized parameters for three synoptic stations. a^* and b^* denote standard parameters for tropical regions and a and b are optimized values

Station name	Longitude (°)	Latitude (°)	Angström's parameters			
			a^*	b^*	a	b
Dori	-0.03	14.03	0.25	0.50	0.24	0.46
Ouagadougou	-1.52	12.35	0.25	0.50	0.24	0.40
Bobo-Dioulasso	-4.30	11.17	0.25	0.50	0.28	0.41

As shown in Figure 2.11, daily mean ETo from the period 1971-2010 decreases southward and varies between 1.5 and 10 mm day^{-1} across BF. The monthly mean ETo ranges from 3 to 6 mm day^{-1}. In general, the spatial variability of the daily mean ETo is relatively low during the rainy season (May-October), particularly during the period June-August where ETo deviation between the North and The South is approximately 1 mm day^{-1}. Lowest values of daily ETo are found on August while highest values of ETo occur from February to April. On average, 10-day cumulative ETo is about 40 mm in Dori, 30 mm in Ouagadougou and between 20 and 30 mm in Bobo-Dioulasso (Figure 2.12). The comparison between 10-day cumulative ETo and rainfall shows that rainfall is likely to meet CWR for two months (July 21th-August 10th) in the North (Figure 2.12a), roughly three months (July-September) in the Center (Figure 2.12b) and five months (June-October) in the South (Figure 2.12c). As in the rainfall probability and dry spell length analyses, the analysis of ET highlights the high risk of crop failure in May due to water stress.

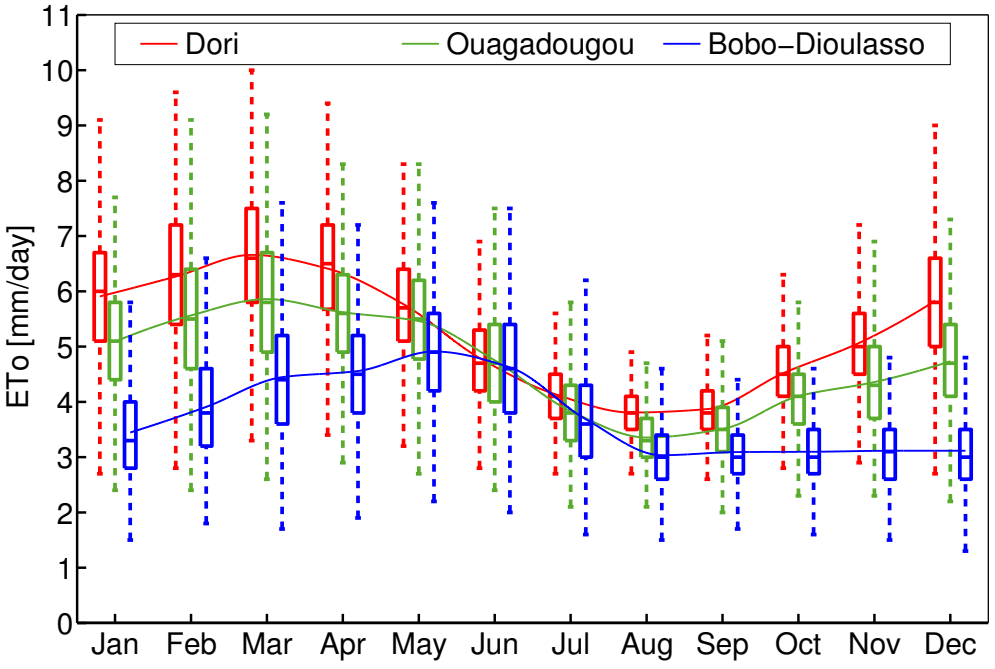

FIGURE 2.11: Variability and annual cycle of reference evapotranspiration (ETo). Given a station and a month, the box and whisker plot (a) represent the distribution of daily ETo during the period 1971-2010. Solid lines represent the annual cycle of monthly mean of daily ETo.

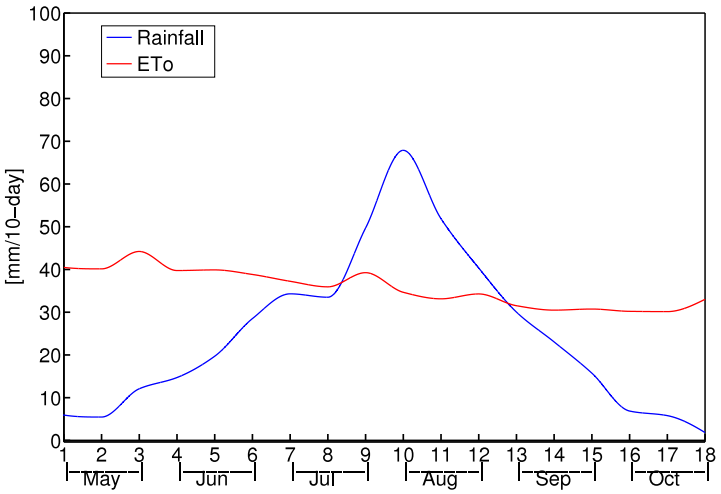

(a) Dori

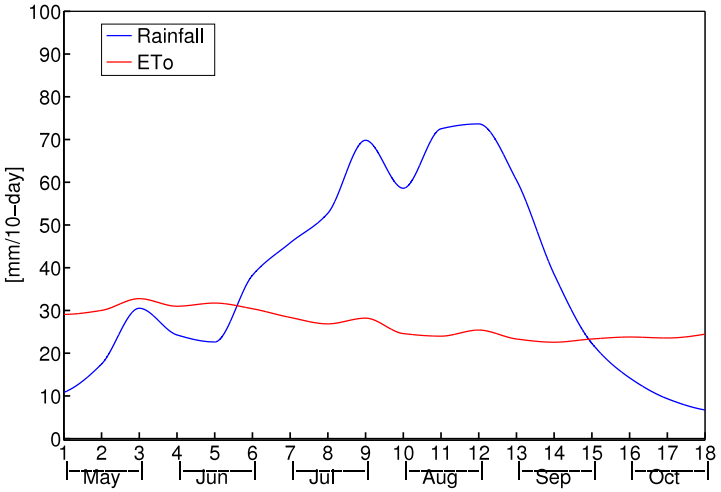

(b) Ouagadougou

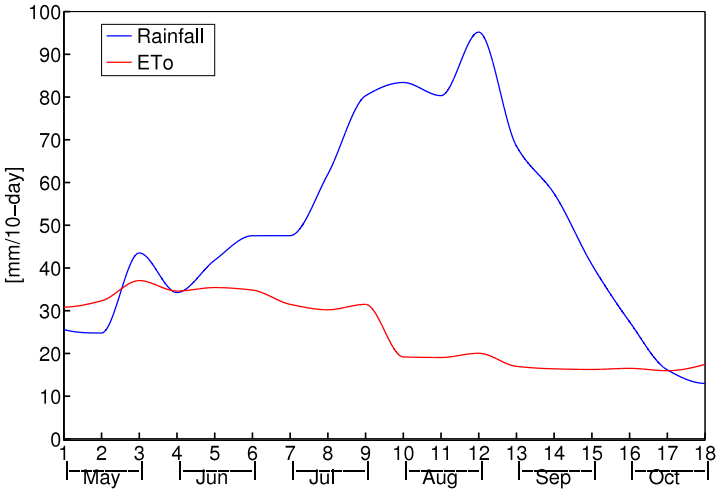

(c) Bobo-Dioulasso

FIGURE 2.12: Seasonal (May-October) cycle of 10-day cumulative reference evapotranspiration (ETo) and rainfall amount at three synoptic stations. Period 1971-2010 is used to compute means of 10-days cumulative ETo and rainfall.

2.5 Characteristics of the growing season in Burkina Faso

2.5.1 Onset of the growing season

From an agronomic point of view water stress conditions which occur at the time of crop germination or during a short period after crop germination are likely to cause crops failures leading farmers to proceed to a resowing. In the aim to alleviate the risk of resowing due to crop failure, rainfall-based methods define the onset of the growing season (OGS) as the date when accumulated rainfall exceeds a specific amount, provided that there was no long dry spell after this date. The rainfall threshold and the length of dry spell are the main parameters of rainfall-based methods. In this section, the following state-of-the-art rainfall-based methods have been selected to carry out the computation of the OGS using daily rainfall data of the period 1971-2010.

1. **Diallo (2001)**: *The date after 1st May, when rainfall accumulated over 3 consecutive days is at least 20 mm and when no dry spell of more than 10 days occurs within the next 30 days.* This approach is currently used at AGRHYMET Regional Center in Niamey (Niger).

2. **Dodd & Jolliffe (2001)**: *The first day of a spell of 5 days in which at least 25 mm of rain falls, on condition that no dry period of more than 7 days occurs in the following 30 days.* This approach is currently in operation as an agricultural decision support tool at the Directorate General of Meteorology (Burkina Faso).

The results show that on average the OGS across BF is between June 1st and July 10th using Diallo's method (Figure 2.13a) and between June 10th and July 20th when Dodd & Jolliffe's method is used (Figure 2.13c). The OGS distribution shows a standard deviation of about 20 days to 40 days irrespectively of rainfall-based methods (Figure 2.13b, d). For both methods, the spatial distribution of OGS follow a North-South gradient with latest OGS in the North and earliest OGS in the South. On average, May is highly risky for planting, using both methods.

In comparison, OGS following Dodd and Jolliffe (2001) is delayed of about 10 days compared to Diallo (2001). In addition, the inter-annual variation of OGS is higher for OGS based on Diallo's method, particularly in the Center region.

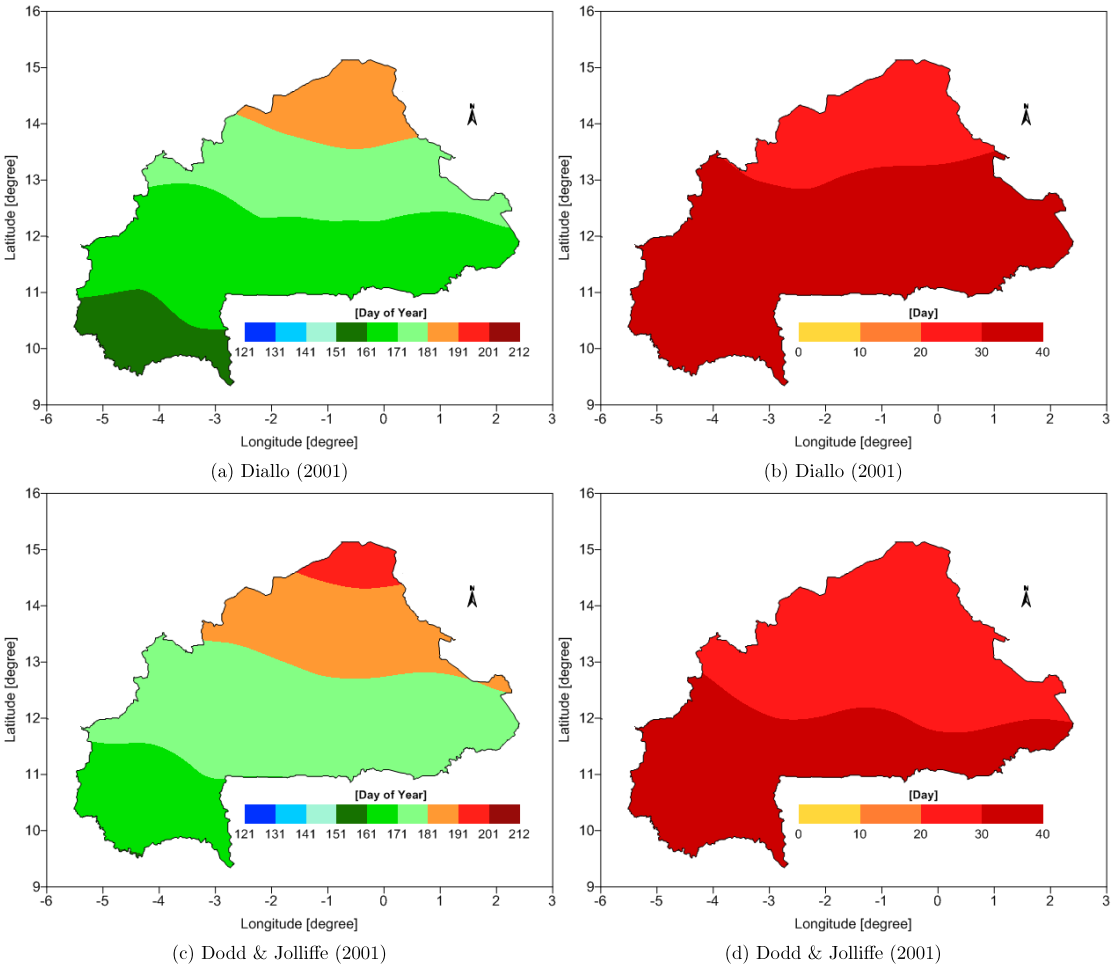

(a) Diallo (2001)

(b) Diallo (2001)

(c) Dodd & Jolliffe (2001)

(d) Dodd & Jolliffe (2001)

FIGURE 2.13: Spatial variability of the onset of the growing season during the period 1971-2010. Ordinary kriging method is used for the interpolation of the mean (left) and standard deviation (right) which is computed based on Diallo (2001) and Dodd and Jolliffe (2001).

2.5.2 Cessation of the growing season

The cessation date of the growing season (CGS) is use in combination with the OGS to compute the length of growing season. At farm level, it corresponds to the period of harvest. Therefore, information on the CGS can be useful for harvest planning activities. Generally speaking, the beginning of the dry season closely follows the onset of an extended period of dry weather. Likewise, the CGS follows the ending of an extended wet period. The first occurrence of a long dry spell

after a specified date is used to estimate the cessation of growing season. Since the harvest time in WA ranges from October till November, September 1^{st} is often used as the starting date for the computation of the the cessation of growing season (Stern et al., 1982, Sivakumar, 1988). The approach commonly used in WA defined the CGS as the date after September 1st in which no rain occurs over a period of 20 days (Stern et al., 1982). A similar approach defines the CGS as the date after September 1st when the soil water content down to 60 cm depth is nil with a daily potential evapotranspiration of 5 mm (Traoré et al., 2000). For a specific location, the later method requires to know the soil water holding capacity for the computation of the CGS . Therefore, Traoré et al. (2000) recommended a value of 100 mm for SSA. With regard to the similarity between the two approaches, the first method is used to compute the CGS for the same time period used to compute the OGS.

As shown in Figure 2.14a, the CGS occurs in the month of October with a standard deviation less than 20 days across BF (Figure 2.14a). Likewise the OGS, a north-south gradient is detected for CGS with earliest CGS occurring in the North while the latest CGS are found in the South. Likewise in previous studies (e.g. Stern et al., 1982, Sivakumar, 1988), the end of the growing season is less variable than the OGS and thereby presenting a lesser degree of risk for farmers.

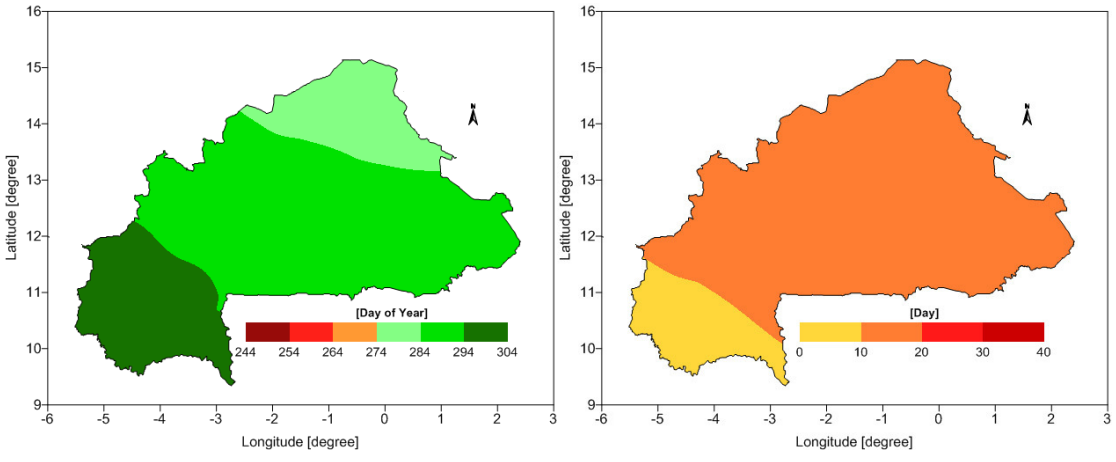

(a) Mean (b) Standard deviation

FIGURE 2.14: Spatial variability of the ending of the growing season during the period 1971-2010. Ordinary kriging method is used for the interpolation of the mean and standard deviation.

2.5.3 Length of the growing season

The information on the LGS is a key component for farmers decision-making. The spatial distribution of the main cereal crops and their importance is related to the LGS. From the computation of the OGS and the CGS, the LGS (day) is taken as the difference $(CGS - OGS)$, provided that CGS and OGS are given as day of year (DOY).

On average, the two rainfall-based methods show a LGS lying between 80 days and 168 days (Figure 2.15a, c). The standard deviation is between 10 days and 40 days regardless of the methods (Figure 2.15b, d). More significantly, the LGS decreases from the South to the North. In addition, the lowest variations of LGS are found in the South while highest variations are in the North.

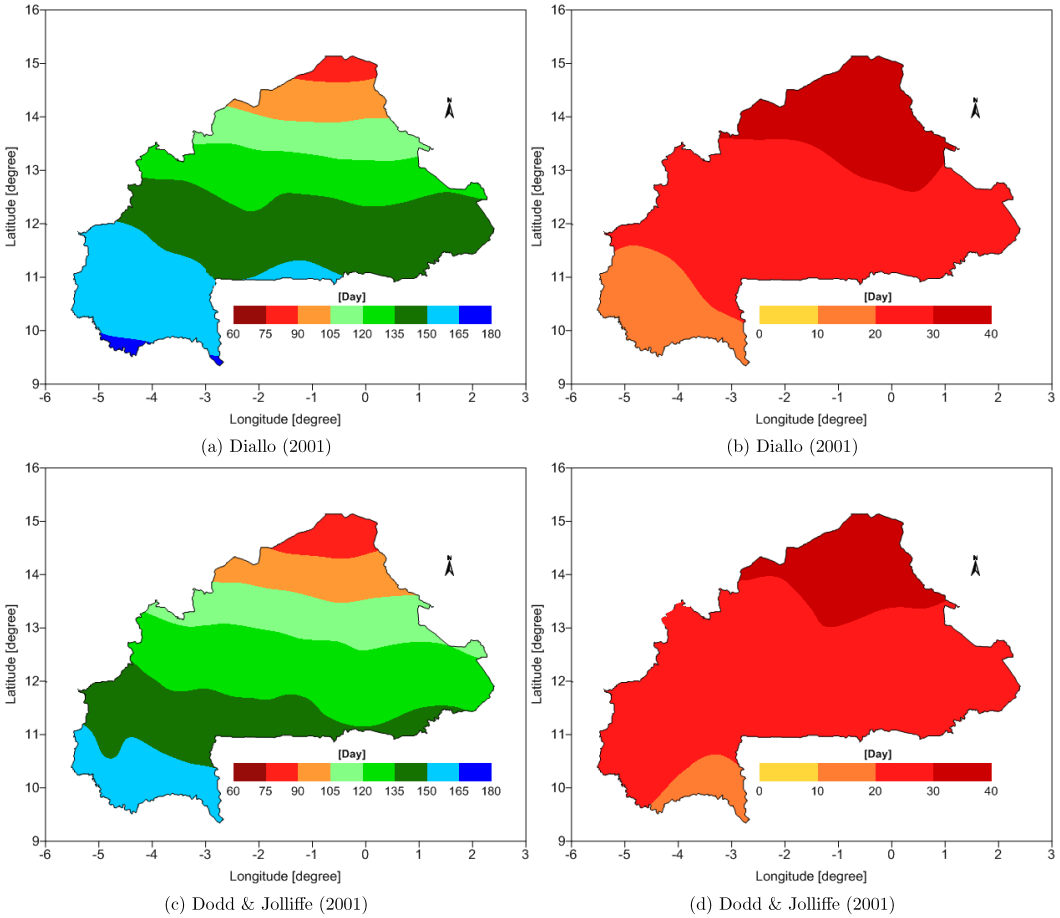

(a) Diallo (2001) (b) Diallo (2001)

(c) Dodd & Jolliffe (2001) (d) Dodd & Jolliffe (2001)

FIGURE 2.15: Spatial variability of the length of the growing season during the period 1971-2010. Ordinary kriging is used for the interpolation of the mean (left) and standard deviation (right) which is computed based on Diallo (2001) and Dodd and Jolliffe (2001).

2.6 Discussion and conclusions

In this chapter, based on historical data for the period 1960-2010, temperature and rainfall variability over BF is analyzed. More specially, rainfall probability, dry spell frequency and crop water balance have been analyzed in order to have an overview of climate-related risks in agriculture over BF. As already highlighted for the SSA region (Oduro-Afriyie, 1989), the spatial distribution of rainfall and temperature in BF indicated a strong north-south gradient with highest (lowest) temperature (rainfall amount) in the North while lowest (highest) temperature (rainfall amount) are found in the South. Similar spatial patterns are found for rainfall probability and dry spell frequency. A positive linear trend of the inter-annual variability of temperature has been detected for the period 1960-2010. The trend is higher for the minimum temperature than for the maximum temperature. More significantly, this analysis highlights that the onset of the growing season is subject to a high risk of long dry spells, lower chances of receiving suitable rainfall amounts to trigger field operations and a higher risk that rainfall amount might not cover crop water requirements throughout the first stage of crop growth. The analysis of the growing season showed that latest (earliest) OGS and shortest (longest) LGS in the North (South) following a strong north-south gradient. Crops with long growing periods might be recommended in the Southern BF and short growing period crops for the Northern BF.

This chapter highlights the particular difference between Northern and Southern BF in terms of agricultural opportunities. In fact, while the climate-related risk is high in the North, the South presents much more potential for cropping a large number of cereal crops including cultivars. However, by overlooking the operational limits of these rainfall-based methods, one can easily argue that the climate-related risk in agriculture is overestimated in the Southern BF. The operational limits of theses methods can be explained by the fact that rainfall-based methods underestimate the magnitude of crop water stress since they only focus on how to alleviate crop failure during the first stage of crop development without any care for further stages of crop growth. Thus, climate conditions, particularly water availability for crops after this first stage of development are not taking into

account to ensure that crops will reach the maturity with a low risk of damage due to water stress. Moreover, these methods are crop-generic. Thereby, arising the question of their relevance for farmers. In fact, farmers used to grow different crops with different agronomical information. In order to tackle these limitations, approaches involving crop models can contribute to derive optimal crop planting dates for a specific crop and a given region. For such approaches both the risk of crop failure and the efficiency of crop production have to be taken into account. To this end, an optimization technique can be apply to ensure that the computed planting dates yield high crop production.

Chapter 3

Data and Methods

3.1 Data

3.1.1 Climate observation and reanalysis data

Climate observation data have been collected from BF Directorate General of Meteorology (DGM). The database encompasses daily minimum and maximum temperature ($°C$) and daily precipitation (mm) for the period 1981-2010. Precipitation data are from 123 rain gauges while temperature data are from synoptic stations in BF (Figure 2.4). In the aim to calibrate the General Large-Area Model for annual crops (GLAM) for maize cropping in BF, European Centre for Medium-Range Weather Forecasts (ECMWF) Interim Re-Analysis (ERA-Interim) data (Dee et al., 2011) have been used. Data on a daily basis from January 1st, 1980 until December 31st, 2010 have been retrieved (available at http://data-portal.ecmwf.int/data/d/interim_daily/) The data encompass minimum and maximum temperature, and incoming shortwave radiation ($MJ\ m^{-2}\ day^{-1}$). A pre-processing of the ERA-Interim data was performed to fit the format, units and time scale required by the crop model. Further, observed precipitation data have been gridded at a resolution of $0.75° \times 0.75°$ (i.e. 51 grid points for the study area) and $0.44° \times 0.44°$ (i.e. 136 grid points for the study area) using Ordinary Kriging (OK). OK is one of the most commonly used method for interpolation. The number of rain gauges (123) was assumed to be acceptable for both $0.75° \times 0.75°$ and $0.44° \times 0.44°$ grid cell interpolation, using OK. The

anisotropy of rainfall variability was well captured. Figure 3.1 illustrates the gridded mean annual precipitation (1980-2010) (Figure 3.1a) as well as the error map (Figure 3.1b) at a resolution of $0.75° \times 0.75°$.

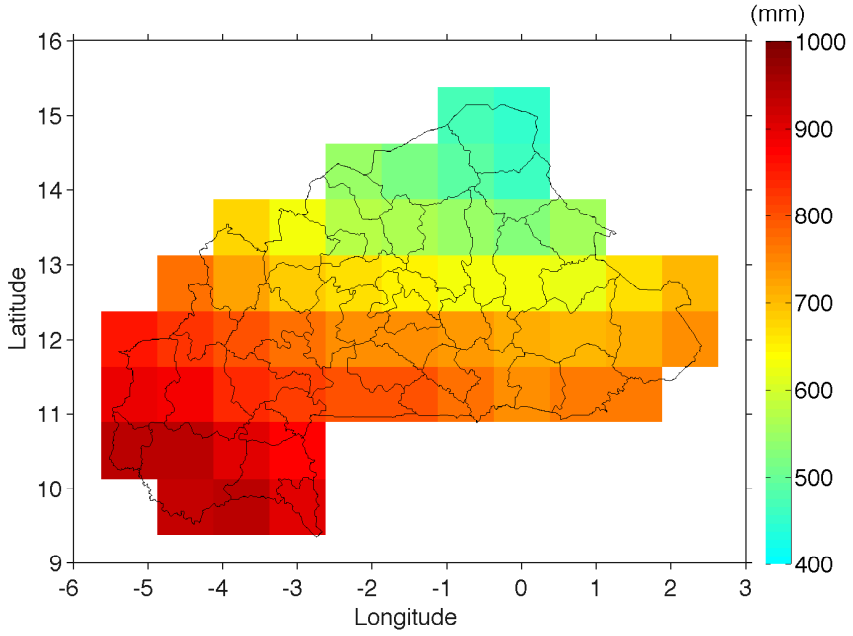

(a)

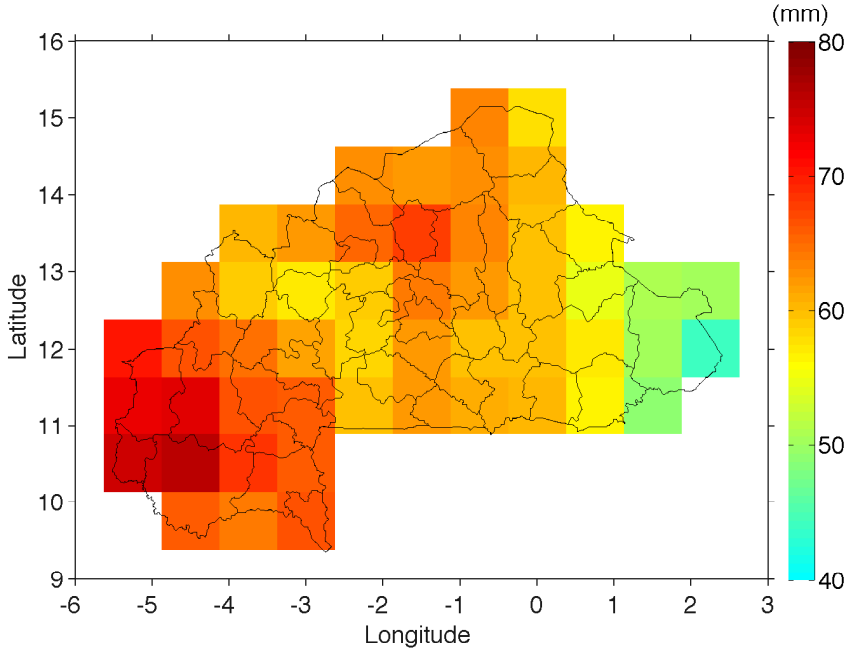

(b)

FIGURE 3.1: Spatial distribution of (a) gridded mean annual rainfall (1980-2010) and (b) gridded root mean squared error (RMSE). RMSE between annual rainfall of any station and its corresponding grid cell is calculated and interpolated using Ordinary Kriging.

3.1.2 Regional climate projections

Nested modeling (i.e. dynamic downscaling modeling) and empirical-statistical downscaling approaches are the most commonly used (Moriondo and Bindi, 2006) to derive climate data at finer scale. The first approach used global circulation models (GCMs) outputs to provide boundary conditions for RCMs which aim to produce regional climate data (Giorgi and Mearns, 1999, Jung and Kunstmann, 2007). The second approach combines assumptions and statistical techniques to downscale locale and regional climate variables from GCM outputs (Bárdossy, 1997). Theses approaches present certain limitations (Leung et al., 2003, Laprise et al., 2008) and they are sources of bias in RCM outputs, particularly regional climate change projection data which, in addition include biases from greenhouse gas (GHG) emission scenarios. However, because of the crucial role of climate models in the process of decision making, these approaches are intensively used to derived regional climate change data which are subsequently used for regional climate change impact studies.

The ongoing CORDEX project is using the nested modeling approach in combination with RCPs (Moss et al., 2008, 2010) to produce projected future climate data at regional scale for different regions worldwide. For instance, in the framework of CORDEX, the RCM group of Swedish Meteorological and Hydrological Institute (SMHI) has used the boundary conditions of eight GCMs (Table 3.1) from the Coupled Model Intercomparison Project - Phase 5 (CMIP5) to drive the latest version of the Rossby Centre Regional Climate Model - RCA4 over Africa domain (Jones et al., 2011, Nikulin et al., 2012). In this study, the SMHI CORDEX-Africa simulations have been used to drive GLAM model. Data at resolution of $0.44° \times 0.44°$, encompassing precipitation, solar shortwave radiation and minimum and maximum temperature on a daily basis have been retrieved from SMHI CORDEX-Africa database. Then, they have been processed and used as climate inputs in GLAM to simulate potential maize yields under future climate change scenarios. The dataset consists of control runs and projections based on the emission scenarios RCP4.5 and RCP8.5. RCP4.5 is a stabilization scenario in which total radiative forcing is stabilized shortly after 2100, without

overshooting the radiative forcing target level 4.5 W/m2 (≈ 650 ppm CO_2 eq) while RCP8.5 is a high emission scenario (i.e. increasing GHG emissions over time) corresponding to a rising radiative forcing pathway leading to 8.5 W/m2 (≈1370 ppm CO_2 eq) by 2100 (Detlef et al., 2009, Allison et al., 2011, Riahi et al., 2011). The retrieved data range from 1989 to 2008 for the CTRL and 2011 to 2050 for the two RCPs.

TABLE 3.1: RCMs and institution names and the corresponding labels used in this study.

RCM (GCM)	GCM's institution name (country)	Label
RCA4 (CanESM2)	CCCma (Canada)	CCCma
RCA4 (CNRM-CM5)	CNRM-CERFACS (France)	CNRM
RCA4 (EC-EARTH)	ICHEC (Europe)	ICHEC
RCA4 (MIROC5)	MIROC (Japan)	MIROC
RCA4 (HadGEM2-ES)	MOHC (UK)	MOHC
RCA4 (MPI-ESM-LR)	MPI-M (Germany)	MPI
RCA4 (NorESM1-M)	NCC (Norway)	NCC
RCA4 (GFDL-ESM2M)	NOAA-GFDL (USA)	NOAA

3.1.3 Soil data

Gridded soil types and their hydrological properties (soil water content at saturation, soil water content at field capacity and soil water content at wilting point) have been derived from Harmonized World Soil Data (HWSD), a 30 arc-second raster soil database (FAO, 1991) in combination with the translator library for raster data, GDAL (available at `http://www.gdal.org`) and a soil water content computation algorithm. First, based on the coordinates of climate data grid cells within the study area, the matching soil mapping unit is derived using GDAL. Then, from HWSD, all soil types at 30 arc-second resolution across BF (Figure 3.2) have been processed and further used to derived the dominant soil type for a given grid cell in the study domain.

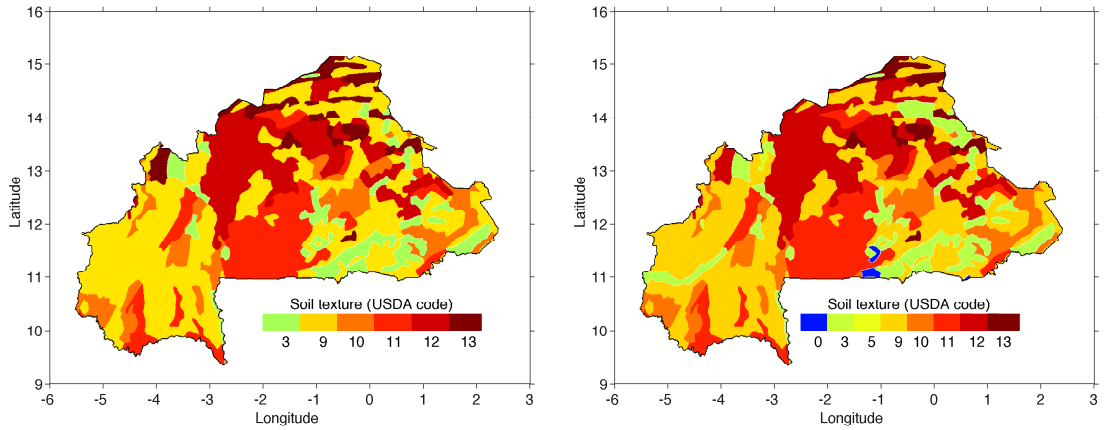

(a) Topsoil (0-30 cm) depth (b) Subsoil (30-100 cm) depth

FIGURE 3.2: Dominant soil texture for the topsoil (a) and the subsoil (b) in BF (data source: HSWD). Numbers refer to USDA soil texture classification. USDA soil codes denote: 0="water body", 3="clay", 5="clay loam", 9="loam", 10=" sandy clay loam", 11="sandy loam", 12=" loamy sand", 13="sand".

Finally, soil hydrological properties of the dominant soil types have been computed using soil properties database from HWSD and an algorithm designed to compute soil water limits (Ritchie et al., 1999, Suleiman and Ritchie, 2001). Figure 3.3 shows the dominant soil texture for the two spatial resolutions ($0.75° \times 0.75°$ and $0.75° \times 0.75°$) across BF.

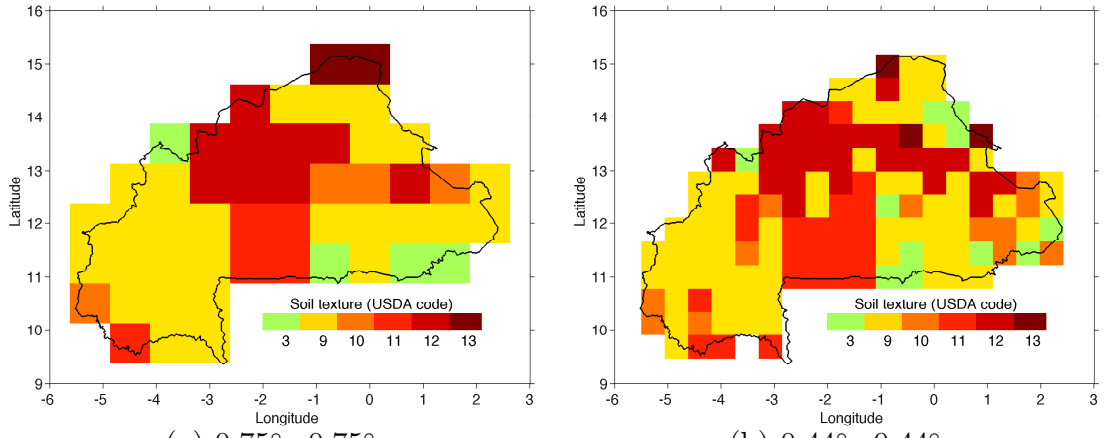

(a) $0.75°\times0.75°$ (b) $0.44°\times0.44°$

FIGURE 3.3: Dominant soil type at a resolutions of $0.75°\times0.75°$ (a) and $0.44°\times0.44°$ (b) over BF. USDA soil codes denote: 3="clay", 5="clay loam', 9="loam", 10=" sandy clay loam", 11="sandy loam", 12=" loamy sand", 13="sand".

3.1.4 Crop yield data

Maize yields on province-level from 2000 to 2010 are used to calibrate the crop model GLAM. Yield data were provided by AGRHYMET Regional Center and the BF National Agricultural Statistic Division. The dataset contains annual rainfed crop production and estimated land area allocated for maize cropping. Given a specific province and year, yield ($kg\ ha^{-1}$) has been computed as a ratio between crop production (kg) and cropping land area (ha). The period 2000-2010 has been selected after a quality analysis of data. The quality analysis is based on data providers experiences and data filtering. Data filtering is performed in two steps. First, from each of the two databases, only those years with a clear separation between rainfed and irrigated maize production have been selected. Then, for each selected year and province, the similarity in data (i.e. maize rainfed production and cropping land area) from the two databases has been checked in order to determine the matching time period which yields the lowest deviation. From this analysis, it is found that the difference between the two databases was less than 5% with no missing data for the period 2000-2010. After data filtering, a consistency analysis of data from the period 2000-2010 has benefited from the experience of data providers. Further, crop yields on a yearly basis, have been gridded at resolutions of $0.44° \times 0.44°$ and $0.75° \times 0.75°$ by using a composite weighted average for provinces that share the same grid cell (Eq.3.1). No detrending has been applied to the data since this period 2000-2010 presented no significant trend in maize yields.

$$Y_{grid}(\mathrm{kg\,ha^{-1}}) = \frac{\sum_{i=1}^{n} w_i \times Y_{district(i)}(\mathrm{kg\,ha^{-1}})}{\sum_{i=1}^{n} w_i} \tag{3.1}$$

where $Y_{grid}(\mathrm{kg\,ha^{-1}})$ is the gridded crop yield, $Y_{district(i)}$ is the crop yield in district i, w_i is the fraction of land area of district i within the grid cell and n is the number of grid cells which share the land area of the grid cell.

3.2 Methods

3.2.1 Large scale crop model GLAM

3.2.1.1 Introduction to crop modeling

Crop response to environment conditions is highly complex and non-linear. The complexity of the modeling approach varies from empirical relationships that describe how a few variables affect crop yield, to more process-based chemical and physical processes occurring during plant growth. In fact, besides the weather, crop yield is influenced by crop characteristics, management strategies, soil properties (i.e. texture and hydrological properties), fertilizers (especially nitrogen, phosphorus and potassium), pests and diseases pressures. Crop simulation models attempt to provide the equations which describe plant physiology and how these processes are affected by crop genotype, environment and farm management practices.

The development of dynamic crop growth models, which started more than thirty years ago, considerably improved existing analytic solution of problems in crop sciences. The first attempts of dynamic crop modeling were models developed to estimate light interception and photosynthesis in crop canopies (e.g. Loomis and Williams, 1963, de Wit, 1965). For instance, Loomis and Williams (1963) developed detailed model to simulate crop growth and yield in sugar beet (Fick et al., 1978).These simple models calculated the light profile in a canopy to assess the sensitivity of crop photosynthetic rates to sun angles, leaf angle distribution and latitudinal position of the crop. Estimation of crop growth and potential yield by accumulation of solar energy through biochemical and biophysical processes as biomass, its partitioning within the plant, completed the infancy phase of crop modeling (Wheeler et al., 2007). For such pioneer models the data requirements are fairly complex in terms of their logic and simulation processes of cropping systems interactions in relation to environment.

With the development of new technologies and advances in computer science, multidisciplinary approaches for modeling soil, water, plant genetics and physiological processes began. They have contributed substantially to modeling the complex

processes and interactions of factors responsible for estimating crop growth and production in response to several management practices. Some of the developments in the chronology were physicochemical measurement for crop microclimate, description of various subcomponents of carbon assimilation, and mimicking the phenology of the crop in the growing season, resulted in complex crop models which is known as process-based crop models such as CERES (Ritchi et al., 1998), SOYGRO (Wilkerson et al., 1985), APSIM (McCown et al., 1996), DSSAT (Jones et al., 1998), and CropSyst (Stöckle et al., 2003). The general mathematical form of such process-based crop model is:

$$\frac{dx}{dt} = f\left(p_1, p_2, w(t), m(t), x(t)\right), \tag{3.2}$$

where

t = time, which goes from 0 at planting to t_n at crop maturity,

$x(t)$ = vector of crop and soil state variables at time t,

$\frac{dx}{dt}$ = vector of rate of changes of the state variables at time t,

f = non-linear set of equations defining dynamic physiological, physical, and chemical processes in plant and soil state variables (it represents many equations of the different crops and soil processes),

p_1 = vector of crop cultivar-specific parameters of equations in f,

p_2 = vector of soil physical and chemical parameters of equations in f,

$w(t)$ = time-varying weather inputs to the model,

$m(t)$ = time-varying management inputs to the model.

Some of these process-based crop models are intensively used. For instance, DSSAT which has been developed to facilitate the application of crop models to agronomic research using a systems approach, has been in use since 1989. It incorporates models of more than 15 different crops with software that facilitates the evaluation and application of the crop models for different purposes. The model APSIM was developed to simulate biophysical processes in farming systems, in particular where there is interest in the economic and ecological outcomes of management practice in the face of climatic risk. It has been used in a broad range of applications, including support for on-farm decision-making, farming

systems design for production or resource management objectives, assessment of the value of seasonal climate forecasting, risk assessment for government policy making, and as a guide to research and education activity.

The development of these complex models was accompanied with the issue of input data to run the models. Indeed, as models became more complex, the number of parameters required to describe the system increased. Many coefficients are necessary to describe cultivar characteristics and estimate these coefficients included the inevitable experimental errors. Some parameters are included in models that could not be measured directly in experiments. These parameters are quantified by calibrating the whole model to achieve outputs that matched relevant observations. Besides the number of parameters for crops, there may be plenty of coefficients and parameters to be obtained for soils and the crop cultivars. A minimum data set of weather is also needed, it comprises rainfall, minimum and maximum temperatures and solar radiation (Wheeler et al., 2007).

In addition to the high demand of input data, the aforementioned process-based crop models are designed to work at plot scale. Therefore the use of these models with global or region climate model outputs is limited since it requires further assumptions and methods to upscale the plot scale information to a regional scale (e.g. Hoogenboom, 2000, Hansen and Jones, 2000, Folberth et al., 2012).

The improvement in the understanding of climate processes has strongly contributed to enhance substantially global and regional climate simulations and thereby enabling climate impact studies at global and regional scales. However, impact models are needed to perform impact studies and therefore to evaluate the potential impact of climate on development sectors such as agriculture. To this end, a new group of process-based crop models have been developed to assess crop production using global or regional climate outputs. These crop models are designed to work at the grid cell corresponding of those from climate models. However, it is known that the spatial scale of a mathematically one-dimensional crop model is defined by the level of detail and spatial aggregation of its input data requirements.

One main advantage of using large scale process-based crop models is that

they require a limited number of input data. In fact, the simulation of crop productivity over a large area needs some simplification of the crop simulation process. A complete set of field-scale inputs will not be readily available over areas of countries and regions, and the grid cell size will encompass spatial heterogeneity in parameters that describe soils, crop genotype and management practices. Thus, large scale crop models combine the benefits of more empirical modeling methods which require a low level of input data, with the benefits of a process-based approach, which have the potential to capture variability due to different sub-seasonal weather patterns, and hence increased their validity under different climates (e.g. Moen et al., 1994, Brock and Brink, 1996, Challinor et al., 2005, Tao et al., 2009). Amongst them, GLAM is designed to be sufficiently process-based to simulate crop productivity over a range of tropical environments, whilst being simple enough to avoid the need for large amounts of location-specific input data.

3.2.1.2 Description of GLAM

Challinor et al. (2004) designed GLAM to simulate the effects of short time-step events such as intra-seasonal variability in rainfall and high temperatures on the crop. GLAM demonstrated good forecasting skills of the model in a hindcast of the groundnut crop aggregated to all India for 1966-1990. As a process-based crop model, it simulates crop growth and development with daily time steps. This crop model operates on spatial scales commensurate with those of global and regional climate models. It can be used to assess the impacts of climate variability and change on annual crops yield. GLAM was initially calibrated and validated for groundnut production in India with possibilities to be applied to a large range of crops as the crop growth processes are generic. In water-limited crop production regions, GLAM has been shown to be able to capture the strong relationship between weather and crop production (Challinor et al., 2004). To simulate a crop growing season, GLAM requires mainly daily time series of precipitation, temperature, and radiation as weather inputs.

Crop growth and development is simulated from the planting date ($t = 0$) to the end of the growing season (t_n). The phenological stages of development depend on the crop and are controlled by the thermal time elapsed within a given development stage. Four phenological stages (i.e. vegetative growth, flowering, grain filling and maturity) are commonly used to describe maize (*Zea mays L.*) growth and development. The thermal time from crop emergence to maturity is specific to each crop. The duration of the different phenological stages strongly depend on the climate. Given a crop development stage in a specific location, the thermal time which is also called growing degree days (GDD) is given by:

$$GDD = \int_{t1}^{t2} (T_{eff} - T_b)\,\mathrm{d}t \tag{3.3}$$

where

t = time unit, which dt corresponds to a day,

$t1$ = starting day of a specific phenological stage,

$t2$ = last day of a specific phenological stage,

$t2 - t1$ = duration of a given phenological stage,

T_b = base temperature, below which crop development ceases,

T_{eff} = effective temperature, which is a function of base, optimum and maximum temperature.

In GLAM, for a specific development stage, daily mean temperature ($\bar{T}$) is used in combination with crop base (T_o), optimum (T_m) and maximum (T_m) temperature to compute the T_{eff} as follows:

$$T_{eff} = \begin{cases} \bar{T} & T_b \leq \bar{T} \leq T_o \\ T_o - (T_o - T_b)\left(\frac{\bar{T} - T_o}{T_m - T_o}\right) & T_o \leq \bar{T} \leq Tm \\ T_b & \bar{T} \geq T_m \ , \ \bar{T} \leq T_b \end{cases}$$

The growth of the crop leaf area is determined by a variable describing soil water stress and a parameter used to reduce leaf area index (LAI) from the physical value to an effective value which accounts for the mean effects of pests, diseases and non-optimal management. The daily fraction of accumulated above ground

biomass (AGB) is determined by:

$$AGB = \begin{cases} T_T \cdot \frac{E_T}{V} & \frac{E_T}{V} \leq E_{TN,max} \\ T_T \cdot E_{TN,max} & \frac{E_T}{V} \geq E_{TN,max} \end{cases}$$

where

T_T = actual rate of transpiration in $cm\ day^{-1}$

V = vapor pressure deficit

E_T = normalized transpiration efficiency in Pa

$E_{TN,max}$ = maximum transpiration efficiency in $g\ kg^{-1}$.

Transpiration (T_T) is determined by considering separately the limitations imposed by plant and soil structure (i.e. physiologically limited transpiration) and energy availability (i.e. energy-limited transpiration). The equation of Priestley and Taylor (1972) is used to estimate the energy-limited transpiration. The extinction coefficient is the key parameter in determining the energy available for transpiration. Thus, for a given day, the lowest transpiration from both estimated transpiration, is taken as the actual transpiration. It is important to mention that the actual transpiration is limited by water availability in the volume of the crop root system. E_T is the key parameter which links the water budget of the root system to biomass production.

The accumulated above-ground biomass is converted into crop yield using the harvest index when the harvest time is reached. Prior, the simulated daily transpiration and the crop transpiration efficiency parameter are used to compute the daily biomass rate from crop emergence to maturity. A harvest index rate parameter is used to increase the harvest index from 0 to a maximum value during the grain filling and maturity stages. Figure 3.4 shows the relational flowchart of GLAM.

The yield responses to e.g. fertilizer, plant population density, pest and diseases separately, have not been explicitly formulated in GLAM. Instead, a unique parameter called yield gap parameter (YGP), which is location specific, is used to take account of yield losses due to the mean effects of nutrient deficiency, non-optimal management, pest and diseases incidence. In GLAM, YGP acts as an

input data bias correction parameter. For any specific location, the YGP is optimized by minimizing the root mean squared error (RMSE) between simulated yields (using all defined values of YGP) and observed yields. For more details on the dynamic processes in GLAM, the reader is referred to Challinor et al. (2004).

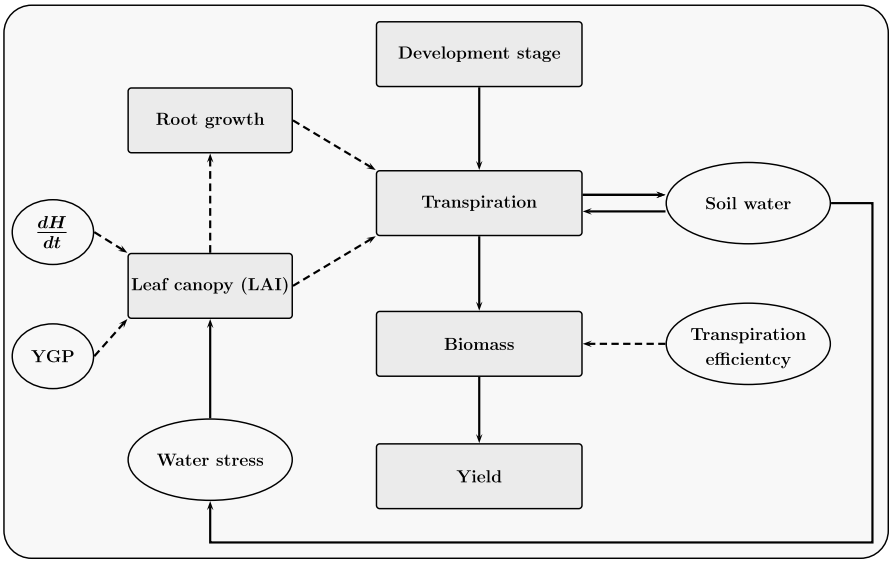

FIGURE 3.4: Relational flowchart of GLAM.

3.2.1.3 GLAM setup

GLAM requires daily weather values as inputs. Weather data encompass maximum and minimum temperature ($^{\circ}C$), precipitation ($mm\ day^{-1}$), and solar radiation ($MJ\ m^{-2}\ day^{-1}$). It also requires input parameters of crop physiological characteristics that control crop development, growth and yield in responses to weather, soil and management factors. GLAM uses these inputs to compute daily changes in the soil and crop state variables, such as LAI, phenological stage of development, above ground biomass and grain yields, which are also outputs from the model.

GLAM code is written in fortran 90 and it is designed to run in two modes: SET and HYP. The SET mode uses a single set of input parameters to simulate crop growth over a spatio-temporal domain while the HYP mode repeats the SET mode a number of times, varying one or more input parameters and producing information on skill for the varying parameters. A text file is used to indicate the path of all directories and files containing GLAM parameters and inputs data such as

weather, soil, management and crop yield data. Grid cells are coded and used subsequently to build input data files. For instance, for a given grid cell and year, ten digits (six and four digits to code grid cells locations and time step (a year), respectively) are used to name each weather file accordingly. Besides input data files, a unique parameter file is used to set up control parameters (e.g. type of season (rainfed or irrigation), the mode (SET or HYP), type of crop or cultivar, CO_2 scenario, output details and files format), crop-specific parameters (e.g. LAI parameters, biomass parameters, phenological parameters), management parameters (i.e. planting date), evapotranspiration parameters (e.g. evaporation coefficient, maximum evapotranspiration, vapor pressure deficit) and soil parameters (e.g. albedo, soil depth). The control options of YGP have to be set in the parameter file. For a specific location, running GLAM in mode HYP in combination with observed crop yield allow to output a YGP file which contains a local optimization of YGP. This file is needed for running GLAM in a SET mode. The different modules of GLAM are summarized in Figure 3.5.

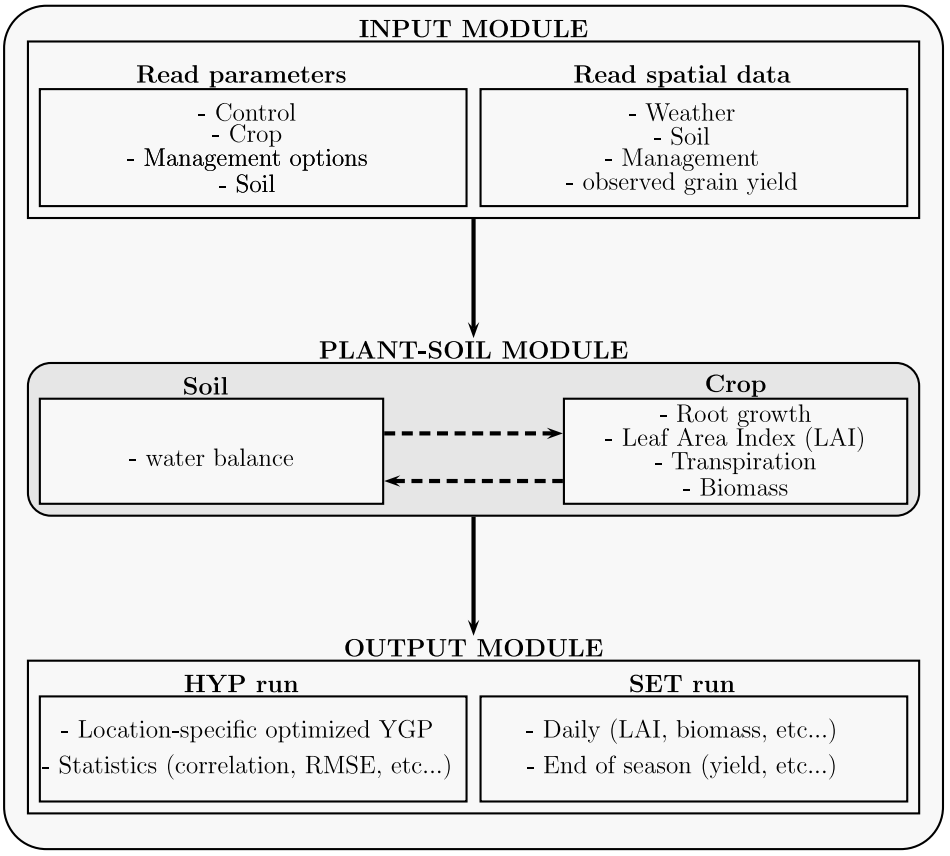

FIGURE 3.5: Simplified structure of GLAM code.

3.2.2 Fuzzy logic for crop planting date definition

3.2.2.1 Introduction to fuzzy logic

It is well known that classical logic is based on the assumptions that there are exactly two truth-values, *false* and *true* , and that the truth-value of any logical formula is uniquely defined by the truth-values of its components. Classical logic is closely connected with classical set theory. Each predicate is uniquely associated with a classical set. In other words, for any given object, a proposition formed by the predicate is true for this object if and only if the object is a member of the associated set. The associated set plays the role of the extension of the predicate. Classical sets deal with sets whose boundaries are crisp. Unfortunately, in the real world, not everything can be described using binary valued sets since the majority of decisions are made in a high level of uncertainty, complexity, or nonlinearity, particularly in environmental sciences. Thus, classical sets were simply not able to play the role of extensions of many-valued predicates, that is, predicates that apply to objects to intermediary degrees.

An alternative approach to classical logic arises from the fuzzy approach of Zadeh (1965), which starts with a truth-value function whose range is the interval from 0 to 1. This means that rather than being *true* or *false*, each proposition has a value which is supposed to provide a measure of its likelihood. Thus, instead of having worlds in which any proposition is *true* or *false*, we have worlds in which the proposition is more likely or less likely. The related discipline of fuzzy logic is proving itself as the most appropriate medium to deal with the need to represent knowledge in a manner that is both faithful to the human style of processing information as well as a form amenable to computer manipulation (Belohlavek and Klir, 2011). Rather than trying to define how things "really are", fuzzy logic accounts for the fact that things in the real world are not either this way or the other way, but most of the relevant properties are in fact gradual ones. Fuzzy logic can be viewed as a language that allows one to translate sophisticated statements from natural language into a mathematical formalism (Celikyilmaz and Türksen, 2009). The basic idea of fuzzy logic is to associate a number with each object indicating the degree to which it belongs to a particular class of objects.

Let X be the *universe of wet-day*, and A a set of elements *"extremely wet-day"* i.e. any day with more than 100 mm as rainfall amount. For classical set theory, it can be defined as follows:

$$A : \{x, m_A(x) = 1\}, m_A(x) = \begin{cases} 1, & x \in A \\ 0, & x \notin A \end{cases}$$

If instead $m_A \in [0, 1]$, we have a fuzzy set A. In this example, the weight of a member of the set "very wet-day" is set to 0 from classical logic point of view whereas it can be set to 0.5 or 0.9 depending on how we defined the membership function in the fuzzy set and also the closeness of the member's rainfall amount to 100 mm. But, it is obvious that a wet-day with 90 mm would produce a different output than a wet-day with 110 mm.

3.2.2.2 Fuzzy logic memberships

The function that associates a number with the object is called *membership function*. The notion of set membership is central to the representation of objects within a universe and to sets defined in the universe. Classical sets contain objects that satisfy precise properties of membership. Likewise, fuzzy sets contain objects that satisfy imprecise properties of membership, i.e. membership of an object in a fuzzy set can be approximate (Şen, 2010). In classical set theory this function is either 1 (the object is belong to the set) or 0 (the object doesn't belong to the set). This means that the membership in a set is binary: an element either is a member of a set or is not. In contrast, fuzzy set theory extended the notion of binary membership to accommodate various "degrees of membership" on the real continuous interval [0, 1], where the endpoints of 0 and 1 conform to no membership and full membership, respectively.

In fuzzy set theory, membership functions have been commonly formulated with straight lines, which are the idealized representations. In real life applications, membership values form scatter-clouds, which are then normalized into idealized shapes such as triangular, trapezoidal, or Gaussian membership functions. Zadeh (1965) argued that fuzzy set membership is the key to decision-making when faced

with linguistic and non random uncertainty.

Suppose that we are interested in classifying a given time series of wet-days in three categories, that is , " Wet", "Very wet" and "extremely wet". Membership functions can be defined to represents "the group of wet-day that can be considered to the wet", "the group of people that can be considered to the very wet" and the "group of people that can be considered to the extremely wet". Let *"Wet"*, *"Very wet"* and *"Extremely wet"* be the fuzzy set which is characterized by its membership functions $\mu_i(X)$ as:

$$\mu_i(x) : X \to [0\ 1], i \in \{"Wet", "Very\ wet", "Extremely\ wet"\}$$

One must decide what the membership function, denoted $\mu_i(x)$ should look like. Figure 3.6 represents a set of possible membership functions of the fuzzy sets " Wet", "Very wet" and "Extremely wet".

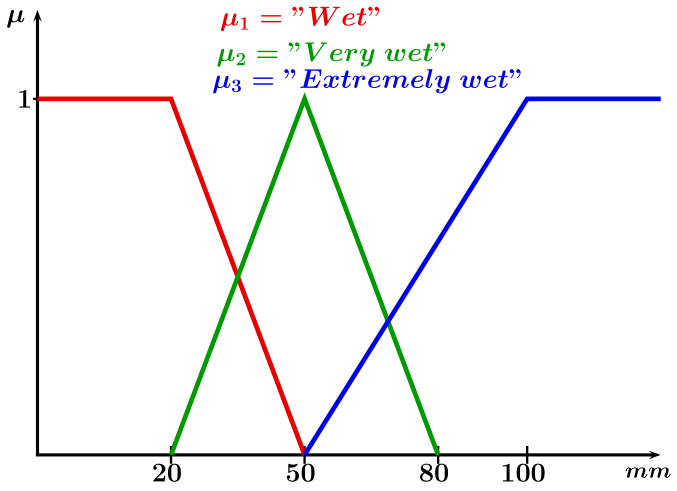

FIGURE 3.6: Membership functions of fuzzy sets "Wet" (red), "Very wet" (green) and "Extremely wet" (blue).

Since the membership value is a fraction between either 0.0 and 1.0 or 0.0 and -1.0, it is clear that one need to find a "defuzzification" method in order to get a non-fuzzy output value for the problem to be solve. Defuzzification is the mathematical process whereby a fuzzy membership function is reduced to a single scalar quantity that best summarizes the function, if a single scalar value is needed (Ross et al., 2002). Thus, one has to define the method that it makes sense for the particular problem. The fuzzy logic membership gives a way to formulate a problem in a

fuzzy sense, but not to deal with optimization problems which require the use of optimization techniques.

3.2.2.3 Fuzzy rule-based planting date definition

Wet conditions are needed to trigger planting activities. After planting, they are also crucial to avoid crop failure. Thus, suitable planting dates for a specific crop have to fulfill at least the following three criterions (Laux et al., 2008, Waongo et al., 2014):

(i) The seed bed must be wet enough for sowing and the water requirements for germination and emergence have to be met. This depends on the specific soil type and crop.

(ii) Prolonged dry spells have to be avoided during the first stage of crop development since crop is more vulnerable to water stress then. Severe water stress during the earlier stage of crop development may lead to crop failure and therefore requires resowing;

(iii) The length of the growing season has to fit with crop duration period in order to ensure sufficient water availability. This criterion is particularly important for water limited regions such as SSA and for crop with reduced water stress resistant such as maize. For instance, latest planting dates which alleviate the risk of prolonged water stress through the rainy season, increase the risk of getting a shorter growing season and might result in a significant loss of production or, even worse a total crop failure if the reproductive stage (i.e. grain filling for maize occurring within the dry season).

The first two criterions are defined to ensure crop germination and an optimum first stage development. During the first stage of crop development, the root system of the crop is still not well developed to cope with longer dry spells. Therefore, crop failure and resowing might be avoided if wet conditions during the first vegetative growth stage occur. To compute planting dates, rainfall-based methods use threshold values to formulate the first two criterions such as rainfall amount and the number of wet-day and dry-spell lengths, for a given period. However, the

uncertainties due to the limited number of observations and measurement errors have to be taken into account when dealing with hydro-meteorological variables, particularly precipitation. To cope with rainfall data uncertainties and the vagueness around the explicit value of these variables, a fuzzy logic based approach has been developed to define the planting date. This approach uses the concept of fuzzy logic membership functions to deal with the cumulative rainfall amount and the wet and dry spell lengths.

Three fuzzy membership functions γ_1, γ_2 and γ_3 for cumulative rainfall amount within a 5 day spell, the number of rainy days within a 5 day spell and the longest dry spell length in the next 30 days after the planting day, respectively, have been defined (Figure 3.7).

The variables a_1 and a_2 of the membership γ_1 vary between 10 and 30 mm, b_1 and b_2 of the membership γ_2 vary between 1 and 5 days and c_1 and c_2 of membership γ_3 vary between 5 and 10 days. The defuzzification parameter k varies between 0.1 and 1. Using a list of if-$then$ clauses, γ_1 is set to 0 is the five days cumulative rainfall is less than a_1 mm and 1 if the five days cumulative rainfall is greater or equal to a_2 mm. For a 5 day cumulative rainfall ranging between a_1 and a_2, the value of γ_1 is obtained by linear interpolation between a_1 and a_2. Similarly, γ_2 and γ_3 are computed based on their specific parameters.

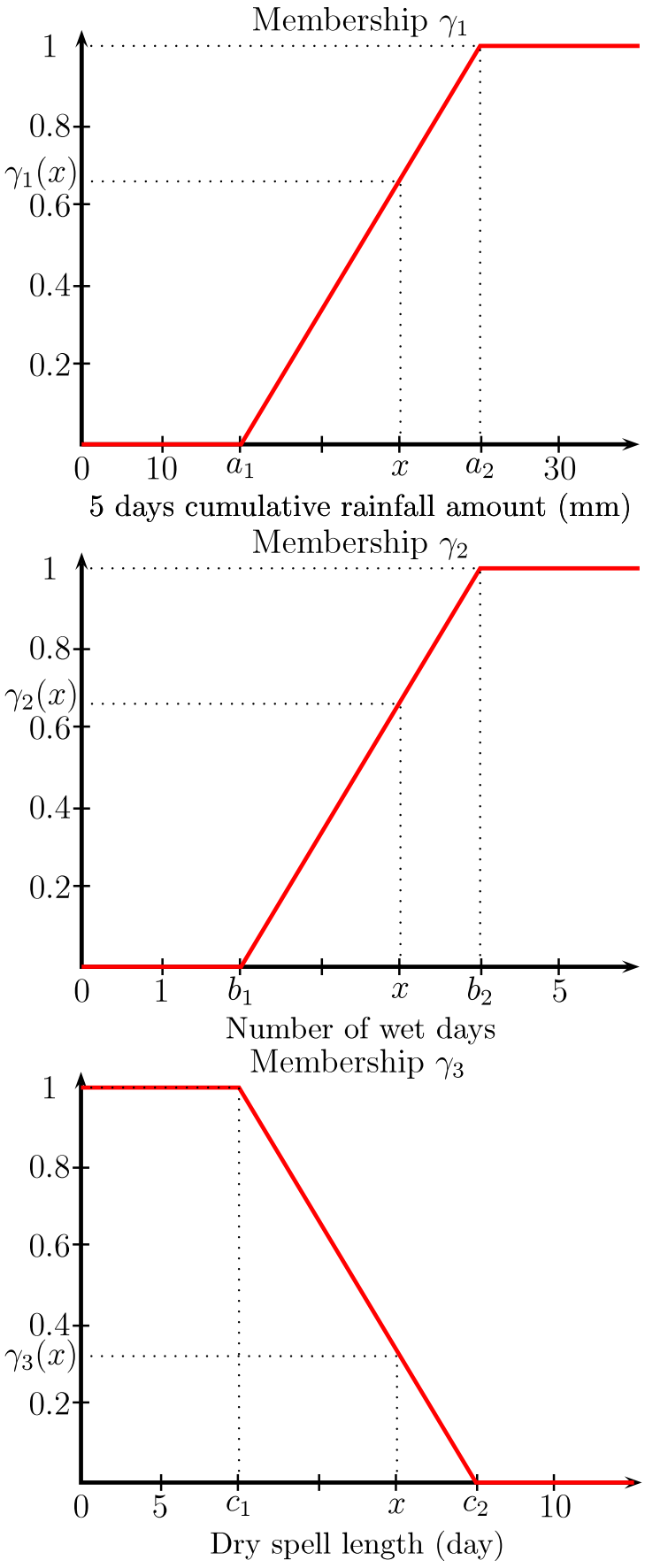

FIGURE 3.7: Fuzzy logic memberships of rainfall amount (top), number of wet days (middle) and dry spell length (bottom) (adapted from Waongo et al., 2014).

3.2.3 Genetic algorithm for planting date optimization

3.2.3.1 Introduction to optimization techniques

The basic principle of optimization is the efficient allocation of scarce resources. Optimization can be applied to any scientific or engineering discipline. An optimization problem may be defined by specifying (1) a set of all potential solutions to the problem and (2) a measure to evaluate the performance of each candidate solution with respect to the objective (Sivanandam and Deepa, 2008). The goal is to find a solution or a set of solutions that perform best with respect to the specified performance measure.

There exist no specific method, which solves all optimization problems. Indeed, the way in which an optimization method samples new candidate solutions and exploits the result of the evaluation of these new solutions limits the class of problems that the method can solve efficiently. For instance, using local operators in conventional search techniques, such as hill-climbing limits the applicability of the algorithm to problems that contain only a few basins of attraction, or problems where an approximate location of the global optimum is known in advance (Pham and Karaboga, 2000).

Optimization techniques can be divided in two major groups: classical optimization and advanced optimization techniques. Classical optimization techniques are useful in finding the optimum solution or unconstrained maxima or minima of continuous and differentiable functions. They are analytical methods and make use of differential calculus in locating the optimum solution. The classical methods have limited scope in practical applications as some of them involve objective functions which are not continuous and/or differentiable. These methods assume that the function is differentiable twice with respect to the design variables and the derivatives are continuous (Rao, 2009). Three main types of problems can be handled by the classical optimization techniques:

- single variable functions
- multivariable functions with no constraints

- multivariable functions with both equality and inequality constraints. In problems with equality constraints the Lagrange multiplier method (Bertseka, 1996) can be used. If the problem has inequality constraints, the Kuhn-Tucker (Kuhn and Tucker, 1951) conditions can be used to identify the optimum solution.

Numerical methods of optimization, such as linear programming, nonlinear programming, integer programming, quadratic programming, dynamic programming and stochastic programming are used to deal with some classical optimization problem. Unfortunately, for more complex nonlinear problems, classical optimization methods lead to a set of nonlinear simultaneous equations that may be difficult to solve. Despite of these limitations, classical techniques of optimization form a basis for developing most of the numerical techniques that have evolved into advanced techniques more suitable to today's practical problems. Hill climbing, simulated annealing, neural-network, ant colony optimization, fuzzy optimization and genetic algorithm, are some of the advanced optimization techniques pham2000. The majority of advanced optimization methods have been developed only in recent years and are emerging as popular methods for the solution of complex engineering problems. For most of them, only the objective function values (and not the derivatives) are required.

Hill climbing: This method is a graph search algorithm where the current path is extended with a successor node which is closer to the solution than the end of the current path. Hill climbing is used widely in artificial intelligence fields, for reaching a goal state from a starting node (Jiang et al., 2013). Choice of next node/starting node can be varied to give a number of related algorithms. The two forms (i.e. simple hill climbing and steepest ascent hill climbing) fail if there is no closer node. This may happen if there are local maxima in the search space which are not solutions.

Simulated annealing method: In simulated annealing method, each point of the search space is compared to a state of some physical system, and the function to be minimized is interpreted as the internal energy of the system

in that state (Yang, 2014). Therefore, the goal is to bring the system from an arbitrary initial state to a state with the minimum possible energy.

Ant colony optimization: It is based on the cooperative behavior of real ant colonies, which are able to find the shortest path from their nest to a food source (Xiao, 2013).

Fuzzy optimization methods: In many practical systems, the objective function, constraints, and the design data are known only in vague and linguistic terms (chun Tang et al., 2014). These methods have been developed for solving such problems.

Neural-network-based methods: In these methods, the problem is modeled as a network consisting of several neurons, and the network is trained suitably to solve the optimization problem efficiently (Khashman, 2011).

3.2.3.2 Genetics algorithm (GA)

A genetic algorithm is a directed random search technique, invented by Holland (1992), which can find the global optimal solution in complex multi-dimensional search spaces. In 1975, Holland developed this idea in his book "Adaptation in natural and artificial systems". He described how to apply the principles of natural evolution to optimization problems and built the first genetic algorithms. A genetic algorithm is modeled on natural evolution in that the operators it employs are inspired by the natural evolution process. These operators manipulate individuals in a population over several generations to improve their fitness gradually. Individuals in a population are similar to chromosomes and usually represented as strings of binary numbers. The basic elements of natural genetics are: reproduction, crossover, and mutation. Evolutionary computation techniques abstract these evolutionary principles in nature into algorithms that may be used to search for optimal solutions to a problem. Therefore, Genetic Algorithm optimization techniques (GAs) uses these natural evolution principles as genetic operators in the genetic search procedure. GAs differ from the traditional methods of optimization in the following respects (Rao, 2009):

1. A population of points (parameter set vectors) is used for starting the procedure instead of a single design point. If the number of parameters is n, usually the size of the population is taken as $2n$ to $4n$. Since several points are used as candidate solutions, GAs are less likely to get trapped at a local optimum.

2. GAs use only the values of the objective function. The derivatives are not used in the search procedure.

3. In GAs the parameters are represented as strings of binary parameters that correspond to the chromosomes in natural genetics. Thus, the search method is naturally applicable for solving discrete and integer programming problems. For continuous design variables, the string length can be varied to achieve any desired resolution.

4. The objective function value corresponding to a design vector plays the role of fitness in natural genetics.

5. In every new generation, a new set of strings is produced by using randomized parents selection and crossover from the old generation (old set of strings). Although randomized, GAs are not simple random search techniques. They efficiently explore the new combinations with the available knowledge to find a new generation with better fitness or objective function values.

3.2.3.3 Parameters in GA

The parameters to be optimized are usually represented in a string form since genetic operators are suitable for this type of representation. The reason for this method being popular is that the binary alphabet offers the maximum number of schemata per bit compared to other coding techniques. Thus, selected parameters for optimization are represented as strings of binary numbers, 0 and 1. More significantly, the method of representation has a major impact on the performance of the GA.

Let X_i be a selected parameter denoted by a four-bit string as **0 1 1 0**, its integer

(decimal equivalent) value will be (Eq. 3.4)

$$X_i = \underbrace{0\ 1\ 1\ 0}_{four-bit\ string} = \overbrace{0 \times 2^3 + 1 \times 2^2 + 1 \times 2^1 + 0 \times 2^0}^{Binary\ to\ decimal} = \underbrace{6}_{Decimal\ equivalent} \tag{3.4}$$

If each parameter $X_i,\ i = 1, 2, 3 \ldots, n$ is coded in a string of length q, the set of n parameters are represented using a string of total length $n \times q$.

For example, if a string of length 4 is used to represent each parameter, a total string of length 12 is used to describe a set of three parameters ($n = 3$). The following string of 12 binary digits denotes the vector of parameters ($x_1 = 5$, $x_2 = 13$, $x_3 = 9$):

$$\overbrace{\underbrace{0\ 1\ 0\ 1}_{x_1=5}\ \underbrace{1\ 1\ 0\ 1}_{x_2=13}\ \underbrace{1\ 0\ 0\ 1}_{x_3=9}}^{String\ of\ length\ 12=\text{"}Chromosome\text{"}}$$

If a parameter X (whose bounds are given by a and b $(a < b)$) is represented by a string of q binary numbers. The decimal value of X can be computed as shown in the below formula:

$$X = a + \frac{b-a}{2^q - 1} \sum_{i=0}^{q-1} (2^i \times b_i)\ ;\ b_i \in \{0, 1\};\ i\text{=bit's position from the right to the left}$$

3.2.3.4 Fitness function and constraints in GA

Since GAs are based on the survival-of-the-fittest principle of nature, they try to maximize a function called the fitness function (Sivanandam and Deepa, 2008). Thus GAs are naturally suitable for solving unconstrained maximization problems. The fitness function, $F(x)$, can be taken to be same as the objective function f(x) of an unconstrained maximization problem so that $F(x) = f(x)$. A minimization problem can be transformed into a maximization problem before applying the GAs. Usually the fitness function is chosen to be nonnegative. The commonly used transformation to convert an unconstrained minimization problem to a fitness function is given by:

$$F(x) = \frac{1}{1 + f(x)}$$

For optimization with constraints $g_i,\ i \in \{1 \ldots n\}$, $F(x)$ can be expressed for

instance as follows:

Maximize$(F(x))$ subject to $\mathbf{g_i(x)} \leq \mathbf{0}$, $i = 1, 2, \ldots, n$ with g_i as a constraint function.

3.2.3.5 Genetic operators and computation process

The choice of operators depends on the problem and the representation scheme employed for the population. For instance, operators designed for binary strings cannot be directly used on strings coded with integers or real numbers. However, there are three common genetic operators: reproduction or selection, crossover and mutation. These operators are inspired by nature. The population in this context is all possible combination of parameters, which have been selected for optimization. The details of the three operations of GAs are given below.

Reproduction: it is the first operation applied to the population to select good strings (set of parameters) of the population to form a mating pool. The reproduction operator is also called the selection operator because it selects good strings of the population. The reproduction operator is used to pick above-average strings from the current population and insert their multiple copies in the mating pool based on a probabilistic procedure. In a commonly used reproduction operator, a string is selected from the mating pool with a probability proportional to its fitness. Thus if F_i denotes the fitness of the ith string in the population of size n, the probability (p_i) for selecting the ith string for the mating pool is given by:

$$p_i = \frac{F_i}{\sum_{j=1}^{n} F_j} \quad , i = 1, 2 \ldots, n$$

These probabilities are used to determine the cumulative probability (P_i) of string i being copied to the mating pool , by adding the individual probabilities of strings 1 through i as follows:

$$P_i = \sum_{j=1}^{i} p_j$$

By this process, the string with a higher (lower) fitness value will be selected more (less) frequently to the mating pool because it has a larger (smaller) range of

cumulative probability. Thus strings with high fitness values in the population, probabilistically, get more copies in the mating pool. The reproduction stage ensures that highly fit individuals (strings or better solution/value of parameters) live and reproduce, and less fit individuals (strings or non suitable solution/value of parameters) die, thereby simulating the principle of "survival-of-the-fittest" of nature.

Crossover: after reproduction, the crossover operator is implemented. The purpose of crossover is to create new strings by exchanging information among strings of the mating pool. Many crossover operators have been used in the literature of GAs. In most crossover operators, two individual strings are picked (or selected) at random from the mating pool generated by the reproduction operator and some portions of the strings are exchanged between the strings. In the commonly used process, known as a single-point crossover operator, a crossover site is selected at random along the string length, and the binary digits (alleles) lying on the right side of the crossover site are swapped (exchanged) between the two strings. The two strings selected for participation in the crossover operators are known as parent strings and the strings generated by the crossover operator are known as child strings (i.e. offsprings).

For example, if two set of parameters (parents or potential solution), each with a string length of 12, are given by

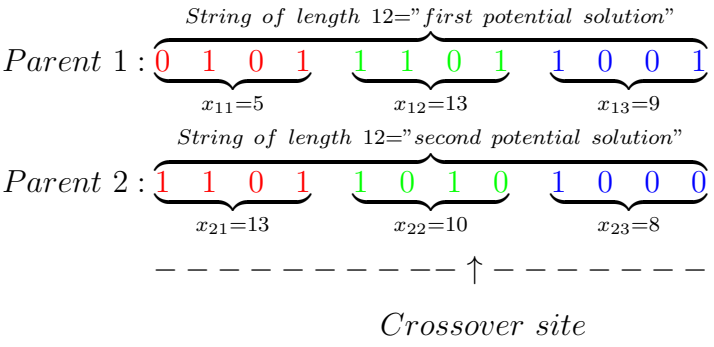

The result after a *single-point* crossover is given by:

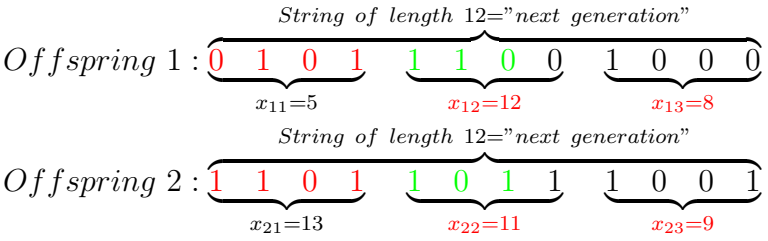

Mutation: the crossover is the main operator by which new strings with better fitness values are created for the new generations. The mutation operator is applied to the new strings with a specific small mutation probability, p_m. The probabilities are expected to be low, since high values may cause strong disruption of promising solutions. The mutation operator changes the binary digit 1 to 0 and vice versa. There are two main types of mutation operators: the standard jump-mutation that acts on the chromosome, sometimes called genotype, and creep-mutation that acts on the decoded individual, sometimes called phenotype. The jump-mutation involves altering only a single gene of a selected member of the population. For instance, when the jump mutation operator acts on one point which is called "single-point mutation", a mutation site is selected at random along the string length and the binary digit at that site is then changed from 1 to 0 or 0 to 1 with a probability of p_m. The creep-mutation operator changes a single individual in a way similar to the jump-mutation operator, but changes each chromosome in small increments rather than drastically changing a single chromosome. The purpose of mutation is (1) to generate a string in the neighborhood of the current string, thereby accomplishing a local search around the current solution, (2) to safeguard against a premature loss of important genetic material at a particular position, and (3) to maintain diversity in the population.

As an example, consider the precedent offsprings and suppose that the "offspring 1" is the one affected by the mutation processes (here a jump-mutation at a single point):

$$Offspring\ 1: \underbrace{0\ \ 1\ \ 0\ \ 1}_{x_{11}=5}\ \ \underbrace{1\ \ 1\ \ 0\ \ 0}_{x_{12}=12}\ \ \underbrace{1\ \ 0\ \ 0\ \ 0}_{x_{13}=8}$$

$$\uparrow$$

Mutation bit (*bit in position* 3 *from the left to the right*)

The result after a *single-point* jump-mutation in this pool of two offsprings is as follows:

$$Offspring\ 1_m: \overbrace{\underbrace{0\ \ 1\ \ 1\ \ 1}_{x_{11}=7}\ \ \underbrace{1\ \ 1\ \ 0\ \ 0}_{x_{12}=12}\ \ \underbrace{1\ \ 0\ \ 0\ \ 0}_{x_{13}=8}}^{String\ of\ length\ 12=\text{"}next\ generation\text{"}}$$

$$Offspring\ 2_m: \overbrace{\underbrace{1\ \ 1\ \ 0\ \ 1}_{x_{21}=13}\ \ \underbrace{1\ \ 0\ \ 1\ \ 1}_{x_{22}=11}\ \ \underbrace{1\ \ 0\ \ 0\ \ 1}_{x_{23}=9}}^{String\ of\ length\ 12=\text{"}next\ generation\text{"}}$$

There is no change observed in *offspring 2* after the mutation since it wasn't affected by the mutation (i.e. $Offspring\ 2_m = Offspring\ 2$) . However, due to the mutation, the value of x_{11} in *offspring 1* changes from 5 to 11, thereby yielding a new individual (i.e. $Offspring\ 1_m \neq Offspring\ 1$).

The solution of an optimization problem by GAs starts with a population of random strings of potential solutions (a matrix of a combinations of parameters). The population size (n) in GAs is usually fixed. Each string is evaluated to find its fitness value. Then, the population is operated by three operators (i.e. reproduction, crossover, and mutation) to produce a new population of parameters. The new population is further evaluated to find the fitness values and tested for the convergence of the process. One cycle of reproduction, crossover, and mutation and the evaluation of the fitness values is known as a generation in GAs. If the convergence criterion is not satisfied, the population is iteratively operated by the three operators and the resulting new population is evaluated for the fitness values. The procedure is continued through several generations until the convergence criterion is satisfied and the process is terminated. A concise flowchart of computation steps of GAs are given in Figure 3.8.

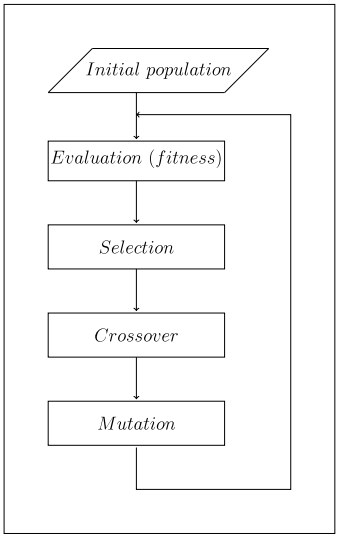

FIGURE 3.8: Flowchart of a basic genetic algorithm.

3.2.4 GLAM model calibration

The calibration of GLAM follows the procedure of Waongo et al. (2014). GLAM has been calibrated for maize in Burkina Faso using a genetic algorithm optimization method. The capability of GAs to approach (and eventually to find) the global optimum in an optimization problem is based on the choice of reproduction operators, their appropriate representation and the formulation of the objective function. The latter is specific to the problem that one is dealing with in terms of the objective to be reached.

In this thesis, the first step in the implementation of the genetic algorithm is to generate an initial population which consists of random selections of potential solutions in the parameter space. A binary encoding is used to encode each member of the population as a binary string of length $p \times 2^n$, where p denotes the number of parameters to be calibrated in the GLAM model and n denotes the number of bits (2^n is the number of possible values for a given parameter) (Carroll, 1996a,b). In GLAM, a total number of 32 parameters have been calibrated for maize for 85-100 days of growing period representing the most dominant group of maize cultivars in BF (Sanon and Dembélé, 2001): phenology parameters (base temperature, optimum temperature, maximum temperature, growing degree days GDD), biomass parameters (temperature efficiency TE, harvest index, maximum value

of normalized TE), evapotranspiration parameters (evaporation coefficient, maximum value of potential transpiration, vapor pressure deficit, soil heat flux coefficient), LAI parameters (critical LAI, daily maximum value of LAI, extinction coefficient, soil water fraction for reduced LAI growth), drainage and uptake parameters (uptake diffusion coefficient, root length density), and soil parameters (albedo, depth of soil over which evaporation occurs, extractable front velocity).

The GDD range for each crop development stage is crucial for the simulation, since the crop phenology and growing period heavily depend on it. To deal with the GDD variability in the target area, the $85-100$ days growing period of maize crop have been transformed in GDD considering four maize growth stages (vegetative growth, flowering, grain filling and maturity). The range of GDD for each development stage has been computed using daily mean temperatures for the target area and crop phenological base temperatures (T_B). T_B is chosen to be in the range of $8-14$°C (Birch et al., 1998). The GDD have been calculated for each grid cell and for each crop development stage. Then, the computation of the GDD mean value (GDD_m) and GDD standard deviation (GDD_{std}) for each development stage is performed over the target area. Finally, assuming a normal distribution, a GDD ranging from $GDD_m - 2 \times GDD_{std}$ to $GDD_m + 2 \times GDD_{std}$ is set for each development stage of maize crop. For the other parameters, the selected range has been taken from GLAM generic parameters file (`http:/www.see.leeds.ac.uk/research/icas/climate_change/glam/glam.html`) and from the literature (Carberry et al., 1989, Muchow and Carberry, 1989, Carberry, 1991, Birch, 1996, Maddonni and Otegui, 1996, Birch et al., 1998, Rasse et al., 2000, Sanon and Dembélé, 2001, Sanon et al., 2002).

In addition to the 32 parameters, planting dates are needed to perform crop simulations with GLAM. Planting dates can be set for simulation in two different ways. Either observed planting dates or computed planting dates can be used as input to GLAM. Observed planting date data are usually not available for large scale analysis in SSA. Therefore, estimated planting dates have been used. To estimate planting dates, the GLAM intrinsic function can be employed. For GLAM calibration purposes, the GLAM intrinsic function has been replaced by a

crop specific soil water balance module for planting date computation. This water balance module uses the water balance module of GLAM. It computes daily soil water balance for the first vegetative growth phase of maize crop, considering daily rainfall, soil characteristics and simulated maize daily actual evapotranspiration. After 1st May, crop specific soil water balance have been computed on daily basis. The estimated planting date is set to be the first day between 1st May and before 31st July for which the crop specific soil water balance is greater than zero for each day in the following 30 days. The planting date is set to 31st July if no planting date is found in the aforementioned period. This soil water balance algorithm should mimic the traditional planting behavior of smallholder farmers in SSA. The resulting planting dates are not optimal in terms of crop yield. Indeed, they have the potential to avoid crop failure but, not to reach optimum crop yield. These dates are used as planting dates for the calibration of GLAM.

The different steps in the process of GLAM calibration for maize crop using a GA have been summarized in Figure 3.9. For optimization purposes, the objective function in the GA has been formulated in a way such that it captures the degree of coincidence between simulated and observed maize yield for the calibration period. In addition, the variability in YGP is part of the objective function. For a specific location, it is assumed that the best setting of parameters in GLAM for the target grid cell should result in a high positive correlation r, and a low $RMSE$, and low variability in YGP. A k-fold cross validation is used to overcome the limited size of the calibration period (2000-2010). To ensure robustness of the calibrated parameters and to reduce the computation time, the value of k is set to five in this study. In the process of 5-fold cross validation, the 11 year-period data is randomly partitioned into five complementary subsets (one subset of three years and four subsets of two years). Out of five, four randomly chosen subsets are used as training sets and the remaining subset is used for validation. 50 loops (10 *initializations* $\times$ 5 *combinations of training/ validation sets*) of cross-validation are performed. Finally, an average over loops is used to compute r and $RMSE$. The minimum and the maximum of YGP over all loops is retained. Thus, for each setting of parameters in GLAM, a fitness value is computed after

the 5-fold cross validation. The highest fitness value should correspond to the best set of parameters. To fulfill these requirements, the fitness function is defined as:

$$f(.) = r \times (1 - rRMSE) \times (\frac{YGP_{min}}{YGP_{max}}), \tag{3.5}$$

where r denotes the Pearson correlation coefficient between simulated yield and observed yield, $rRMSE$ is the relative Root Mean Square Error, and YGP_{min} and YGP_{max} denote the minimum (maximum) value of (YGP).

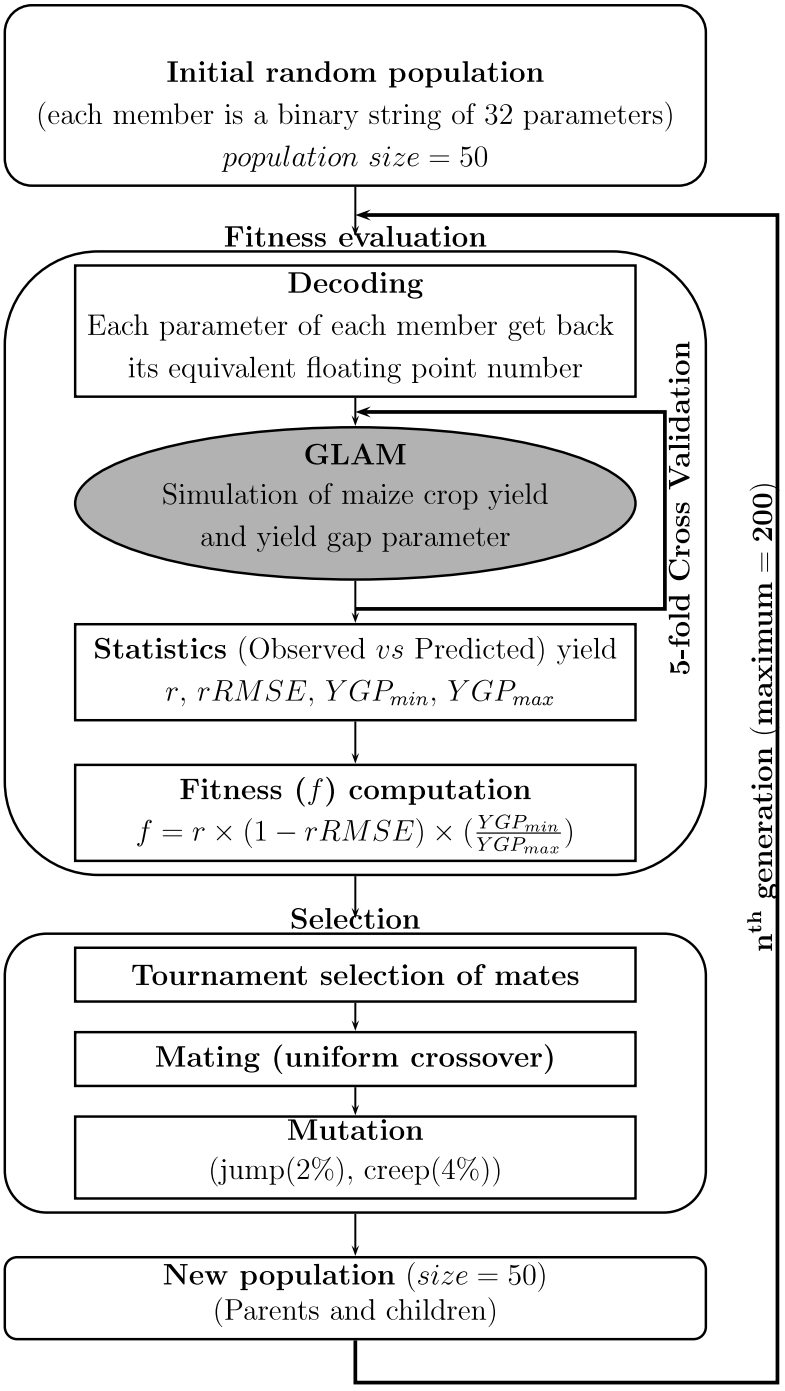

FIGURE 3.9: Flowchart of GLAM calibration for maize crop using a genetic algorithm (adapted from Waongo et al., 2014).

3.2.5 Computation of Optimized Planting Dates (OPDs)

The computation of Optimized Planting Dates (OPDs) follows the procedure of Waongo et al. (2014). GAs coupled with the fuzzy logic memberships for planting date and the calibrated GLAM has been used to derive ten ensemble members which are composed of optimized sets of fuzzy parameters (a_1, a_2, b_1, b_2, c_1, c_2, k). The flowchart of the respective process is illustrated in Figure 3.10. The optimized fuzzy parameters are crop and location specific. For the optimization process, a fitness function is defined to discriminate the different sets of parameters in terms of performance. The objective is to optimize planting dates so that they increase crop production and also reduce the variability at the same time. Therefore, the fitness function is defined as:

$$f(.) = \bar{Y}_{sim}^{(1-CV)}, \tag{3.6}$$

where CV is the coefficient of variation in crop yield, $\bar{Y}_{sim}$ is the mean value of the simulated crop yield.

For a specific location, the optimization process yielded a set of optimum fuzzy parameters. From this set, an ensemble of ten members is retained. The ten ensemble members consist of parameter sets which result in high crop yields and low variability of simulated crop yield (i.e. higher fitness) over time.

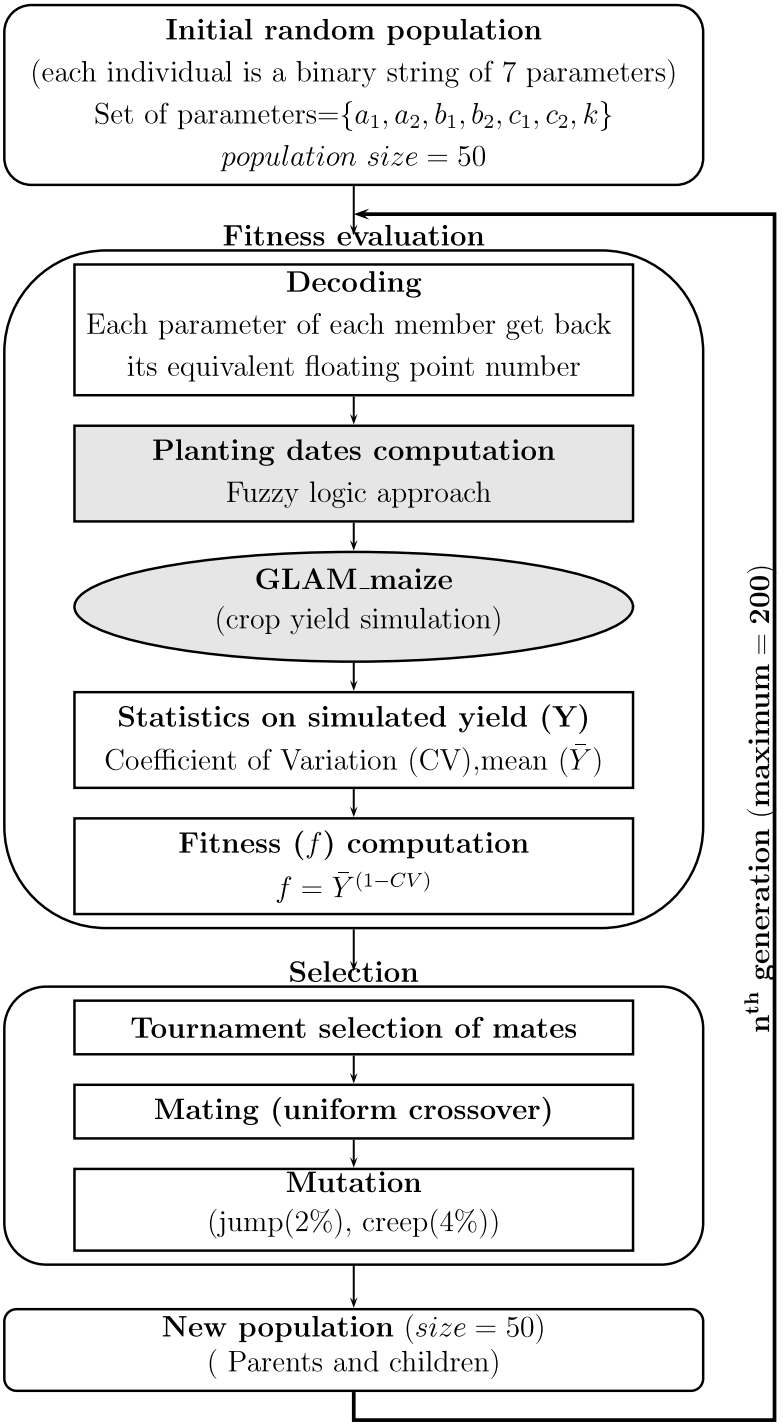

FIGURE 3.10: Flowchart of planting dates optimization using a genetic algorithm (adapted from Waongo et al., 2014).

Using a time series of rainfall of a specific grid cell with the ensemble of optimized fuzzy parameter sets, an ensemble of optimized planting dates for maize has been computed by applying the algorithm of the fuzzy rule-based planting date. The flowchart in Figure 3.11 illustrates the individual steps.

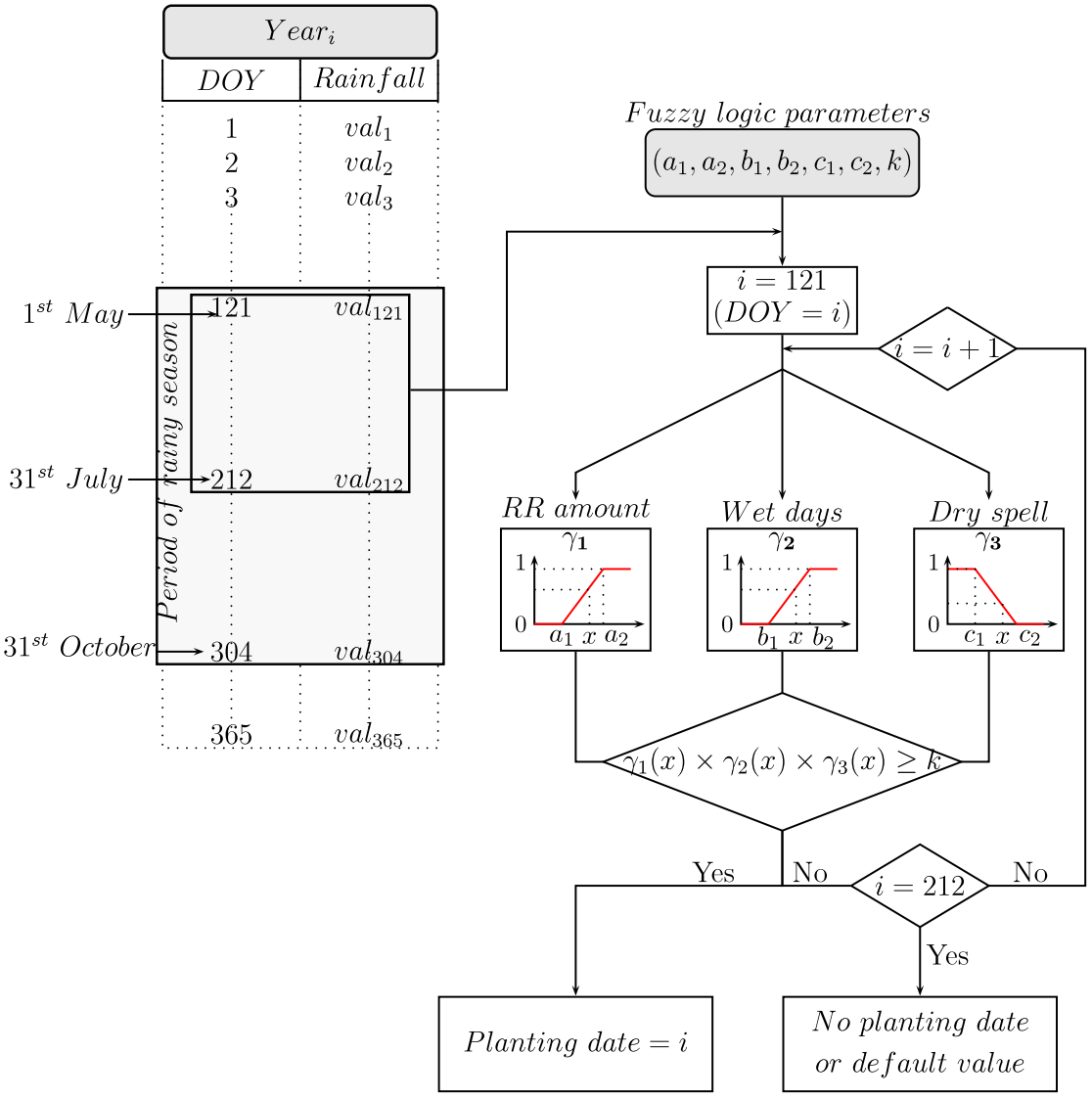

FIGURE 3.11: Flowchart of planting dates computation based on daily rainfall and the optimized fuzzy logic parameters (adapted from Waongo et al., 2014). The box spanning the period between May 1st and July 31st represents the potential crop planting window within the rainy season (May 1st- October 31st) in SSA.

In order to evaluate the efficiency of the OPDs, two state-of-the-art and regionally established approaches have been used to calculate planting dates for comparison. These two approaches are as follows:

1. Diallo (2001): *The date after 1st May, when rainfall accumulated over 3 consecutive days is at least 20 mm and when no dry spell of more than 10 days occurs within the next 30 days.* This approach is currently used at AGRHYMET Regional Center in Niamey (Niger).

2. Dodd and Jolliffe (2001): *The first day of a spell of 5 days in which at least 25 mm of rain falls, on condition that no dry period of more than 7 days occurs in the following 30 days.* This approach is currently in operation as an agricultural decision support tool at the BF Directorate General of Meteorology.

A deviation of planting dates and a relative deviation of maize mean yield are used to compare the different approaches. The deviation of planting date (D_{PD}) is calculated as:

$$D_{PD}\,(days) = OPD - P_D \tag{3.7}$$

where P_D are the planting dates either based on Diallo (2001) or Dodd and Jolliffe (2001).
The relative deviation of mean maize yields (D_{yield}) is given as:

$$D_{yield}\,(\%) = 100 \times \frac{(YIELD_{OPD} - YIELD)}{YIELD} \tag{3.8}$$

where $YIELD$ is the mean yield either based on Diallo (2001) or Dodd and Jolliffe (2001), $YIELD_{OPD}$ is the mean yield based on OPD.

3.2.6 OPDs impact on maize production under climate change

3.2.6.1 RCMs control run analysis

Regional climate models usually have significant biases for precipitation, particularly in WA (Cook and Vizy, 2006, Kim et al., 2014). For decision making support, it is essential to characterize their accuracies. To this end, the bias of temperature and precipitation is analysed for the RCM control runs for the whole BF and the three agroecological zones (AEZs) separately. The AEZs are defined on the basis of climatic zones described by Sivakumar and Gnoumou (1987) and a 30-yr mean annual rainfall distribution as follows:

(i) "North", which corresponds to the region where the mean annual rainfall is less than 600 mm and located in the North of BF. This region corresponds roughly to the sahelian zone and includes three synoptic stations;

(ii) "South", which corresponds to the region where the mean annual rainfall is more than 900 mm and is located in the South-West of BF. This region corresponds roughly to the South soudanian zone and includes four synoptic stations;

(iii) "Centre", which corresponds to the transition zone between North and South. The mean annual rainfall is more than 600 mm and less than 900 mm. This region corresponds roughly to the Centre-North soudanian zone and includes three synoptic stations.

For each AEZ, the cycles of temperature and precipitation from the RCM control runs are analyzed at monthly and seasonal (May-October) time scales. Synoptic stations per AEZ are thereby compared to their corresponding grid cells. In addition, the Taylor diagram is plotted for temperature and precipitation to draw conclusions about how well the RCMs control runs match the corresponding observations from synoptic stations in terms of correlation, root-mean-square difference (RMSD) and ratio of variances (Taylor, 2001). Taylor diagrams provide a way to summarize how closely climate model simulations match the observations. To this

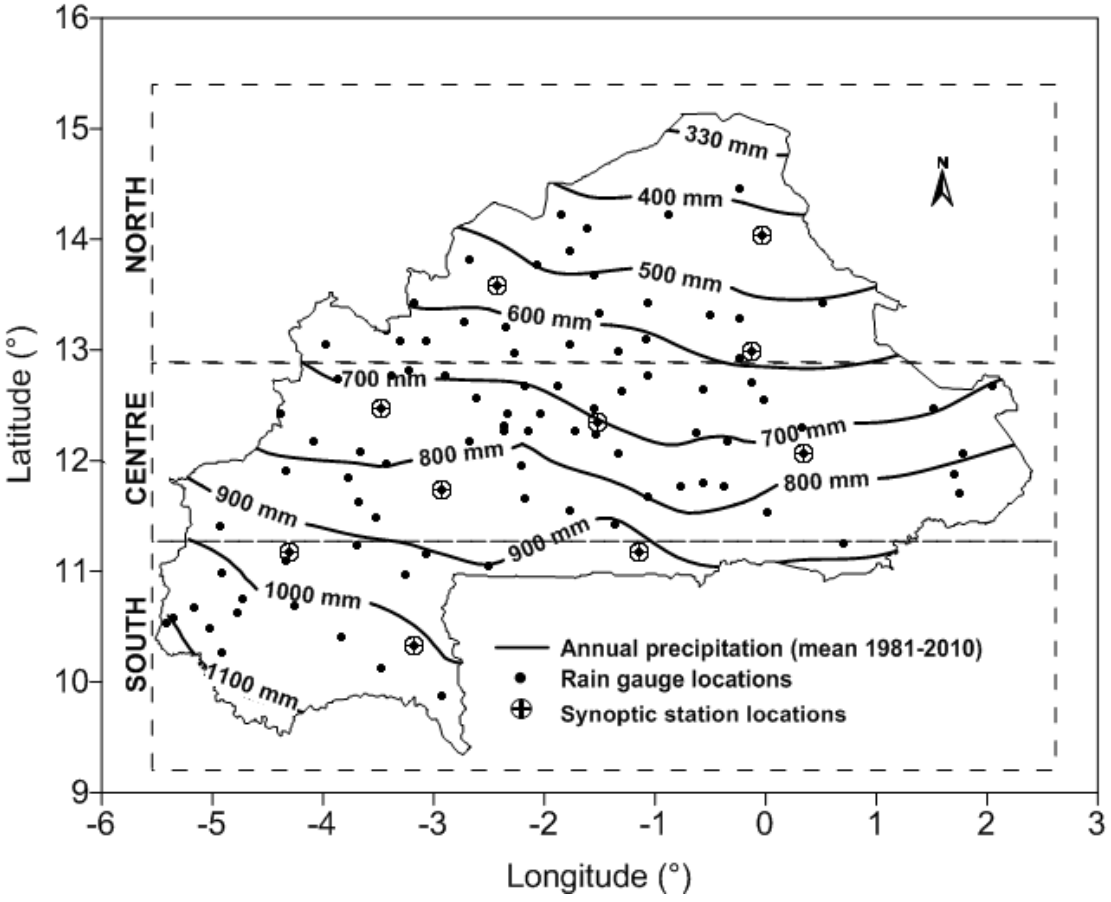

FIGURE 3.12: Mean annual precipitation (30-yr mean isohyets). Precipitation interpolation has been performed using an ordinary krigging (OK) method. The dotted Boxes represent roughly the three agroecological zones (North, Centre, South) across BF.

end, climate data for the period 1989-2008 from synoptic stations and RCMs grids cells matching the synoptic station locations have been used for the computation.

3.2.6.2 Maize yield simulation under climate change

One of the most popular methods for estimating the impacts of climate change on agriculture relies on crop models. First, the crop model is calibrated for a specific crop and selected region. Then, different climate change scenarios are run for each region given a particular management practice. Likewise, in this study, maize yield is simulated using the calibrated GLAM, climate data from eight RCMs and two planting date options. The simulations are performed for each RCM using CTRL, RCP4.5 and RCP8.5 data. This results in eight crop yield simulations for CTRL and 32 crop yield projections. The planting date

approaches of Diallo (2001) and Waongo et al. (2014) are used as management strategies. In this study, unlike the approach of Diallo (2001), Waongo et al. (2014) computes planting dates for climate change simulations in two steps. First, optimized location-specific planting rules are derived using a GA, the calibrated GLAM, observed climate data for the period 1989-2008 and the OPD approach. Second, the optimized location-specific planting rules are used in combination with the RCMs data to estimate future OPDs. The simplified steps in the process of potential maize yield simulations under climate change are shown in Figure 3.13.

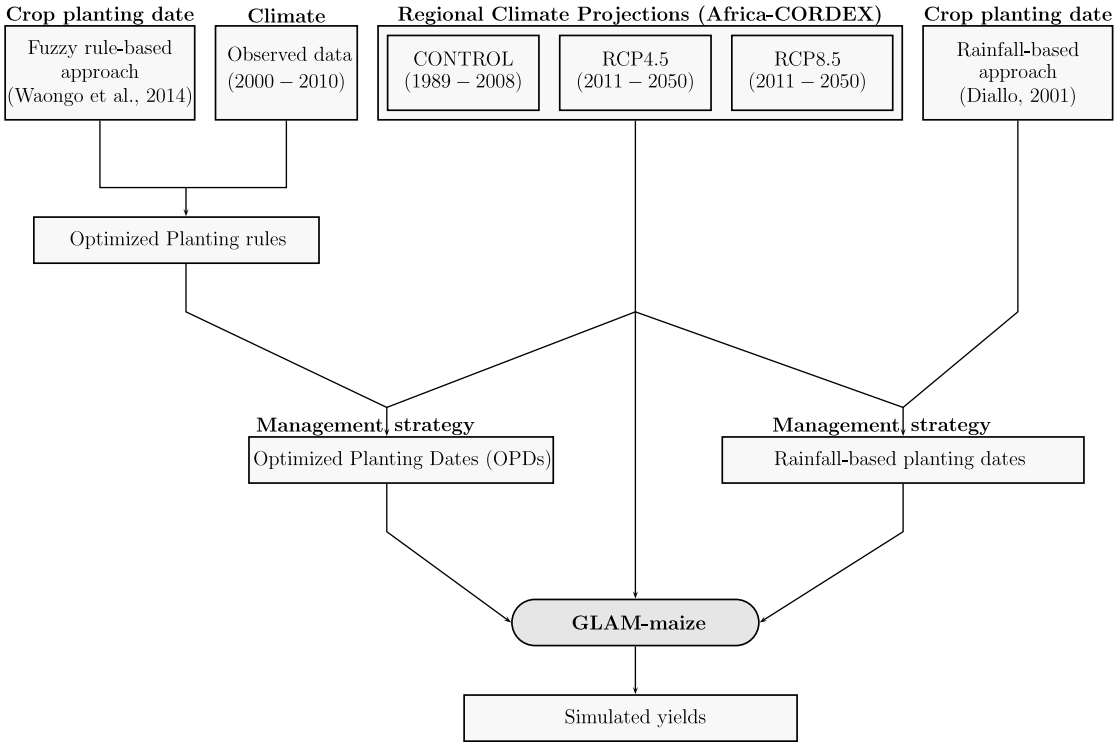

FIGURE 3.13: Flowchart of maize yield simulation under regional climate projection and planting dates options.

Chapter 4

OPDs for agricultural decision-making

4.1 Results

4.1.1 GLAM calibration for maize in Burkina Faso

Since GLAM has not yet been calibrated for maize in WA, a GA based calibration has been performed at two resolutions ($0.75° \times 0.75°$ and $0.44° \times 0.44°$). The performance of the calibration has been evaluated using Pearson's correlation coefficient (r) and the $RMSE$ between simulated and observed yields over the period 2000-2010.

Figure 4.1*a* depicts the location specific r at resolution of $0.75° \times 0.75°$ over BF. The minimum r is 0.6, while r is larger than 0.75 for 80% of all locations (41 out of 51 grid cells). At the significance level $\alpha = 0.05$, the r values are statistically significant (Figure 4.1*b*). Figure 4.1*a* reveals a distinct homogeneous high correlation ($r \geq 0.8$) in the South West of BF. On average, the calibrated GLAM is able to capture 50% ($R^2 = 0.5$) of the variability of maize yield for the period 2000-2010. The relative $RMSE$, shown in Figure 4.1*c*, is less than 50% for all locations. The simulated maize yield in the majority of locations deviates from the respective observed yield by less than 25% and even less in the South West of BF. The range of variability of calibrated parameters is given in Appendix B.

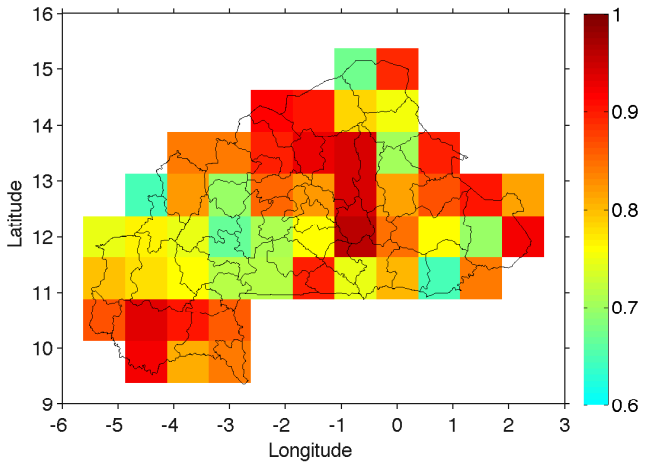

(a)

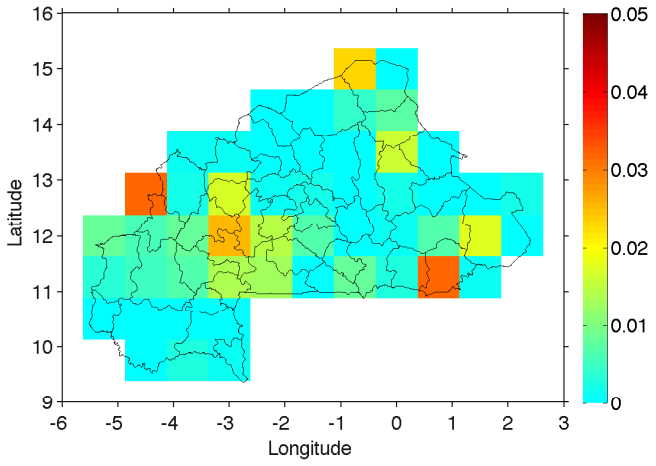

(b)

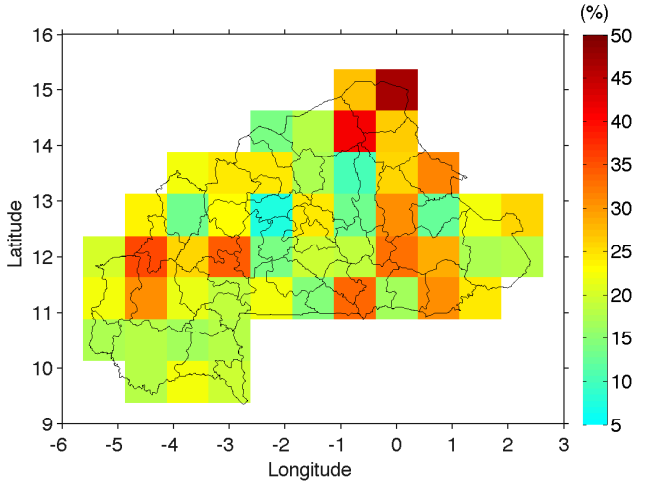

(c)

FIGURE 4.1: Measures of the performance of the calibrated GLAM at resolution of $0.75° \times 0.75°$. (a) Pearson correlation coefficient between observed and simulated maize crop yield, (b) p-value of Pearson's correlation coefficient, and (c) Relative RMSE between observed and simulated maize yield.

At resolution of $0.44° \times 0.44°$, r ranges between 0.52 and 0.93 at a significant level $\alpha = 5\%$ (Figure 4.2*a*). The highest values of r are found in the northernmost and south-western BF while in the south-eastern BF, r values are lower than 0.7. The relative $RMSE$ values are lower than 40% over BF with lowest values in the northern and south-eastern BF (Figure 4.2*b*).

From the two calibrations, it is evident that the performance of the calibrated GLAM for maize clearly depends on the location and the resolution.

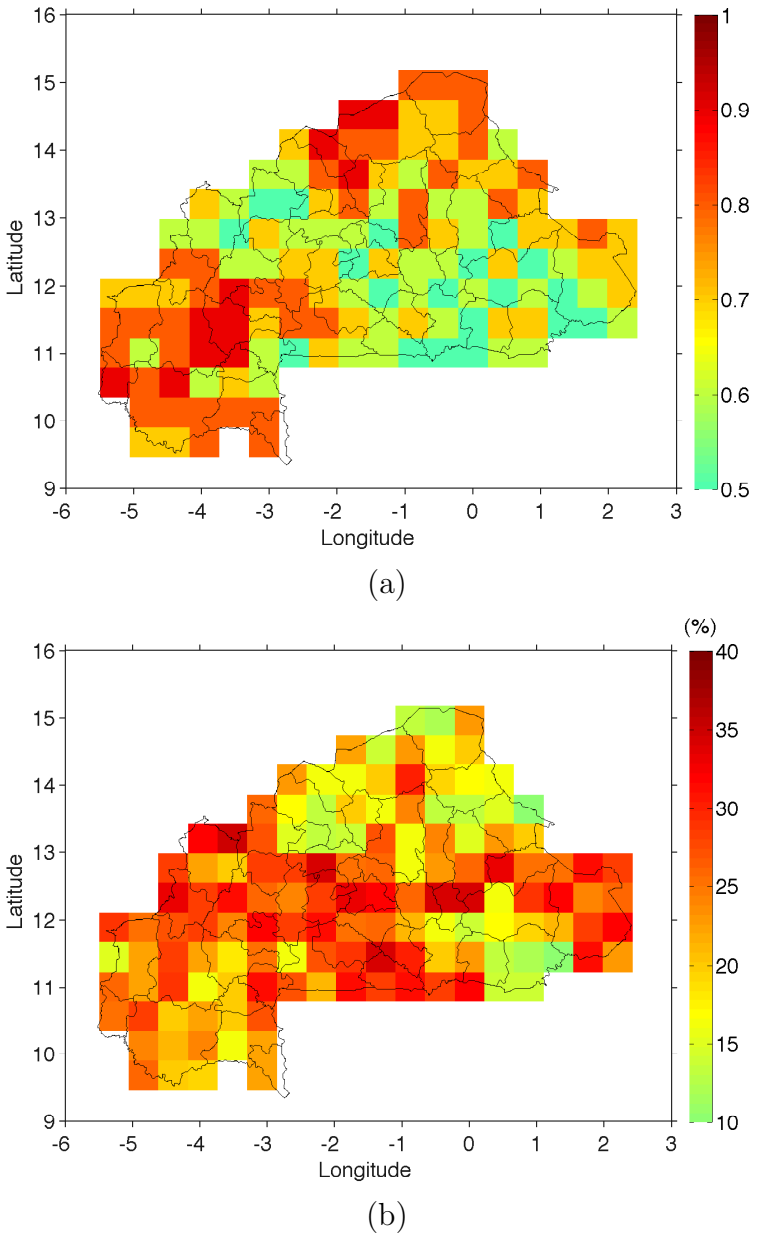

FIGURE 4.2: Pearson correlation coefficient (a) and relative RMSE (b) between observed and simulated maize achieved by GLAM calibration at resolution of $0.44° \times 0.44°$.

4.1.2 OPDs and simulated yields for maize over Burkina Faso

A 10 ensemble members of fuzzy logic parameter sets is used to derive OPDs over the period 1980-2010 (see section 3.2.5). The ensemble mean values of the fuzzy logic parameters are presented in Appendix C. The results shown in Figure 4.3 depict (a) the mean OPD ($\overline{OPD}$) and (b) the standard deviation of OPD (σ_{OPD}) for a sample of 310 (10 $members \times$ 31 $years$) optimized planting dates for each grid cell. $\overline{OPDs}$ vary between the 7th of May and the 5th of July across the country following a north-south gradient. In general, earliest OPDs occur in May in the the Southern part whereas the latest OPDs occur in June-July in the Northern part of BF. Following a similar spatial pattern, σ_{OPD} varies between 2 and 18 days. The variability of OPDs is greater in the Northern than in the Southern parts of the country.

The OPDs have been used as input in GLAM to simulate maize yield. Figure 4.3*c* shows the spatial distribution of mean maize yield over the period 1980-2010. The mean yield varies between 500 kg ha^{-1} and 3000 kg ha^{-1} with highest (lowest) yields in the southernmost (northernmost) parts of BF. The highest simulated mean yields can be found in Southwestern Burkina Faso, whereas yields are less than 2000 kg ha^{-1} for the Central and Northern part of the country.

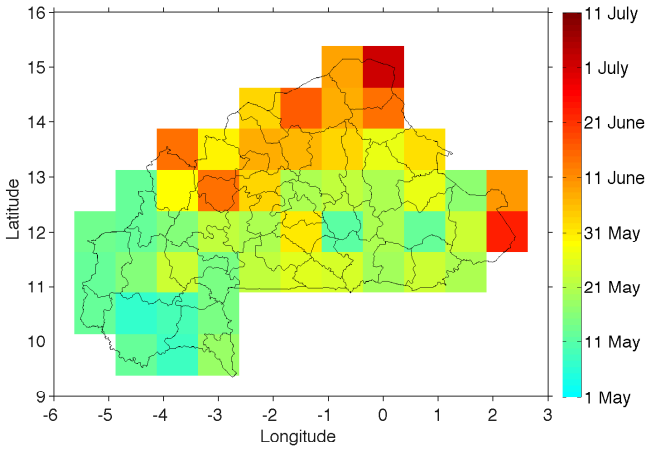

(a) Mean optimized planting dates

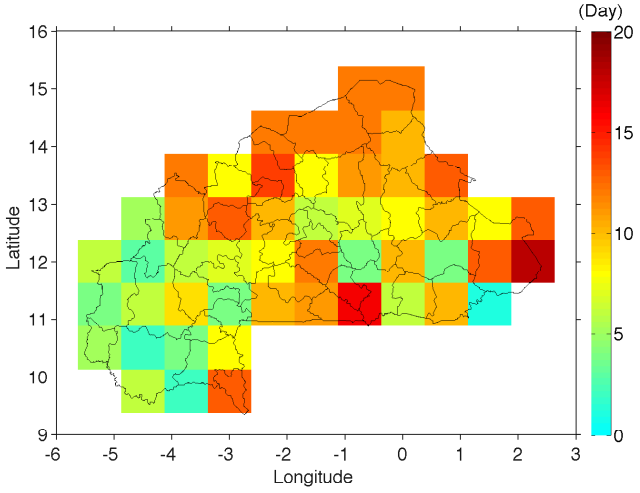

(b) Standard deviation of optimized planting dates

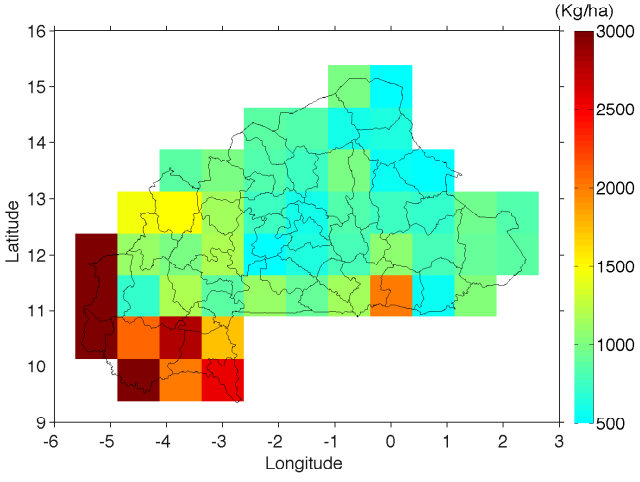

(c) Mean simulated maize yield using optimized planting dates

FIGURE 4.3: Maize optimized planting dates and simulated maize yield in Burkina Faso at resolution of 0.75°×0.75° for the period 1980-2010.

4.1.3 Performance of the OPD approach under present climate

Climate observation data are used in combination with OPDs to simulate maize yields. For comparison, planting dates and maize yield are computed using Diallo (2001) and Dodd and Jolliffe (2001) approaches. OPD-based planting dates and simulated yields are compared to the approaches of Diallo (2001) and Dodd and Jolliffe (2001) then. On average, the deviation in planting dates between OPD approach and the approaches of Diallo (2001) and Dodd and Jolliffe (2001) varies between −20 and +12 days for both Diallo (2001) (Figure 4.4*a*) and Dodd and Jolliffe (2001) (Figure 4.4*b*). The lowest (highest) deviation magnitude is mainly located in the Southwestern (Northern) part of BF. In general, the OPD approach yielded earliest planting dates if compared to the planting dates computed by the approaches of Diallo (2001) and Dodd and Jolliffe (2001).

The deviation of maize potential yield ranges between −10% and +60% while positive values prevail (Figures 4.4*c* and 4.4*d*). Except for the Southern part, the potential yield obtained by OPDs results in an increase of at least 10% in mean yield compared to those obtained by Diallo (2001) and Dodd and Jolliffe (2001). For the southern part of the country, however, this increase in mean yield is less pronounced.

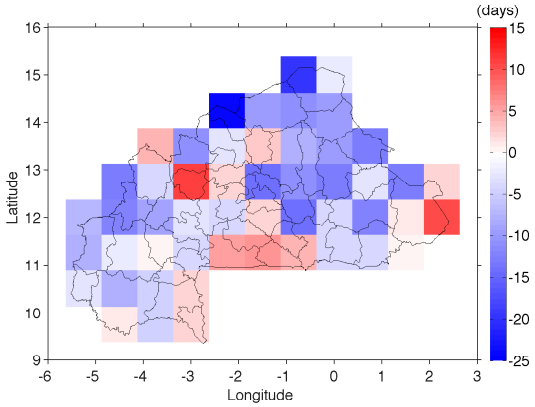

(a) Planting date deviations (OPD-Diallo (2001))

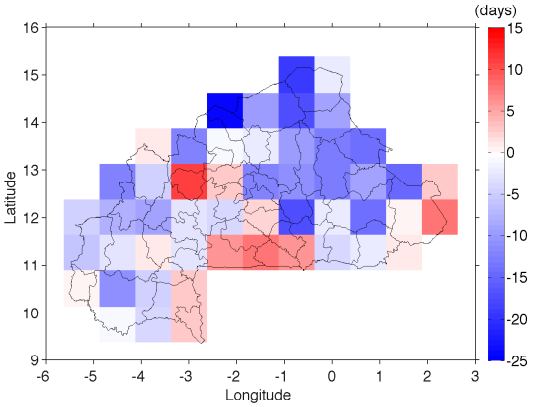

(b) Planting date deviations (OPD-Dodd and Jolliffe (2001))

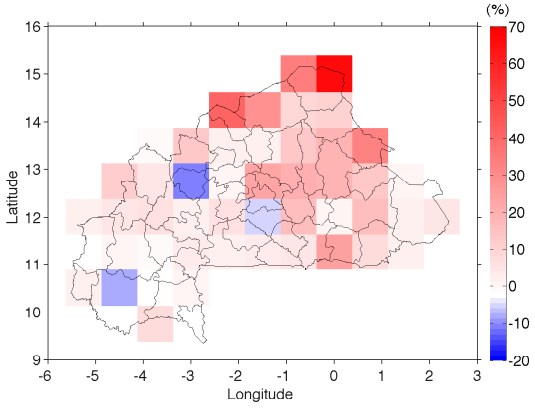

(c) Relative deviation of mean maize potential yield (OPD-Diallo (2001))

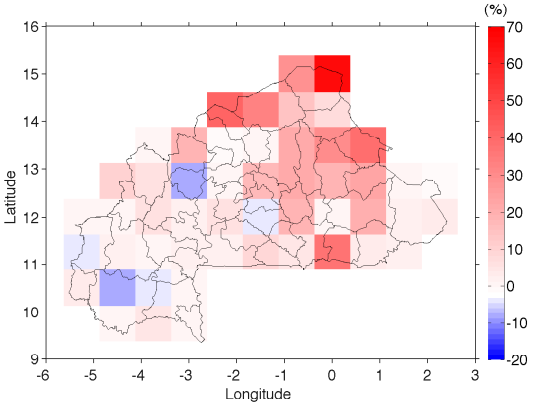

(d) Relative deviation of mean maize potential yield (OPD-Dodd and Jolliffe (2001))

FIGURE 4.4: Comparison of planting dates (a, b) and simulated yield (c, d) obtained by OPDs and approaches of Diallo (2001) and Dodd and Jolliffe (2001), for maize cultivation in Burkina Faso.

4.1.4 RCMs temperature and precipitation analysis

Temperature and precipitation patterns for RCM control runs are compared with observed data from synoptic stations in BF for the period 1989 to 2008. Figure 4.5 summarizes the statistical relationship between RCMs simulations and observations. Statistics are calculated for four spatial domains, that is whole BF (National) and the three AEZs. As shown in Figure 4.5, the correlation coefficients (r) between RCMs simulations and observations are less than 0.6 for precipitation and 0.8 for temperature, irrespectively of the RCMs, variables (temperature and precipitation) and spatial domains. Among the RCMs, precipitation and temperature patterns from CNRM showed the highest correlation coefficients and the lowest RMSD while NCC showed the lowest correlation coefficient and the highest RMSD. However, the precipitation variance of the NCC model is similar to the observed precipitation variance. At the national scale, the precipitation patterns have found to be similar for the models CCCma, ICHEC,MIROC and MOHC. However, there is a clear difference between the models in the three AEZs. These differences are more pronounced for precipitation patterns than temperature pattern.

Figure 4.6 shows that all RCMs are in general able to capture the intra-seasonal cycle of mean temperature and precipitation during the main growing season (June-September). However, only the intra-seasonal variance of temperature are well capture by RCMs (Figure 4.7). Moreover, the variance of temperature is lower than precipitation variance. For all AEZs, RCMs underestimate the mean and variance of monthly precipitation in August. With regards to RCMs, the model CCCma outcome the largest biases for precipitation, particularly for the period July-October. Largest biases of mean temperature is observed with models CCCma (i.e, an overestimation) and ICHEC ((i.e, an underestimation) during July-September. On average, the RCMs fail to reproduce precipitation and temperature in May. Indeed, the RCMs strongly overestimate precipitation and underestimate temperature in May over all AEZs.

The seasonal precipitation gradient from the South to the North is reasonably

captured by the RCMs (Figure 4.8). Likewise Figure 4.6 and 4.7, the underestimation of the mean and variance of precipitation over all AEZs by CCCma model can be observed in Figure 4.8. Moreover, Figure 4.8 shows that NOAA model tends to overestimate seasonal precipitation over the AEZs with a high variability of seasonal precipitation amount. Since no systematic bias has been detected, we do not perform a bias correction for subsequent analyses.

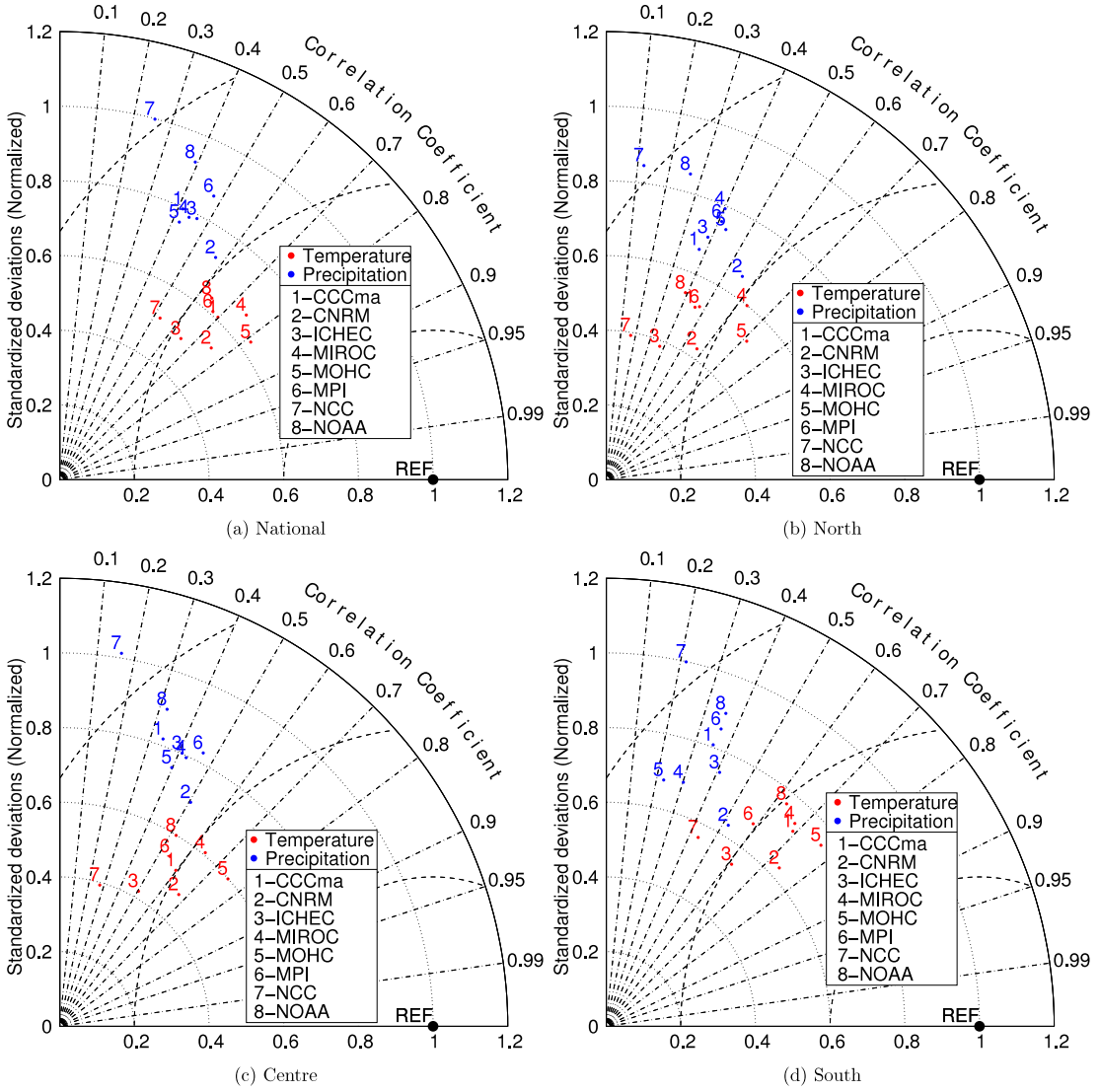

(a) National (b) North

(c) Centre (d) South

FIGURE 4.5: Diagrams displaying temperature and precipitation statistics in comparison to observations for the AEZs and whole Burkina Faso. Statistics are based on RCM control runs data for period 1989-2008. The centered root-mean-square difference and the standard deviation of temperature and precipitation have been normalized. REF depicts observations derived from synoptic stations.

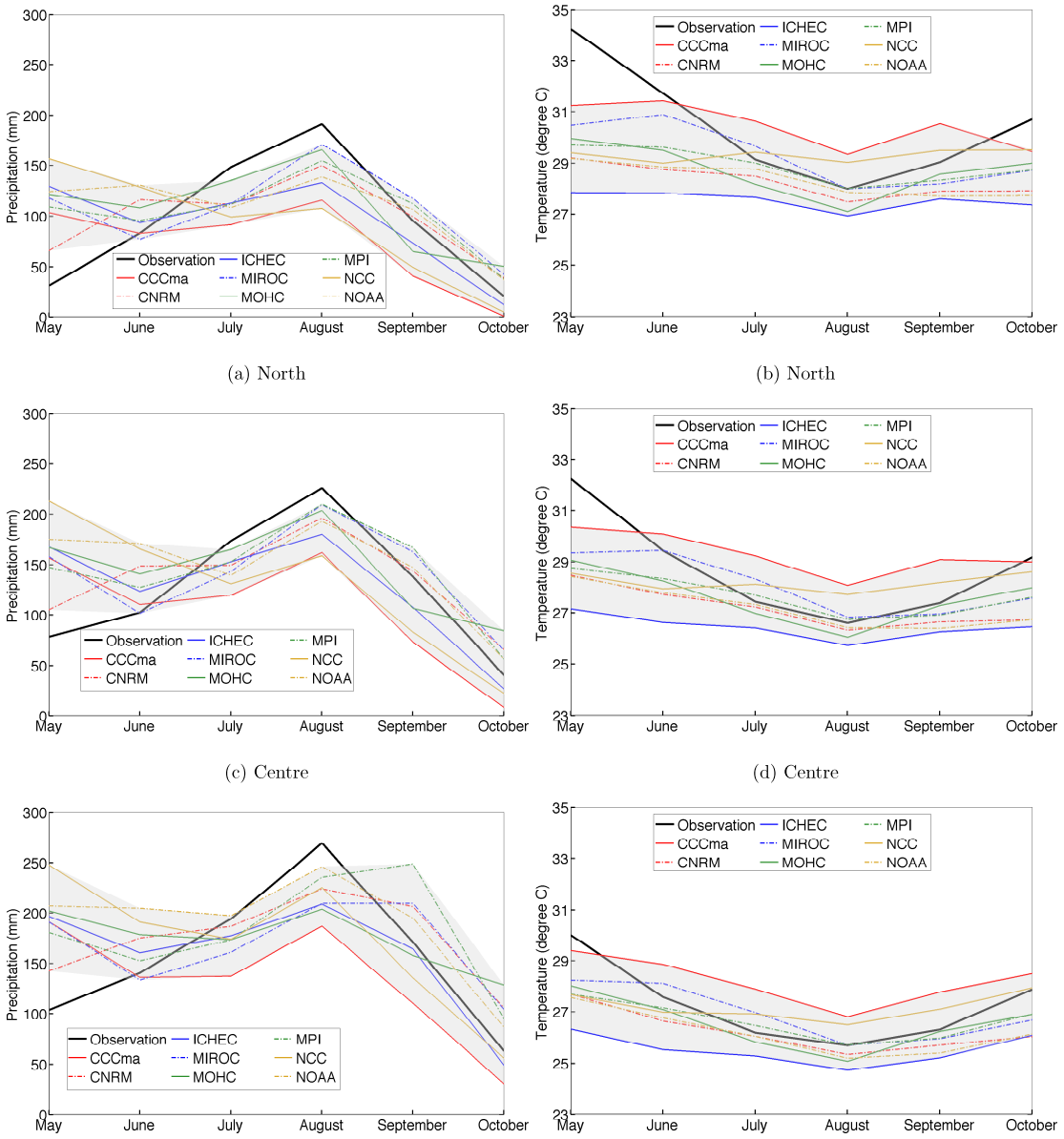

(a) North (b) North

(c) Centre (d) Centre

(e) South (f) South

FIGURE 4.6: Intra-seasonal cycle of RCM control runs precipitation (left) and temperature (right) for the AEZs. The black lines represent the monthly mean of observations from synoptic stations located in each AEZ. The light grey shading represents the range of variation of monthly precipitation amounts from all RCM control runs.

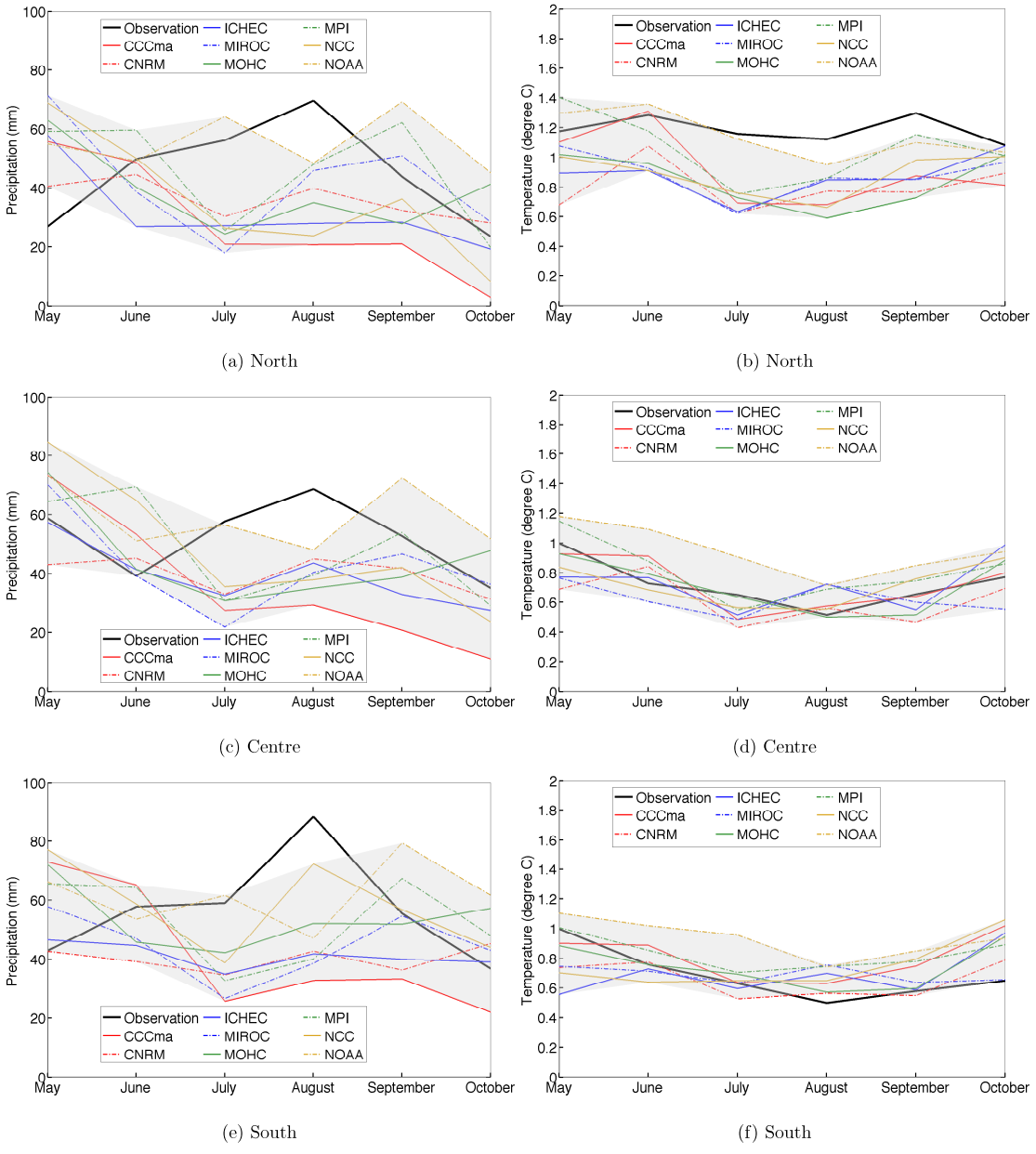

(a) North (b) North

(c) Centre (d) Centre

(e) South (f) South

FIGURE 4.7: Standard deviation of RCM control runs for monthly precipitation (left) and temperature (right) for the different AEZs. The black line represents the standard deviation of observations in each AEZ. The light grey shading represents the range of the standard deviations from all RCM control runs.

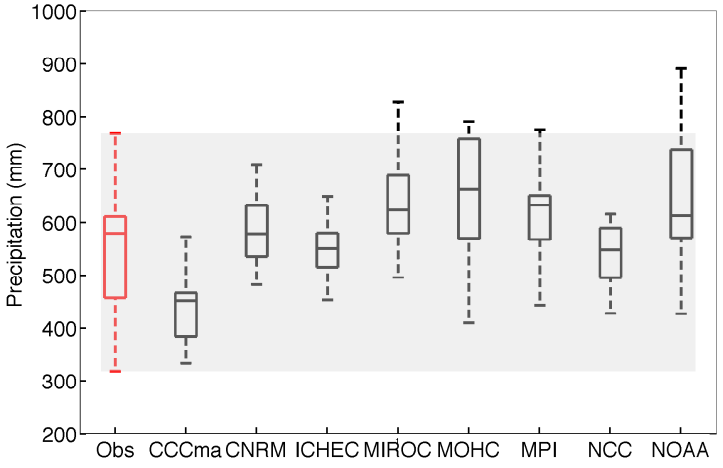

(a) North

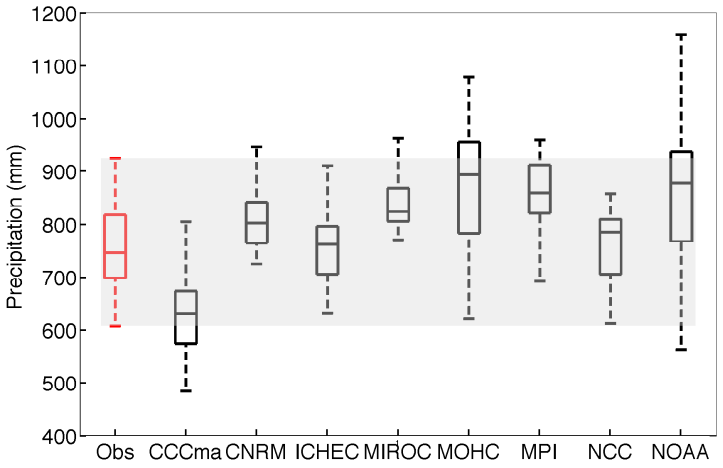

(b) Centre

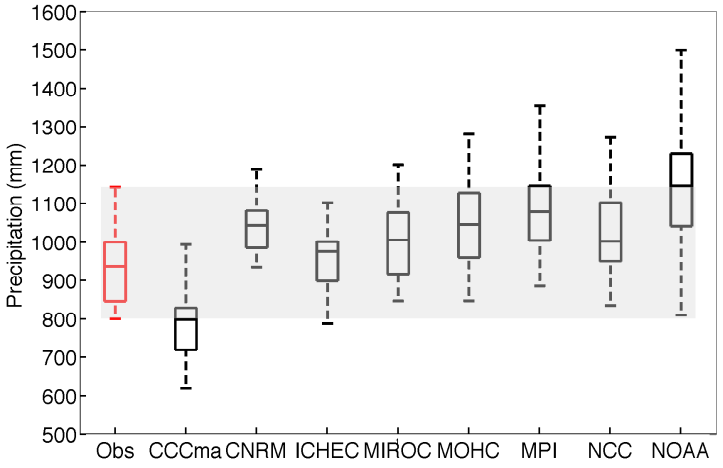

(c) South

FIGURE 4.8: Observation and RCM long-term seasonal precipitation amount distribution for the different AEZs. The red box-and-whisker plot represent the distribution of observed seasonal precipitation derived from synoptic stations for each AEZ for the period 1989-2008. The light grey shading highlights the range of variation of observations. X-axis denotes observations (Obs) and RCM labels.

4.1.5 Comparative performance of the OPD approach under climate change

By using regional climate change data (spatial resolution of 0.44°×0.44°), OPDs' impact on future maize production is evaluated in comparison with the planting date approach of Diallo (2001). The analysis is performed for two time periods (2011-2030 and 2031-2050), two emission scenarios (RCP4.5 and RCP8.5) and the three AEZs (North, Centre and South) as well as national scale. In general, as shown in Figure 4.9, OPDs achieve higher potential maize yield if compared to the approach of Diallo (2001) regardless of the RCMs, time periods and spatial domains. The mean yield achieved by OPDs is at least 15% larger than the mean yield achieved by the approach of Diallo (2001). Concerning the spatial scale, the mean and the variance of yield deviation decrease from the North to the South. For illustration, the high performance of OPDs (yield deviation $\geq 30\%$) observed in the North is also associated with a high variability, regardless of RCM. In the South, yield deviation is in general positive and less variable.

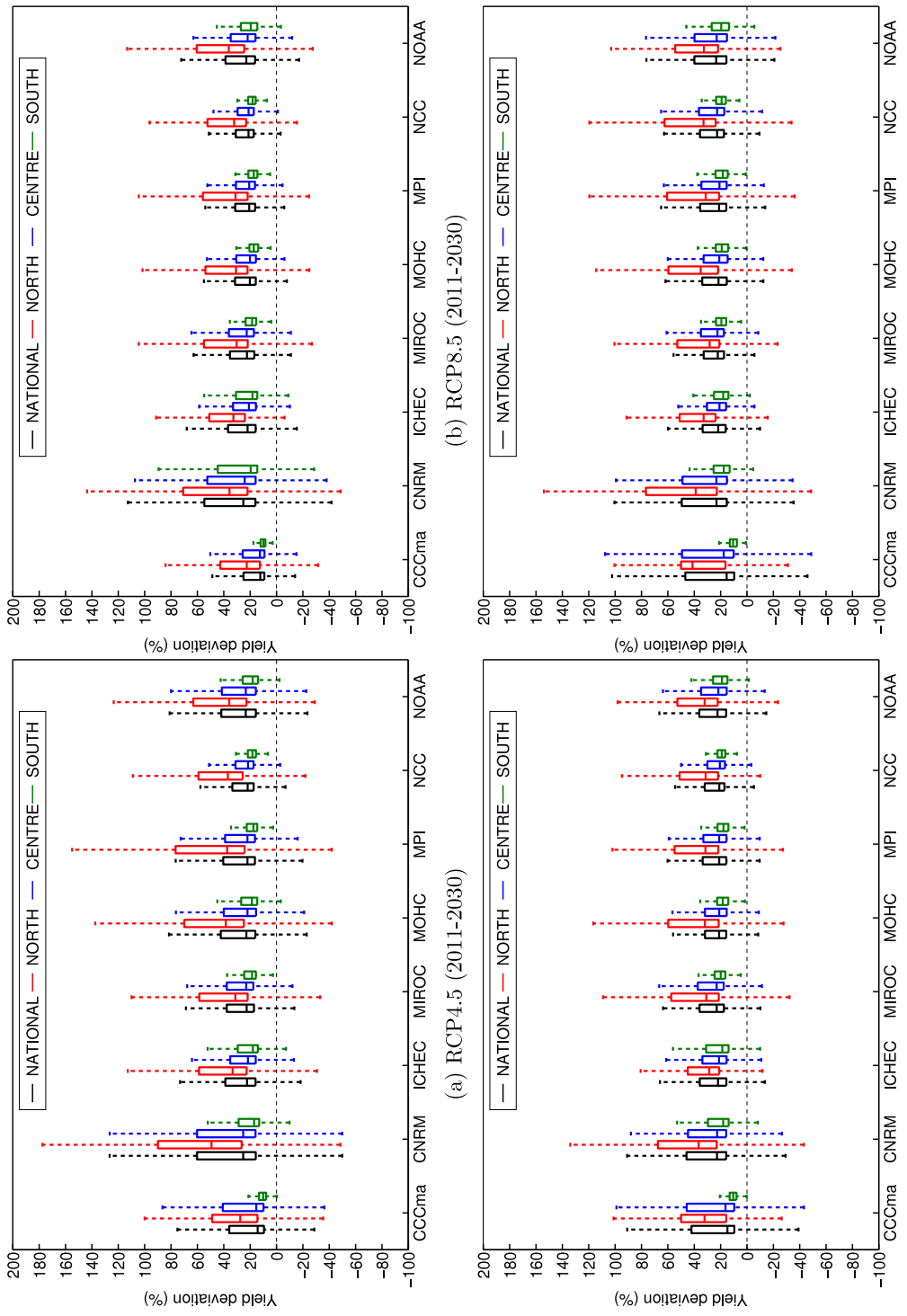

(a) RCP4.5 (2011-2030) (b) RCP8.5 (2011-2030)

(c) RCP4.5 (2031-2050) (d) RCP8.5 (2031-2050)

FIGURE 4.9: Comparison between simulated maize yield obtained by OPD and Diallo (2001) under RCP4.5 and RCP8.5. For a given year, simulated yield obtained by Diallo (2001) is used as baseline to compute relative deviations (expressed in %) of yield obtained by OPD approach. X-axis denote RCM labels. The dotted horizontal line separated cases where OPDs achieved higher potential yield than Diallo (2001) (boxplots above the dotted line) and cases where OPDs achieved less potential yield than Diallo (2001) (boxplots below the dotted line).

4.1.6 OPDs impact on maize yield under regional climate change

OPDs in combination with future climate projections from 8 RCMs have been used to estimate the climate change impacts on maize production. Simulated maize yields for the baseline period (i.e. RCMs control runs 1989-2008) show that yield obtained by OPDs (Appendix D) are significantly higher ($> 10\%$) than yields obtained by Diallo (2001) (Appendix E). The spatial variability of potential maize yield for the period 2011-2050 has been evaluated under RCP4.5 (Figure 4.10 and Figure 4.12) and RCP8.5 (Figure 4.11 and Figure 4.13). Across RCMs, the change in mean yield varies between -23% and 34% from the baseline for the majority of grid cells. On average, a negative changes of mean yield is observed. For the period 2011-2050, RCMs ensemble mean of yield change is -3.4% for RCP4.5 and -8.3% for RCP8.5. RCP4.5 shows an almost equally number of locations with negative and positive change of yield, regardless of the RCM (Figure 4.14a). In contrast, a clear discrimination of mean yield changes is observed with RCP8.5, particularly for the period 2031-2050 where a negative change in the mean yield is dominantly observed for six out of eight RCMs (Figure 4.14b).

With regards to RCMs, a decrease in yield is observed with CCCma and MIROC models for the majority of locations in the South-West and Centre-East of BF, irrespectively of the RCP and period. However, ICHEC model shows a higher positive change ($> 40\%$) of mean yield in the South-West of BF, regardless of RCP and period. In the North and Centre-East, RCP8.5 yields a more pronounced decrease in mean yield during the period 2031-2050 for CNRM, ICHEC, MOHC, MPI and NOAA models.

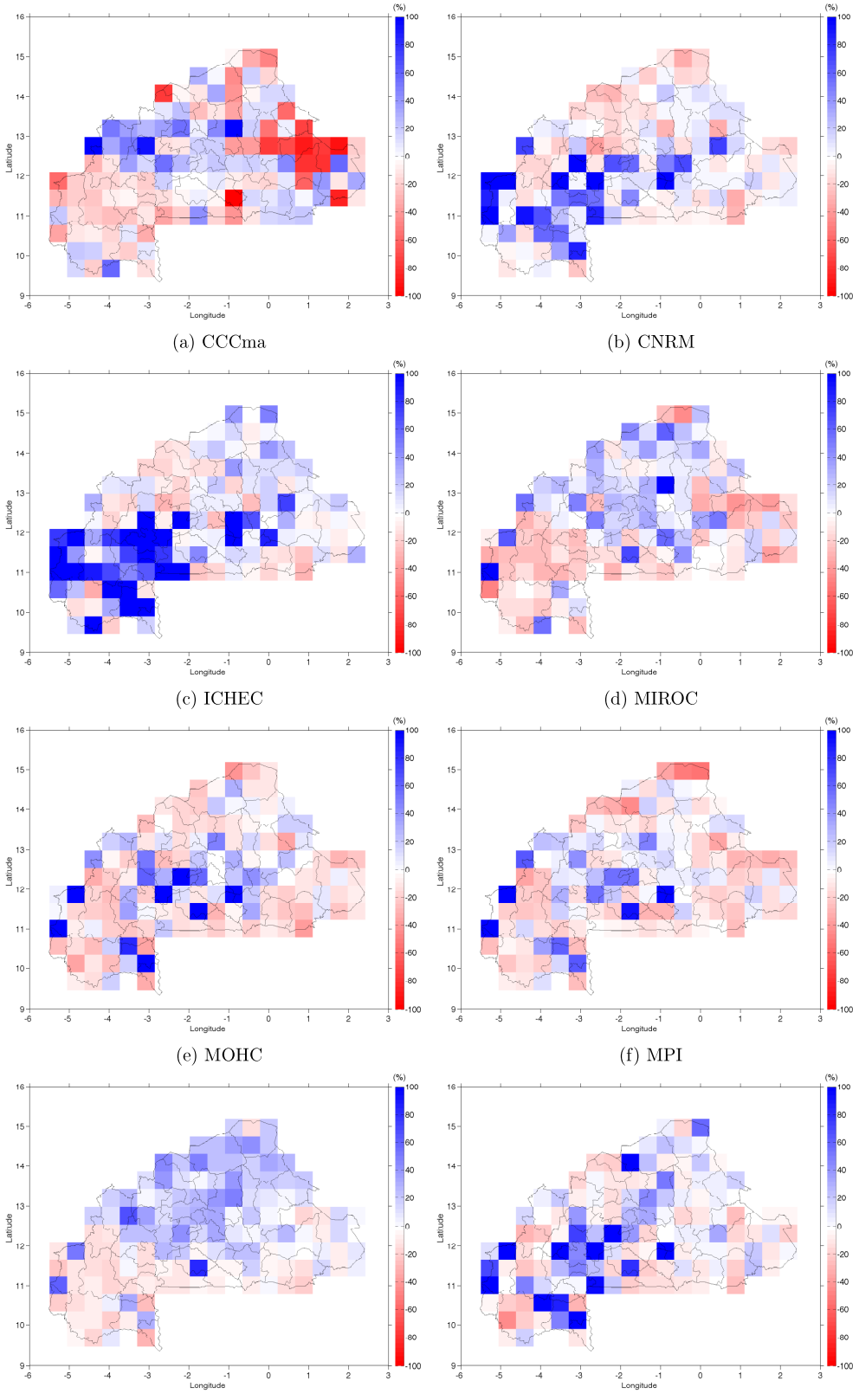

(a) CCCma (b) CNRM

(c) ICHEC (d) MIROC

(e) MOHC (f) MPI

(g) NCC (h) NOAA

FIGURE 4.10: Maize mean yield changes for eight RCMs under the emission scenario RCP4.5 and OPD approach for the period 2011-2030. The change in yield is expressed in % of the mean yield achieved by RCM control runs (period 1989-2008).

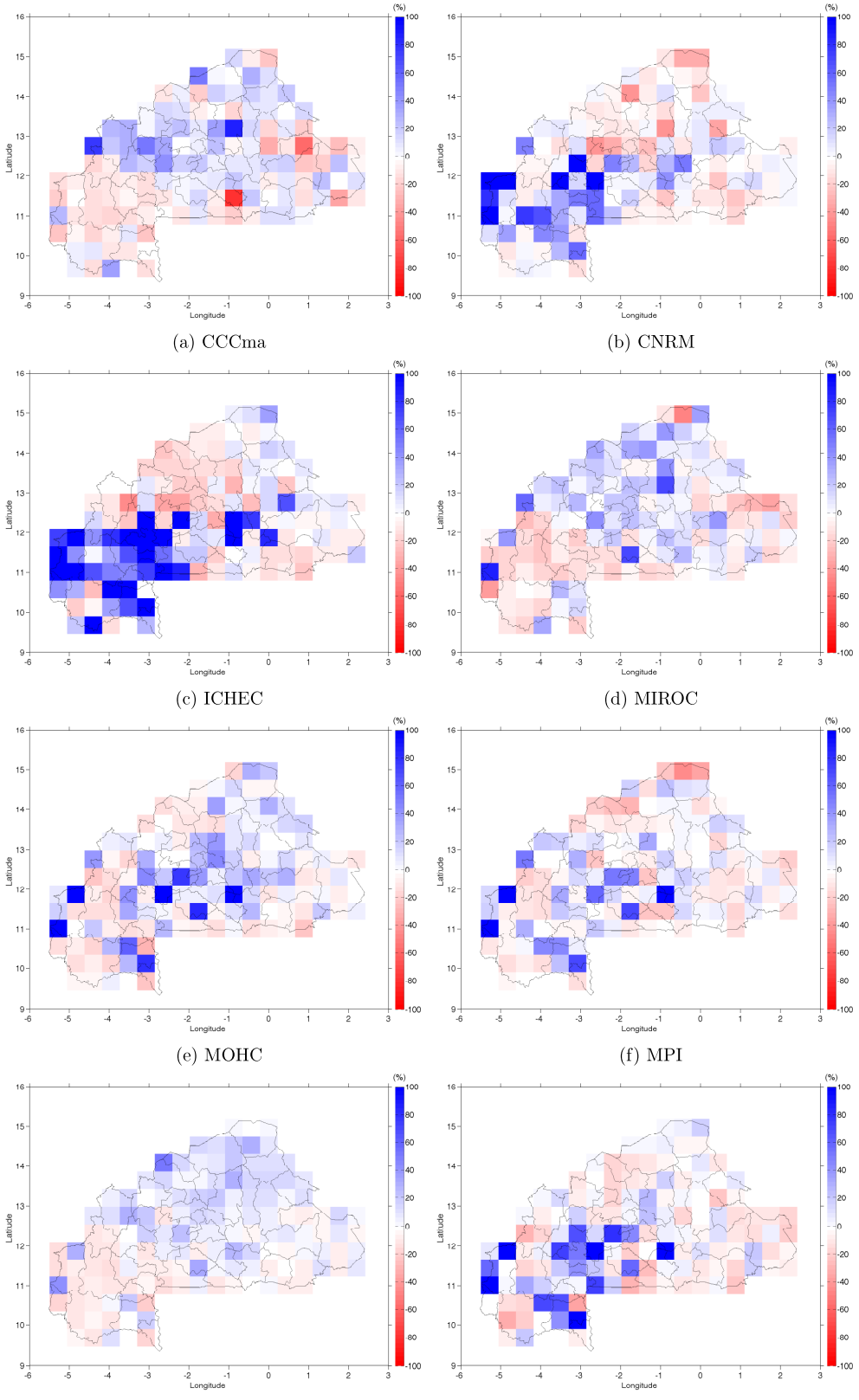

(a) CCCma (b) CNRM

(c) ICHEC (d) MIROC

(e) MOHC (f) MPI

(g) NCC (h) NOAA

FIGURE 4.11: Maize mean yield changes for eight RCMs under the emission scenario RCP8.5 and OPD approach for the period 2011-2030. The change in yield is expressed in % of the mean yield achieved by RCM control runs (period 1989-2008).

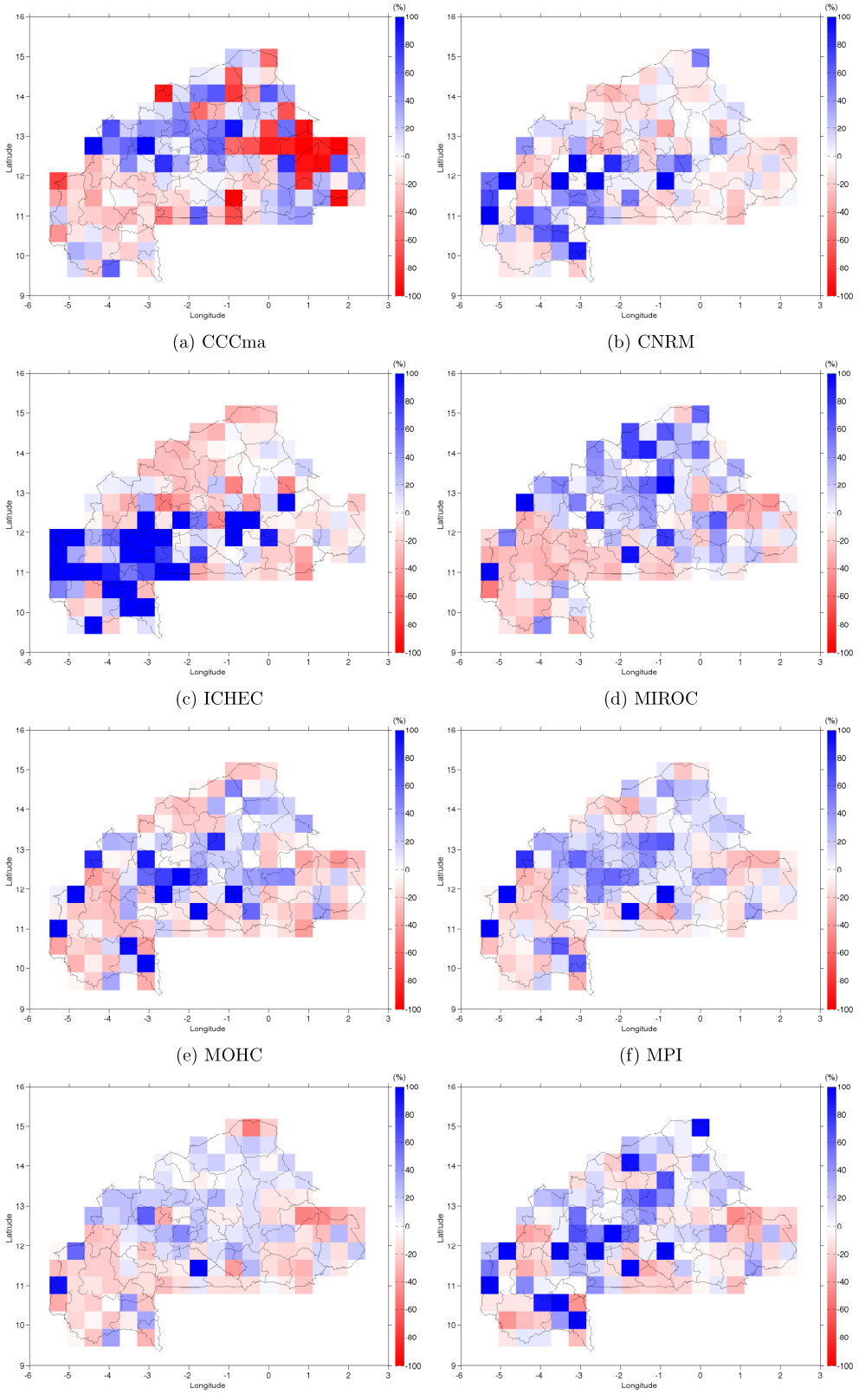

(a) CCCma (b) CNRM

(c) ICHEC (d) MIROC

(e) MOHC (f) MPI

(g) NCC (h) NOAA

FIGURE 4.12: Maize mean yield changes for eight RCMs under the emission scenario RCP4.5 and OPD for the period 2031-2050. The change in yield is expressed in % of the mean yield obtained by RCM control runs (period 1989-2008).

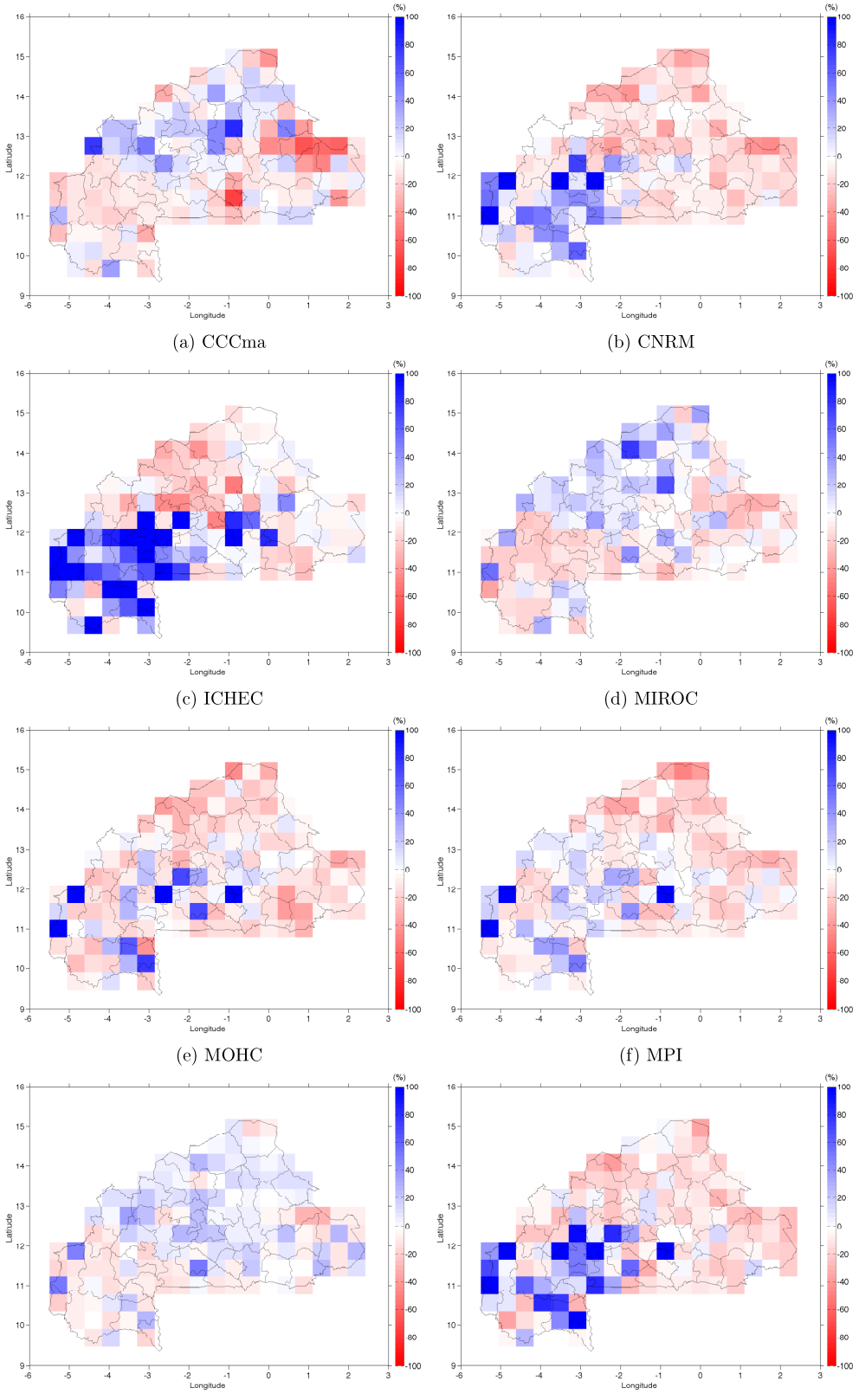

(a) CCCma (b) CNRM

(c) ICHEC (d) MIROC

(e) MOHC (f) MPI

(g) NCC (h) NOAA

FIGURE 4.13: Maize mean yield changes for eight RCMs under the emission scenario RCP8.5 and OPD for the period 2031-2050. The change in yield is expressed in % of the mean yield obtained by RCM control runs (period 1989-2008).

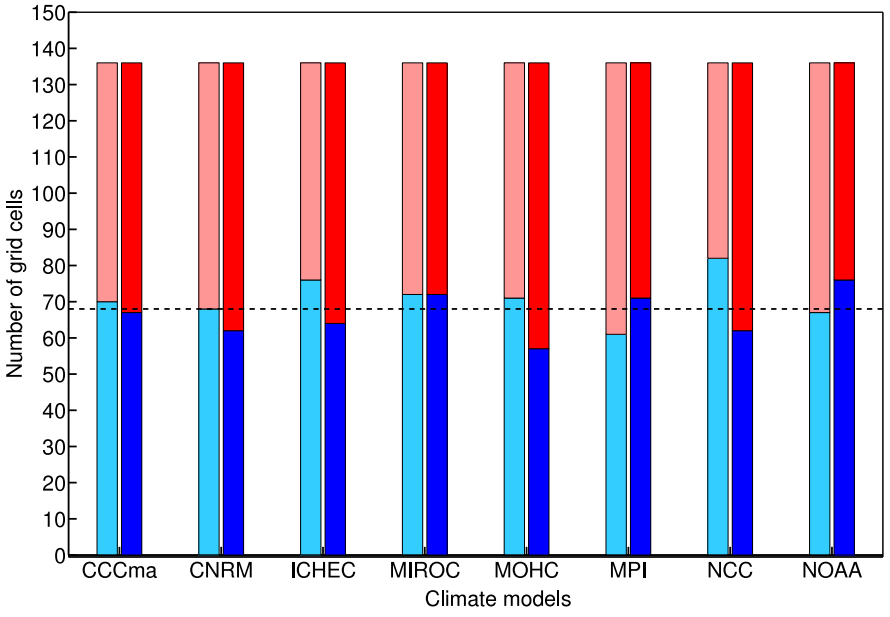

(a) RCP4.5

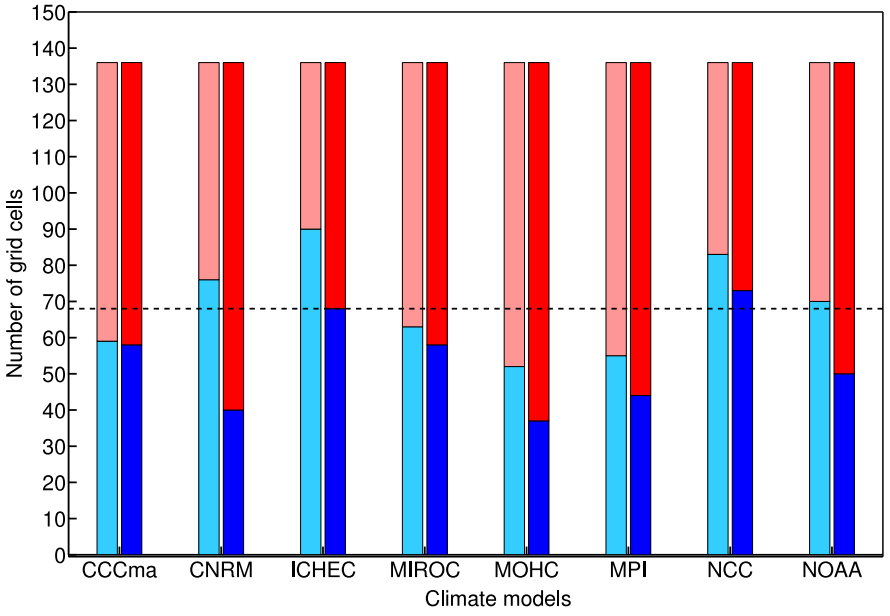

(b) RCP8.5

FIGURE 4.14: Number of locations affected by a negative change (red and light red) and a positive change (blue and light blue) of simulated yield in comparison to the baseline 1989-2008. Light red and light blue boxes represent the period 2011-2030 while red and blue boxes represent the period 2031-2050. X-axis represents RCMs and the horizontal dotted line represents the half of the total number of grid cells (136) in the study domain.

4.2 Discussion

An approach to objectively derive crop planting dates is presented and applied for the first time for maize cultivation in WA. The approach accounts for crop-specific meteorological and soil requirements during the whole growing period. The results show that the optimized planting dates generally follow the prevailing north-south gradient of rainfall with earlier (later) planting in the South (North). This gives evidence that planting dates depend strongly on the location. This finding is in agreement with studies of Kniveton et al. (2009) and Laux et al. (2010) accounting for local and regional differences, respectively. The OPD approach is similar to the approach of Laux et al. (2010). Instead of using a crop model designed to work on local scale, the crop model GLAM is used. A genetic algorithm is used to derive robust planting rules at a regional scale, which significantly reduces the required iterations, and thereby computing time.

In WA, several methods to estimate the onset of the rainy season are in operation, giving recommendations for planting dates. These approaches are usually applied at the local scale. At the BF National Meteorological services and the Regional Center AGRHYMET, the approaches of Diallo (2001) and Dodd and Jolliffe (2001) which are regionally adapted versions of Stern et al. (1981, 1982), are currently in operation to support agricultural decision-making in WA. For the Southeast of Burkina Faso, the OPD approach reaches a similar performance in terms of potential yields compared to the two well-established methods, i.e. these approaches are already well adapted for this intensively used and maize-dominated agricultural region. Compared to these approaches in operation, the proposed OPD approach has the following advantages:

1. Once a calibrated process-based crop model is available, agrometeorological and crop yield data are required to derive crop and location specific planting rules and to estimate planting dates. Besides the required knowledge to calibrate the crop model, this approach can be seen as fully objective. However agronomic and agrometeorological knowledges are still required to validate the outcome of this study.

2. Instead of relying exclusively on rainfall amount and distribution around planting, the OPD approach does not only account for plant water requirements and availability throughout the whole growing period, but also for solar radiation and temperature. This information is inherently included by coupling the planting rules to a process-based crop model.

3. The use of fuzzy-logic to estimate planting rules instead of binary logic gives further flexibility to estimate reliable planting dates where strict thresholds may fail. This is exemplarily illustrated for the amount of rainfall in a 5 day spell. For instance A strict value of 25 mm as used in the approach of Dodd and Jolliffe (2001) would exclude a reasonable planting date in which for instance, 24.9 mm of rain are recorded, even if significant rain and favorable conditions for crop growth follow.

4. Lastly, the OPD approach is not elaborating a single specific planting date, but rather suggesting a set of reasonable planting rules, leading to a time window for planting of approximately 2 weeks. This can help to increase the adoptability of this approach for smallholders, because their decision about planting also depends on other external factors such as availability of seeds, labour, machines, etc.

Based on regional climate change scenarios and two planting date approaches (OPD and Diallo, 2001), maize yield has been simulated using GLAM model. The results showed that the OPD approach achieves significantly higher potential yield compared to the planting date approach of Diallo (2001). In agreement with Waongo et al. (2014), the findings confirmed the potential benefit of OPDs in BF. Thus, based on present and projected future climate, it is demonstrated that the OPD approach achieves higher potential yields across BF compared with the methods currently in operation in WA. However, detailed in-field validation is required before implementation as agricultural management strategy at national and regional centers.

This study assessed also the impact of climate change on maize productivity in conjunction with OPD approach as adaptation strategy. The results show

that on average, potential maize yield is expected to be decreased in future for the majority of locations across BF, particularly for RCP8.5 during the period 2031-2050. With regards to the finding, planting dates based on OPD approach have to be associated with others management strategies in order to be able to strengthen climate change adaptation. The fact is that there are not many decisions in farming that are simple based on a single factor nor are they made in line with a purely tactical response to current information. For long-term adaptations, farmers need to jointly adapt several farming practices to adequately respond to climate risks. However, in WA, the constraints imposed by poor supportive policies and the extreme poverty of farmers are still the major limitation for the adoption of various strategies (Antwi-Agyei et al., 2013), thereby making adaption to climate change more complex in this region. It is also worth to highlight that this study evaluates the potential impacts of climate change on maize production based on one single RCM (i.e. RCA4) which is driven by eight GCMs (Nikulin et al., 2012). In addition, the possibility that potential management strategies (e.g. adoption of new crop varieties, enhancement of the use of fertilizers, development of irrigation options) which decision-makers might strongly promote and farmers might adopt in future to cope with climate change are not expressed in GLAM model for the long term runs.

Chapter 5

Final conclusions and outlook

Rainfed farming in SSA is the most vulnerable agricultural system since it is characterized by smallholder farming with a limited use of production inputs. Since farmers' options for coping climate variability and adapting climate change are particularly limited in that region, planting date, a low-cost agricultural management strategy, aiming to alleviate crop water stress can contribute to enhance decision-making as a strategic decision for farmers as well as a climate change adaptation strategy.

An approach to objectively derive OPDs is presented and applied for the first time for maize cultivation in WA. By taking into account, the inherent uncertainties in rainfall measurements and computation issues, three fuzzy logic memberships have been developed to represent the three main criterions used to defined planting date. Then, the process-based crop model GLAM and the fuzzy logic approach for planting date have been coupled with a genetic algorithm to calibrate GLAM for maize cropping and further to derive OPDs. The approach accounts for crop-specific meteorological and soil requirements throughout the whole crop growing period.

Based on present climate and regional climate change data, maize yield has been simulated using GLAM and both OPDs and two state-of-the-art methods. Results have shown that for both present climate and climate change scenarios, OPDs achieved significantly higher potential maize yield in comparison to the state-of-the-art methods. With regards to the findings, the OPDs approach can

be a valuable agricultural management strategy and can be used to support rain-fed agriculture in WA. However, in-field experiments are crucial to validate the findings before any operational used of OPDs approach.

In this study, only RCMs data from SMHI-Africa CORDEX were available at the time of this study. However, with regards to the complexity of climate change, multi-model ensemble simulations (multiple RCMs driven by multiple GCMs and emissions scenarios) are necessary to quantify the uncertainties of impacts of possible climate realizations on crop production. Therefore, with the objective of enhancing climate-related risk adaptation options, further studies might be necessary to capture the whole range of climate uncertainties.

This research was the first step toward an operational use of OPDs, therefore it did not deal with how to effectively achieve the implementation of OPDs for an operational use in WA. Further studies should be conducted in order to evaluate the potential benefits of the OPD approach if combined with improved seasonal climate predictions accounting for the intra-seasonal rainfall variability. The West African Seasonal Climate Outlook (PRESAO in French) is made routinely and provides mainly tercile (below normal, near normal, above normal) probabilities of the three-monthly rainfall amount for the upcoming season. Although, economic values of PRESAO at farm level have been found in SSA (Sultan et al., 2010), the adoption of the current seasonal climate outlook by farmers is low. One of the main reason of the low uptake have been highlighted by Ingram et al. (2002), which found that farmers expressed a strong interest in receiving PRESAO, but they were much more interested in receiving information on the onset and cessation of the wet season, and the risk of long dry spell occurrence during the growing season. Therefore, it is obvious that farmers are interested in having this information included in PRESAO. Since the limited skill of the seasonal prediction of the local-scale onset of the wet season have been demonstrated (e.g. Marteau et al., 2009), research on the predictability of OPDs over WA is crucial before suggesting the implementation of the OPD approach in the PRESAO framework. This avenue of research can substantially contribute to enhance farmers strategic decision-making regarding when to plant and subsequently which crop or cultivar

to choose and also on-time preparation of farm lands.

APPENDIX A

Climate observation network operated by DGM in BF. Names in bold are synoptic stations

Station name	Longitude (°)	Latitude (°)
OUAGADOUGOU	-1.52	12.35
OUARKOYE	-3.67	12.08
ORONKUA	-3.10	11.28
NANDALIA	-2.18	12.33
KANTCHARI	1.52	12.47
GUIEDOUGOU	-3.42	12.98
DIONKELE	-4.72	11.78
BOUROUM BOUROUM	-3.23	10.53
BARABOULE	-1.85	14.22
DJIBO	-1.62	14.10
ARIBINDA	-0.87	14.23
GORGADJI	-0.52	14.03
GOROM GOROM	-0.23	14.45
DORI	-0.03	14.03
MARKOYE	0.07	14.63
BOMBOROKUY	-3.98	13.05
KASSOUM	-3.30	13.08
TOENI	-3.18	13.43
TOUGAN	-3.07	13.08
KIEMBARA	-2.72	13.25
TIOU OUAHIGOUYA	-2.67	13.82
OUAHIGOUYA	-2.43	13.58
GOURCY	-2.35	13.20
TITAO	-2.07	13.77
SEGUENEGA	-1.97	13.43
POBE	-1.77	13.90
TEMA	-1.77	13.05
TIKARE	-1.73	13.28
BOURZANGA	-1.55	13.68
BAM TOURCOING	-1.50	13.33
KAYA	-1.08	13.10

BARSALOGHO	-1.07	13.42
BOUROUM	-0.65	13.60
TOUGOURI	-0.50	13.32
DAKIRI	-0.23	13.28
BANI	-0.17	13.72
SEBBA	0.52	13.43
TANSILLA	-4.38	12.42
SOLENSO	-4.08	12.18
NOUNA	-3.87	12.73
DEDOUGOU	-3.48	12.47
SOUROU GASSAN	-3.22	12.82
SAFANE	-3.22	12.13
TOMA	-2.90	12.77
TIOGO	-2.68	12.18
REO AGRI	-2.37	12.32
KOUDOUGOU	-2.37	12.27
IMANSGHO	-2.33	12.43
YAKO	-2.27	12.97
SARIA	-2.15	12.27
KINDI	-2.03	12.43
BOUSSE	-1.88	12.67
KOKOLOGHO	-1.88	12.18
TANGHIN DASSOURI	-1.72	12.27
PABRE	-1.57	12.52
BOULBI	-1.53	12.23
SABA	-1.42	12.37
MANE	-1.33	12.98
GUILONGOU	-1.30	12.62
KORSIMORO	-1.07	12.82
MOGTEDO	-0.83	12.28
ZORGHO	-0.62	12.25
BOULSA	-0.57	12.65
KOUPELA	-0.35	12.18
KOSSOUDOUGOU	-0.23	12.93
BOGANDE	-0.13	12.98
PIELA	-0.13	12.70
LANTAOGO	-0.08	12.02
BILANGA	-0.02	12.55

FADA NGOURMA	0.35	12.07
YAMBA	0.33	12.30
GAYERI	0.48	12.65
MATIAKOUALY	1.03	12.37
DIAPAGA	1.78	12.07
SAMOROGOUAN	-4.93	11.40
FARAKOBA AGRO	-4.33	11.10
BOBO DIOULASSO	-4.30	11.17
BONDOUKUY	-3.77	11.85
KOUMBIA	-3.70	11.23
BEREBA	-3.68	11.62
HOUNDE	-3.52	11.48
WONA	-3.43	11.97
BAGASSI	-3.30	11.75
DANO	-3.07	11.15
BOROMO	-2.92	11.73
BOURA	-2.50	11.05
TIOU KOUDOUGOU	-2.20	11.95
GAO	-2.18	11.65
LEO	-2.10	11.10
SAPOUY	-1.77	11.55
BETARE	-1.37	11.43
PO	-1.15	11.17
MANGA	-1.07	11.67
TIEBELE	-0.97	11.10
GON BOUSSOUGOU	-0.77	11.40
NIAOGHO	-0.77	11.77
GARANGO	-0.57	11.80
TENKODOGO	-0.38	11.77
OUARGAYE	0.02	11.53
KOMIN YANGA	0.13	11.73
PAMA	0.70	11.25
MAHADAGA	1.75	11.70
LOUMANA	-5.35	10.58
SOUBAKANIEDOUGOU	-5.02	10.48
ORODARA	-4.92	10.98
NIANGOLOKO	-4.92	10.27
BANFORA	-4.77	10.63

BANFORA AGRICULTURE	-4.77	10.62
SIDERADOUGOU	-4.25	10.68
OUO	-3.83	10.40
KAMPTI	-3.47	10.13
DIEBOUGOU	-3.25	10.97
GAOUA	-3.18	10.33
DISSIN	-2.93	10.93
LEGMOIN	-2.90	10.15
BATIE	-2.92	9.88
LERI	-3.38	12.77
BOTOU	2.05	12.67
DIONKELE NDOROLA	-4.82	11.77
VALLEE DU KORI	-4.38	11.37
BEREGADOUGOU	-4.73	10.75
OUANGOLODOUGOU	-4.80	10.08

APPENDIX B

Summary of the range of variability of GLAM calibrated parameters at resolution of $0.75^{\circ} \times 0.75^{\circ}$

Parameter	Minimum	Maximum
Base temperature for all development stages ($^{\circ}C$)	8	14
Optimum temperature for all development stages ($^{\circ}C$)	25	35
Maximum temperature for all development stages ($^{\circ}C$)	35	45
Growing degree day from emergence to anthesis ($^{\circ}C$)	500	1000
Growing degree day from anthesis to grain filling ($^{\circ}C$)	300	800
Growing degree day from grain filling to maximum LAI ($^{\circ}C$)	150	300
Growing degree day from maximum LAI to maturity ($^{\circ}C$)	200	500
Maximum LAI growth ($m^2\ m^{-2}\ day^{-1}$)	0.01	0.21
Constante of soil heat flux (-)	0.1	0.8
Extenction coefficient for PAR (-)	0.1	0.9
Soil water content fraction threshold (-)	0.3	0.8
Extractable front velocity ($cm\ day^{-1}$)	0.2	1.1
Depth of soil over which evaporation occurs (mm)	20	50
Albedo (-)	0.1	0.3
Uptake diffusion coefficient ($cm^2\ day^{-1}$)	0.3	0.7
LAI corresponding to maximum transpiration (-)	0.6	2.4
Maximum of potential transpiration (cm)	0.4	0.6
Vapor pressure deficit (kPa)	0.6	1.1
Transpiration efficiency (Pa)	1	4

APPENDIX C

Mean values of optimized fuzzy parameters set at resolution of 0.75°×0.75°

Latitude	Longitude	$a_1(mm)$	$a_2(mm)$	$b_1(day)$	$b_2(day)$	$c_1(day)$	$c_2(day)$	k
15.00	-0.75	11	13	2	3	7	9	0.70
15.00	0.00	12	18	2	3	7	8	0.60
14.25	-2.25	14	24	3	5	7	9	0.80
14.25	-1.50	11	14	2	4	7	9	0.70
14.25	-0.75	11	16	2	4	7	9	0.70
14.25	0.00	14	21	2	4	6	8	0.60
13.50	-3.75	13	20	2	3	7	9	0.60
13.50	-3.00	10	13	2	3	7	9	0.70
13.50	-2.25	13	16	2	3	7	8	0.60
13.50	-1.50	19	23	2	3	7	9	0.80
13.50	-0.75	11	13	2	4	7	9	0.80
13.50	0.00	10	14	2	3	7	9	0.70
13.50	0.75	11	13	2	3	7	9	0.80
12.75	-4.50	12	15	2	3	7	9	0.80
12.75	-3.75	11	13	1	3	7	8	0.80
12.75	-3.00	21	25	2	3	7	9	0.80
12.75	-2.25	18	26	3	4	6	9	0.80
12.75	-1.50	11	15	3	4	6	9	0.60
12.75	-0.75	11	14	2	3	7	9	0.60
12.75	0.00	11	14	2	4	6	8	0.70
12.75	0.75	10	13	2	4	6	8	0.80
12.75	1.50	12	18	2	3	7	9	0.50
12.75	2.25	18	23	2	3	7	8	0.70
12.00	-5.25	12	18	1	3	6	9	0.70
12.00	-4.50	11	14	2	3	6	9	0.70
12.00	-3.75	11	15	2	3	7	8	0.60
12.00	-3.00	12	18	1	3	7	9	0.60
12.00	-2.25	10	13	2	3	7	9	0.80
12.00	-1.50	12	16	3	4	7	8	0.70
12.00	-0.75	12	16	2	3	7	9	0.60
12.00	0.00	15	23	1	3	6	8	0.60

12.00	0.75	11	14	1	3	6	8	0.60
12.00	1.50	13	19	2	3	7	9	0.80
12.00	2.25	17	24	2	4	8	9	0.90
11.25	-5.25	15	23	2	3	7	9	0.50
11.25	-4.50	13	20	3	4	7	9	0.50
11.25	-3.75	19	25	2	4	7	9	0.70
11.25	-3.00	12	18	3	4	6	9	0.60
11.25	-2.25	15	20	2	4	6	8	0.80
11.25	-1.50	18	25	2	3	7	9	0.80
11.25	-0.75	17	22	2	4	7	9	0.70
11.25	0.00	11	16	2	3	6	8	0.70
11.25	0.75	11	17	2	4	6	8	0.60
11.25	1.50	15	19	2	4	6	8	0.90
10.50	-5.25	17	22	2	3	6	8	0.70
10.50	-4.50	14	20	2	3	6	9	0.60
10.50	-3.75	11	16	3	4	7	8	0.70
10.50	-3.00	15	23	3	4	7	8	0.80
9.75	-4.50	17	24	2	3	7	9	0.60
9.75	-3.75	11	16	4	5	6	9	0.80
9.75	-3.00	15	22	2	3	6	8	0.70

APPENDIX D

Maize mean yield obtained by OPDs and using RCM control runs (1989-2008)

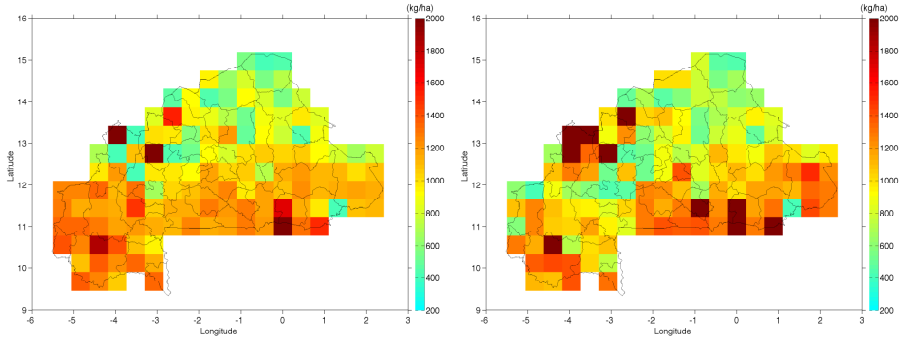

(a) CCCma

(b) CNRM

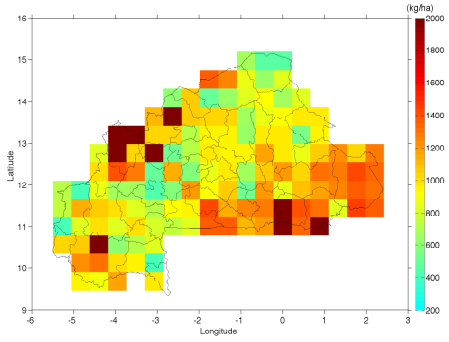

(c) ICHEC

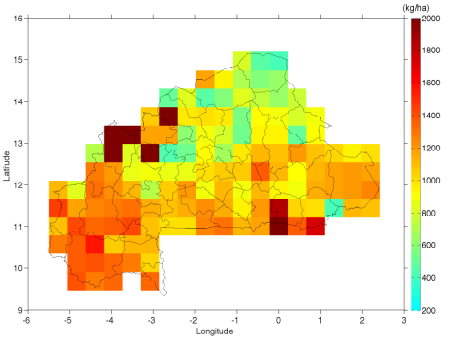

(d) MIROC

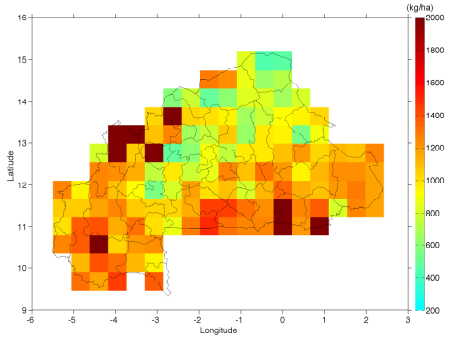

(e) MOHC

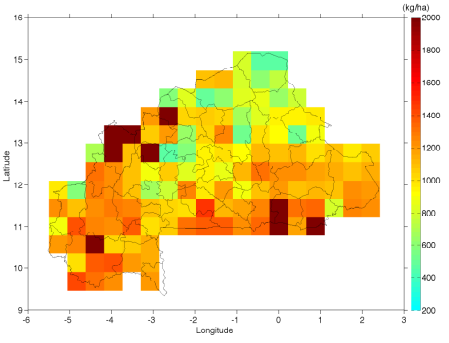

(f) MPI

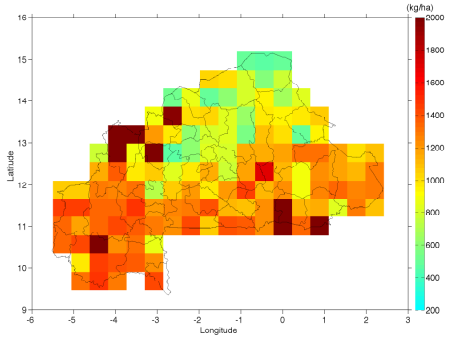

(g) NCC

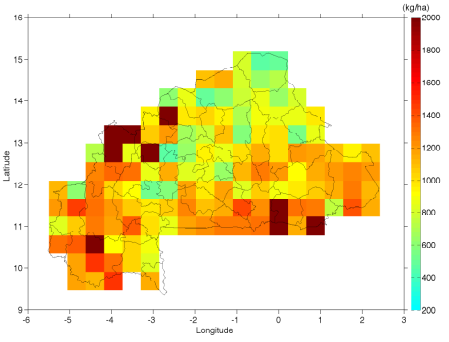

(h) NOAA

APPENDIX E

Mean yield of maize obtained by Diallo(2001) and using RCM control runs (1989-2008)

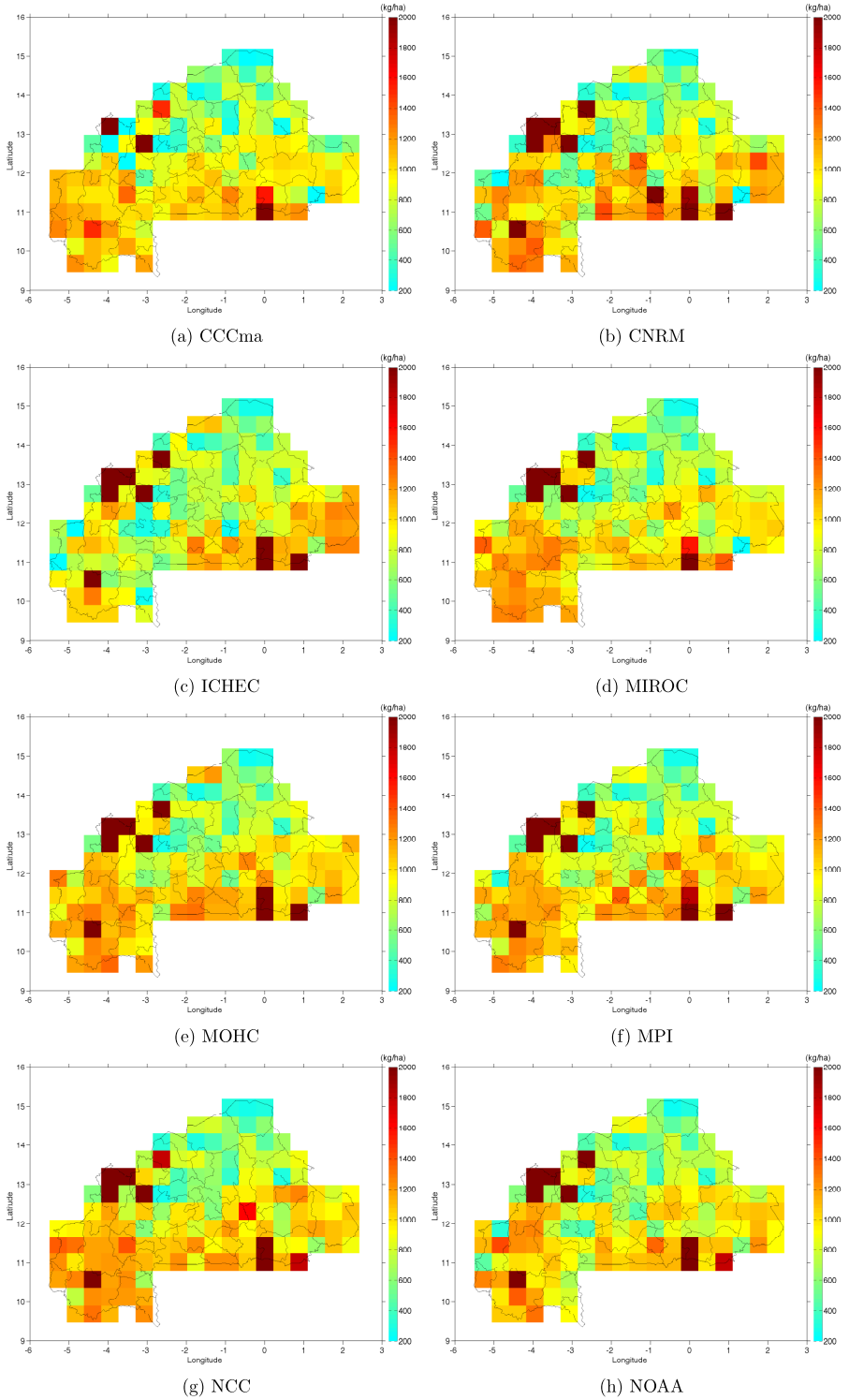

(a) CCCma (b) CNRM

(c) ICHEC (d) MIROC

(e) MOHC (f) MPI

(g) NCC (h) NOAA

Bibliography

Adeboye, O. B., J. A. Osunbitan, K. O. Adekalu, and D. A. Okunade, 2009: Evaluation of fao-56 penman monteith and temperature based models in estimating reference evapotranspiration. *Agricultural Engineering International*, **XI**, 1–25, the CIGR Ejournal.

Allen, R. G., L. S. Pereira, D. Raes, and M. Smith, 1998: Crop evapotranspiration: Guidelines for computing crop water requirements, fao irrigation and drainage paper no. 56. Tech. Rep., Food and Agriculture Organization of the United Nations (FAO), Rome, Italy.

Allison, M. T., K. V. Calvin, S. J. Smith, G. P. Kyle, A. Volke, P. Patel, S. Delgado-Arias, B. Bond-Lamberty, M. A. Wise, L. E. Clarke, and J. A. Edmonds, 2011: Rcp4.5: a pathway for stabilization of radiative forcing by 2100. *Climatic Change*, **109**, 77–94, doi:10.1007/s10584-011-0151-4.

Antwi-Agyei, P., A. J. Dougill, and L. C. Stringer, 2013: Barriers to climate change adaptation in Sub-Saharan Africa: evidence from northeast Ghana & systematic literature review. Technical report, Centre for Climate Change Economics and Policy, Working Paper No. 154, Leeds, UK.

Azoumah, Y., E. Ramdé, G. Tapsoba, and S. Thiam, 2010: Siting guidelines for concentrating solar power plants in the sahel: Case study of Burkina Faso. *Solar Energy*, **84**, 1545–1553, doi:10.1016/j.solener.2010.05.019.

Badini, O., O. S. Claudio, and H. F. Eldon, 1987: Application of crop simulation modeling and GIS to agroclimatic assessment in Burkina Faso. *Agriculture,*

Ecosystems and Environment, **64**, 233–244, doi:10.1016/S0167-8809(97)00041-8.

Barbara, G. B., R. W. Katz, and A. H. Murphy, 1986: On the Economic Value of Seasonal-Precipitation Forecasts: The Fallowing/Planting Problem. *Bulletin American Meteorological Society*, **67**, 833–841.

Barbier, B., H.Yacouba, H. Karambiri, M. Zorome, and B. Some, 2009: Human vulnerability to climate variability in the sahel: farmers' adaptation strategies in northern Burkina Faso. *Environmental Management*, **43**, 790–803, doi:10.1007/s00267-008-9237-9.

Bárdossy, A., 1997: Downscaling from gcms to local climate through stochastic linkages. *Journal of Environmental Management*, **49**, 7–17, doi:10.1006/jema.1996.0112.

Belohlavek, R. and G. J. Klir, 2011: *Concepts and Fuzzy Logic*. MIT Press, 287 pp.

Benoît, P., 1977: The start of the growing season in Northern Nigeria. *Agricultural Meteorology*, **18**, 91–99.

Bertseka, D. P., 1996: *Constrained Optimization and Lagrange Multiplier Methods*. Athena Scientific, Belmont, Massachusetts, 410 pp.

Biazin, B., G. Sterk, M. Temesgen, A. Abdulkedir, and L. Stroosnijder, 2012: Rainwater harvesting and management in rainfed agricultural systems in sub-Saharan Africa – a review. *Physics and Chemistry of the Earth*, **47-48**, 139–151.

Birch, C. J., 1996: Testing the performance of two maize simulation models with a range of cultivars of maize (zea mays) in diverse environments. *Environmental Software*, **11**, 91–98.

Birch, C. J., G. L. Hammer, and K. G. Rickert, 1998: Temperature and photoperiod sensitivity of development in five cultivars of maize (Zea maysL.) from emergence to tassel initiation. *Field Crops Research*, **55**, 93–107.

Brock, J. and J. E. Brink, 1996: Estimating millet production for famine early warning: an application of crop simulation modelling using satellite and ground-based data in Burkina Faso. *Agric. For. Meteor.*, **83**, 95–112.

Brooks, K., S. Zorya, A. Gautam, and A. Goyal, 2013: Agriculture as a Sector of Opportunity for Young People in Africa. Technical Report 4, Agriculture and Environmental Services Department,The World Bank Sustainable Development Network. Policy Research Working Paper 6473, Washington DC, USA.

Carberry, P. S., 1991: Test of leaf area development in CERES-Maize - a correction. *Field Crops Research*, **27**, 159–167.

Carberry, P. S., R. C. Muchow, and R. L. McCown, 1989: Testing the CERES-Maize simulation model in a semi-arid tropical environment. *Field Crops Research*, **20**, 297–315.

Carroll, D. L., 1996a: Chemical Laser Modeling with Genetic Algorithms. *AIAA J.*, **34**, 338–346.

Carroll, D. L., 1996b: Genetic Algorithms and Optimizing Chemical Oxygen-Iodine Lasers. *Developments in Theoretical and Applied Mechanics*, The University of Alabama, School of Engineering, 411–424.

Celikyilmaz, A. and I. B. Türksen, 2009: *Modeling Uncertainty with Fuzzy Logic. With Recent Theory and Applications*. Springer, 443 pp.

Challinor, A. J., T. R. Wheeler, C. Garforth, P. Q. Craufurd, and A. Kassam, 2007: Assessing the vulnerability of food crop systems in Africa to climate change. *Climate Change*, **83**, 381–399, doi:10.1007/s10584-007-9249-0.

Challinor, A. J., T. R. Wheeler, J. M. Slingo, P. Q. Craufurd, and D. I. F. Grimes, 2004: Design and optimisation of a large-area process-based model for annual crops. *Agricultural and Forest Meteorology*, **124**, 99–120, doi:10.1016/j.agrformet.2004.01.002.

Challinor, A. J., T. R. Wheeler, J. M. Slingo, P. Q. Craufurd, and D. I. F. Grimes, 2005: Simulation of crop yields using the ERA40 re-analysis: limits to skill and non-stationarity in weather-yield relationships. *J. Appl. Meteor.*, **44**, 516–531.

Chamberlin, P. and M. Diop, 2003: Application of daily rainfall principal component analysis to the assessment of the rainy season characteristics in Senegal. *Climate Research*, **23**, 159–169.

chun Tang, Z., Z. zhou Lu, and J. xiang Hu, 2014: An efficient approach for design optimization of structures involving fuzzy variables. *Fuzzy Sets and Systems*, **255**, 52–73, doi:http://dx.doi.org/10.1016/j.fss.2014.05.017.

Cochemé, I. and P. Franquin, 1967: An agroclimatology survey of a semi-arid area in Africa, South of the Sahara. Tech. Rep., World Meteorological Organization of the United Nations (WMO), Geneva, Switzerland.

Conway, G., 2006: *The Doubly Green Revolution: Food for All in the 21st Century*. Cornell University Press, New York, USA, 360 pp.

Conway, G., 2008: The science of climate change in africa: impacts and adaptations. Tech. Rep., Department of International Development, UK.

Cook, K. H. and E. K. Vizy, 2006: Coupled model simulations of the West African monsoon system: twentieth- and twenty-first-century simulations. *Journal of Climate*, **19**, 3681–3703, doi:http://dx.doi.org/10.1175/JCLI3814.1.

Cooper, P. J. M., J. Dimes, K. P. C. Rao, B. Shapiro, B. Shiferawa, and S. Twomlow, 2008: Coping better with current climate variability in the rain-fed farming systems of sub-saharan africa: an essential first step in adapting to future climate change. *Agriculture, Ecosystem and Environment*, **126**, 24–35, doi:10.1016/j.agee.2008.01.007.

Cooper, P. J. M., K. P. C. Rao, P. Singh, J. Dimes, P. Traore, K. K. Rao, P. Dixit, and S. J. Twomlow, 2009: Farming with current and future climate risk: Advancing a 'hypothesis of hope' for rain-fed agriculture in the semi-arid tropics. *Journal of Semi-Arid Tropical Agricultural Research*, **7**, ejournal.icrisat.org.

Şen, Z., 2010: *Fuzzy Logic and Hydrological Modeling*. Taylor and Francis Group, LLC, 354 pp.

de Wit, C. T., 1965: Photosynthesis of leaf canopies. Tech. Rep., Agricultural Research Report No. 663, Pudoc, Wageningen, The Netherlands.

Dee, D. P., S. M. Uppala, A. J. Simmons, P. Berrisford, P. Poli, S. Kobayashi, U. Andrae, and M. A. Balmaseda et al., 2011: The ERA-Interim reanalysis: configuration and performance of the data assimilation system. *Quart. J. Roy. Meteor. Soc.*, **137**, 553–597, doi:10.1002/qj.828.

Detlef, P., van Vuuren, J. Edmonds, M. Kainuma, K. Riahi, A. Thomson, K. Hibbard, G. C. Hurtt, T. Kram, V. Krey, J.-F. Lamarque, T. Masui, M. Meinshausen, N. Nakicenovic, S. J. Smith, and S. K. Rose, 2009: The representative concentration pathways: an overview. *Climatic Change*, **109**, 5–31, doi:10.1007/s10584-011-0148-z.

Diallo, M. A., 2001: Statistical analyse of agroclimatic parameters based on regional meteorological database. Technical report, Centre Régional AGRHYMET, Niamey, Niger.

Diao, X., P. Hazell, D. Resnick, and J. Thurlow, 2007: The Role of Agriculture in Development, Implications for Sub-Saharan Africa. Technical Report 153, International Food Policy Research Institute (IFPRI), Washington DC, USA.

Dodd, D. E. S. and I. T. Jolliffe, 2001: Early detection of the start of the wet season in semiarid tropical climates of western Africa. *International Journal of Climatology*, **21**, 1251–1262, doi:10.1002/joc.640.

Doorenbos, J. and W. O. Pruit, 1977: Crop water requirements, fao irrigation and drainage paper no. 24. Tech. Rep., Food and Agriculture Organization of the United Nations (FAO), Rome, Italy.

FAO, 1991: Digitized Soil Map of the World. World Soil Resources Report 67. Technical report, FAO, Rome, Italy.

Fick, G. W., R. S. Loomis, and W. A. William, 1978: *Sugar beet*, Cambridge University Press, Cambridge, UK, chapter Crop physiology. 310–354.

Folberth, C., T. Gaiser, K. C. Abbaspour, R. Schulin, and H. Yang, 2012: Regionalization of a large-scale crop growth model for sub-Saharan Africa: Model setup, evaluation, and estimation of maize yields. *Agriculture, Ecosystems and Environment*, **151**, 21–33, doi::10.1016/j.agee.2012.01.026.

Giorgi, F. and L. O. Mearns, 1999: Introduction to special section: regional climate modeling revisited. *Journal of Geophysical Research*, **104**, 6335–6352, doi:10.1029/98JD02072.

Godfray, C., J. Beddington, I. Crute, L. Haddad, D. Lawrence, J. Muir, J. Pretty, S. Robinson, S. Thomas, and C. Toulmin, 2010: Food security: the challenge of feeding 9 billion people. *Science*, **327**, 812–818, doi:10.1126/science.1185383.

Hansen, J. W. and J. W. Jones, 2000: Scaling-up crop models for climatic variability applications. *Agricultural Systems*, **65**, 43–72.

Hargreaves, G. L. and Z. A. Samani, 1982: Estimating potential evapotranspiration. *Irrigation and Drainage Engineering*, **108**, 225–230.

Hellmuth, M. E., A. Moorhead, M. C. Thomson, and J. Williams, 2007: Climate risk management in africa: Learning from practice. Tech. Rep., International Research Institute for Climate and Society (IRI), Columbia University, New York, USA.

Henao, J. and C. Baanante, 2006: Agricultural production and soil nutrient mining in africa : implications for resource conservation and policy development. Tech. Rep., International Center for Soil Fertility and Agricultural Development, Muscle Shoals, USA.

Holland, J. H., 1992: *Adaptation in natural and artificial systems: An Introductory Analysis with Applications to Biology, Control, and Artificial Intelligence*. MIT Press, 218 pp.

Holmén, H. and G. Hudén, 2011: *African smallholders : food crops, markets and policy*, CAB international, chapter 2. 23–43.

Hoogenboom, G., 2000: Contribution of agrometeorology to the simulation of crop production and its application. *Agric. For. Meteor.*, **103**, 137–157.

Ingram, K., M. Roncoli, and P. Kirshen, 2002: Opportunities and constraints for farmers of west africa to use seasonal precipitation forecasts with burkina faso as a case study. *Agricultural Systems*, **74**, 331–349, doi:http://dx.doi.org/10.1016/S0308-521X(02)00044-6.

IPCC, 2013: The physical science basis: Contribution of working group i to the fourth assessment report of the intergovernmental panel on climate change. Tech. Rep., Intergovernmental Panel on Climate Change (IPCC), Cambridge University Press, Cambridge, UK and New York, USA.

IPCC, 2014: Climate change 2014: Impacts, adaptation, and vulnerability. working group II contribution to the fifth assessment report of the Intergovernmental Panel on Climate Change. Technical report, Cambridge University Press, Cambridge, UK and New York, USA.

Janicot, S., B. Harzallah, B. Fontaine, and V. Moron, 1998: West African monsoon dynamics and eastern equatorial Atlantic and Pacific SST anomalies (1970-1988). *Journal of Climatology*, **11**, 1874–1882.

Jiang, T., G. Ren, and X. Zhao, 2013: Evacuation Route Optimization based on Tabu Search Algorithm and Hill-climbing Algorithm. *Procedia-Social and Behavioral Sciences*, **96**, 865–872, doi:http://dx.doi.org/10.1016/j.sbspro.2013.08.098.

Jones, C., F. Giorgi, and G. Asrar, 2011: The Coordinated Regional Downscaling Experiment: CORDEX, an international downscaling link to CMIP5. *CLIVAR Exchanges No. 56*, **16**, 34–40.

Jones, J. W., G. Y. Tsuji, G. Hoogenboom, L. A. Hunt, P. K. Thornton, D. T. Imamura, W. T. Bowen, and U. Singh, 1998: *Understanding options for agricultural production*, Kluwer Academic, Dordrecht, The Netherlands, chapter Decision Support System for Agrotechnology Transfer; DSSAT V3. 157–177.

Jung, G. and H. Kunstmann, 2007: High-resolution Regional Climate Modelling for the Volta Basin of West Africa. *Journal of Geophysical Research - Atmosphere*, **112**, 1–17, doi:10.1029/2006JD007951.

Kaboré, P. D. and C. Reij, 2004: The emergence and spreading of an improved traditional soil and water conservation practice in Burkina Faso. Discussion paper 114. Technical report, Environment and Production Technology Division, IFPRI, Washington DC, USA.

Khashman, A., 2011: Credit risk evaluation using neural networks: Emotional versus conventional models . *Applied Soft Computing*, **11**, 5477–5484, doi:http://dx.doi.org/10.1016/j.asoc.2011.05.011.

Kim, J., D. E. Waliser, C. A. Mattmann, C. E. Goodale, A. F. Hart, P. A. Zimdars, D. J. Crichton, C. Jones, G. Nikulin, B. Hewitson, C. Jack, C. Lennard, and A. Favre, 2014: Evaluation of the CORDEX-Africa multi-RCM hindcast: systematic model errors. *Climate Dynamics*, **42**, 1189–1202, doi:10.1007/s00382-013-1751-7.

Kniveton, D. R., R. Layberry, C. J. R. Williams, and M. Peck, 2009: Trends in start of the wet season over Africa. *Int. J. Climatol.*, **29**, 1216–1225.

Knox, J., T. Hess, A. Daccache, and T. Wheeler, 2012: Climate change impacts on crop productivity in Africa and South Asia. *Environmental Research Letters*, **7**, 034032, doi:10.1088/1748-9326/7/3/034032.

Kuhn, H. W. and A. W. Tucker, 1951: Nonlinear programming, in J. Neyman, ed., Proceedings of the Second Berkeley Symposium on Mathematical Statistics and Probability. *University of California Press, Berkeley, CA*, **65**, 481–492.

Laprise, R., R. Elía, D. Caya, S. Biner, P. Lucas-Picher, E. Diaconescu, M. Leduc, A. Alexandru, and L. Separovic, 2008: Challenging some tenets of Regional Climate Modelling. *Meteorolology and Atmospheric Physics*, **100**, 3–22, doi:10.1007/s00703-008-0292-9.

Lauer, J. G., P. R. Carter, T. M. Wood, G. Diezel, D. Wiersma, R. Rand, and M. J. Mlynarek, 1999: Corn hybrid response to planting date in the northern corn belt. *Agronomy Journal*, **91**, 834–839, doi:10.2134/agronj1999.915834x.

Laux, P., 2009: *Statistical modeling of precipitation for agricultural planning in the Volta Basin of West Africa*. Ph.D. thesis, Mitteilungen, Institut für Wasserbau, Heft 179, Stuttgart, 198pp.

Laux, P., G. Jäckel, R. M. Tingem, and H. Kunstmann, 2010: Impact of climate change on agricultural productivity under rainfed conditions in Cameroon - A method to improve attainable crop yields by planting date adaptations. *Agricultural and Forest Meteorology*, **150**, 1258–1271, doi:10.1016/j.agrformet.2010.05.008.

Laux, P., H. Kunstmann, and A. Bárdossy, 2008: Predicting the regional onset of the rainy season in West Africa. *International Journal of Climatology*, **28**, 329–342, doi:10.1002/joc.1542.

Laux, P., S. Wagner, A. W. A. Bárdossy, J. Jacobeit, and H. Kunstmann, 2009: Modelling daily precipitation features in the Volta basin of West Africa. *International Journal of Climatology*, **29**, 937–954, doi:10.1002/joc.1852.

Leung, L. R., L. O. Mearns, F. Giorgi, and R. L. Wilby, 2003: Regional climate research: Needs and opportunities. *Bulletin of the American Meteorological Society*, **82**, 89–95, doi:10.1175/BAMS-84-1-89.

Lobell, D. B., M. Burke, C. Tebaldi, M. D. Mastrandrea, W. P. Falcon, and R. L. Naylor, 2008: Prioritizing climate change adaptation needs for food security in 2030. *Science*, **319**, 607–610, doi:10.1126/science.1152339.

Long, S. P., E. A. Ainsworth, A. D. B. Leakey, D. R. Ort, J. Nosberger, and D. Schimel, 2007: Crop models, co_2, and climate change - response. *Science*, **315**, 459–460.

Loomis, R. S. and W. A. Williams, 1963: Maximum crop productivity: an estimate. *Crop Science*, **3**, 67–72, doi:10.2135/cropsci1963.0011183X000300010021x.

Maddonni, G. A. and M. E. Otegui, 1996: Leaf area, light interception, and crop development in maize. *Field Crops Research*, **48**, 81–87.

Marteau, R., V. Moron, and N. Philippon, 2009: Spatial Coherence of Monsoon Onset over Western and Central Sahel (1950-2000). *Journal of Climate*, **22**, 1313–1324, doi:http://dx.doi.org/10.1175/2008JCLI2383.1.

McCown, R. L., G. L. Hammer, J. N. G. Hargreaves, D. P. Holzworth, and D. M. Freebairn, 1996: APSIM: a novel software system for model development, model testing and simulation in agricultural systems research. *Agricultural Systems*, **50**, 255–271.

Moen, T. N., K. M. Kaiser, and S. J. Riha, 1994: Regional yield estimation using a crop simulation model: concepts, methods and validation. *Agricultural Systems*, **46**, 79–92.

Moriondo, M. and M. Bindi, 2006: Comparison of temperatures simulated by gcms, rcms and statistical downscaling: potential application in studies of future crop development. *Climate Research*, **30**, 149–160, doi:10.3354/cr030149.

Moss, R. H., M. Babiker, S. Brinkman, E. Calvo, T. Carter, J. Edmonds, I. Elgizouli, S. Emori, L. Erda, K. Hibbard, R. Jones, M. Kainuma, J. Kelleher, J. F. Lamarque, M. M. B. Matthews, J. Meehl, L. Meyer, J. Mitchell, N. Nakicenovic, B. O'Neill, R. Pichs, K. Riahi, S. Rose, P. Runci, R. Stouffer, D. van Vuuren, J. Weyant, T. Wilbanks, J. P. van Ypersele, and M. Zurek, 2008: Towards New Scenarios for Analysis of Emissions, Climate Change, Impacts, and Response Strategies. IPCC Technical Summary, Geneva, Switzerland. Technical Summary, Intergovernmental Panel on Climate Change, WMO, Geneva, Switzerland.

Moss, R. H., J. A. Edmonds, K. A. Hibbard, M. R. Manning, S. K. Rose, D. P. van Vuuren, T. R. Carter, S. Emori, M. Kainuma, T. Kram, G. A. Meehl, J. F. B. Mitchell, N. Nakicenovic, K. Riahi, S. J. Smith, R. J. Stouffer, A. M. Thomson, J. P. Weyant, and T. J. Wilbanks, 2010: The next generation of scenarios for climate change research and assessment. *Nature*, **463**, 747–756, doi:10.1038/nature08823.

Muchow, R. C. and P. S. Carberry, 1989: Environmental control of phenology and leaf growth in a tropically-adapted maize. *Field Crops Research*, **20**, 221–236.

Müller, C., W. Cramer, W. L. Hare, and H. Lotze-Campen, 2011a: Climate change risks for African agriculture. *Nature Clim. Change*, **108**, 4313–4315, doi:10.1073/pnas.1015078108.

Müller, C., W. Cramer, W. L. Hare, and H. Lotze-Campen, 2011b: Climate change risks for african agriculture. *Proc. Nat. Acad. Sci.*, **108**, 4313–4315, doi:10.1073/pnas.1015078108.

Nelson, G. C., M. W. Rosegrant, J. Koo, R. Robertson, T. Sulser, T. Zhu, C. Ringler, S. Msangi, A. Palazzo, M. Batka, M. Magalhaes, R. Valmonte-Santos, M. Ewing, and D. Lee, 2009: Climate Change: Impact on Agriculture and Costs of Adaptation. Technical report, International Food Policy Research Institute, Washington DC, USA.

Nicholson, S. E. and J. P. Grist, 2003: The Seasonal Evolution of the Atmospheric Circulation over West Africa and Equatorial Africa. *Journal of Climate*, **16**, 1013–1030.

Nikulin, G., C. Jones, P. Samuelsson, F.Giorgi, M. B. Sylla, G. Asrar, M. Büchner, R. Cerezo-Mota, O. B. Christensen, M. Déqué, J. Fernandez, A. Hänsler, E. van Meijgaard, and L. Sushama, 2012: Precipitation Climatology in an Ensemble of CORDEX-Africa Regional Climate Simulations. *Journal of Climate*, **25**, 6057–6078, doi:http://dx.doi.org/10.1175/JCLI-D-11-00375.1.

Oduro-Afriyie, A., 1989: On the mean monthly equivalent potential temperature and rainfall in West Africa. *Theoretical and Applied climatology*, **39**, 188–193.

Omotosho, J. B., 1992: Long-range prediction of the onset and end of the rainy season in the West African Sahel. *International Journal of climatology*, **12**, 369–382, doi:10.1002/joc.3370120405.

Omotosho, J. B., A. A. Balogun, and K. Ogunjobi, 2000: Predicting monthly and seasonal rainfall, onset and cessation of the rainy season in West Africa using only surface data. *International Journal of climatology*, **20**, 865–880.

Padgham, J., 2009: Agriculture development under a changing climate: Opportunities and challenges for adaptation. Tech. Rep., World Bank, Washington DC, USA.

Pedzisa, T., I. Minde, and S. Twomlow, 2010: An evaluation of the use of participatory processes in wide-scale dissemination of research in micro dosing and conservation agriculture in zimbabwe. *Research Evaluation*, **19**, 145–155.

Penman, H. L., 1948: Natural evaporation from open water, bare soil and grass. *Proc. Royal. Soc.*, **193**, 120–145.

Pham, D. and D. Karaboga, 2000: *Intelligent Optimization Techniques. Genetic Algorithms, Tabu Search, Simulated Annealing and Neural Networks*. Springer, 307 pp.

Priestley, C. H. and R. J. Taylor, 1972: On the assessment of the surface heat flux and evaporation using large-scale parameters. *Monthly Weather Review*, **100**, 81–92.

Rao, S. S., 2009: *Engineering Optimization Theory and Practice*. John Wiley & Sons, 829 pp.

Rasse, D. P., J. T. Ritchie, W. W. Wilhelm, J. Wei, and E. C. Martin, 2000: Simulating inbred-maize yields with CERES-IM. *Agronomy Journal*, **92**, 672–678.

Renkow, M. and D. Byerlee, 2010: The impacts of cgiar research: a review of recent evidence. *Food Policy*, **35**, 391–402.

Riahi, K., S. Rao, V. Krey, C. Cho, V. Chirkov, G. Fischer, G. Kindermann, N. Nakicenovic, and P. Rafaj, 2011: Rcp 8.5–a scenario of comparatively high greenhouse gas emissions. *Climatic Change*, **109**, 33–57, doi:10.1007/s10584-011-0149-y.

Ritchi, J., D. C. Godwin, and W. T. Down, 1998: *Understanding options for agricultural production*, Kluwer Academic, Dordrecht, The Netherlands, chapter CERES growth, development and yield. 79–98.

Ritchie, J. T., A. Gerakis, and A. A. Suleiman, 1999: Simple model to estimate field-measured soil water limits. *Trans. ASAE.*, **42**, 1609–1614, doi:10.13031/2013.13326.

Roncoli, C., K. Ingram, and P. Kirshen, 2001: The costs and risks of coping with drought: livelihood impacts and farmers' responses in Burkina Faso. *Climate Research*, **19**, 119–132, doi:10.3354/cr019119.

Rosegrant, M. W., X. Cai, and S. A. Cline, 2002: World water and food to 2025 : Dealing with scarcity. Tech. Rep., International Food Policy Research Institute (IFPRI), Washington DC, USA.

Ross, T. J., J. M. Booker, and W. J. Parkinson, 2002: *Fuzzy Logic and Probability Applications: Bridging the Gap*. American Statistical Association and Society for Industrial and Applied Mathematics (ASA-SIAM), 434 pp.

Roudier, P., B. Sultan, P. Quirion, and A. Berg, 2011: The impact of future climate change on West African agriculture: what does the recent literature say? *Global Environmental Change*, **21**, 1073–1083, doi:10.1016/j.gloenvcha.2011.04.007.

Sacks, W. J., D. Deryng, and J. A. F. N. Ramankutty, 2010: Crop planting dates: an analysis of global patterns. *Global Ecology and Biogeography*, **19**, 607–620, doi:10.1111/j.1466-8238.2010.00551.x.

Sanon, M. and Y. Dembélé, 2001: Etude de quatre niveaux d'irrigation de complément et du pluvial strict sur le maïs et le cotonnier dans la plaine du sourou. Technical Report 25, INERA, Ouagadougou, Burkina Faso.

Sanon, M., Y. Dembélé, and L. Somé, 2002: Evapotranspiration du blé, de l'oignon, du maïs et du cotonnier au nord-ouest du burkina faso. *5ème Conférence Inter-Régionale sur l'Environnement*, EIER-ETSHER, Ouagadougou, Burkina Faso, 38–48.

Sawadogo, H., 2011: Using soil and water conservation techniques to rehabilitate degraded lands in northwestern Burkina Faso. *International Journal of Agricultural Sustainability*, **9**, 120–128, doi:10.3763/ijas.2010.0552.

Sivakumar, M. V. K., 1988: Predicting rainy season potential from the onset of rains in Southern Sahelian and Sudanian climate zones of West Africa. *Agricultural and Forest Meteorology*, **42**, 295–305, doi:10.1016/0168-1923(88)90039-1.

Sivakumar, M. V. K. and F. Gnoumou, 1987: Exploiting rainy season potential from the onset of rains in the Sahelian zone of West Africa. Research Bulletin 23, ICRISAT, Niamey, Niger.

Sivanandam, S. N. and S. N. Deepa, 2008: *Introduction to Genetic Alghorithms*. Springer, 442 pp.

Stehfest, E., M. Heistermann, J. A. Priess, D. S. Ojima, and J. Alcamo, 2007: Simulation of global crop production with the ecosystem model DayCent. *Ecological Modelling*, **209**, 203–219.

Stern, R. D., M. D. Dennett, and I. C. Dale, 1982: Analyzing daily rainfall measurements to give agronomically useful results. 1. Direct methods. *Experimental Agriculture*, **18**, 223–236, doi:10.1017/S001447970001379X.

Stern, R. D., M. D. Dennett, and D. J. Garbutt, 1981: The start of the rains in West Africa. *Journal of Climatology*, **1**, 59–68, doi:10.1002/joc.3370010107.

Stöckle, C. O., M. Donatelli, and R. Nelson, 2003: CropSyst, a cropping systems simulation model. *European Journal of Agronomy*, **18**, 289–307.

Suleiman, A. A. and J. T. Ritchie, 2001: Estimating saturated hydraulic conductivity from soil porosity. *Trans. ASAE.*, **42**, 235–239, doi:10.13031/2013.4683.

Sultan, B., B. Barbier, J. Fortilus, S. M. Mbaye, and G. Leclerc, 2010: Estimating the Potential Economic Value of Seasonal Forecasts in West Africa: A Long-Term Ex-Ante Assessment in Senegal. *Weather, Climate, and Society*, **2**, 69–87, doi:http://dx.doi.org/10.1175/2009WCAS1022.1.

Sultan, B. and S. Janicot, 2000: Abrupt shift of the ITCZ over West Africa and intra-seasonal variability. *Geophysical Research Letters.*, **27**, 3353–3356.

Tao, F., M. Yokozawa, and Z. Zhang, 2009: Modelling the impacts of weather and climate variability on crop productivity over a large area: A new process-based model development, optimization, and uncertainties analysis. *Agric. For. Meteor.*, **149**, 831–850.

Taylor, K. E., 2001: Summarizing multiple aspects of model performance in a single diagram. *Journal of Geophysical Research*, **106**, 7183–7192, doi:10.1029/2000JD900719.

Traoré, S. B., F. N. Reynier, M. Koné, B. Sidibé, A. Yoroté, K. Yattara, and M. Kouressy, 2000: Adaptation a la sécheresse des écotype locaux de sorgho du Mali. *Sécheresse*, **11**, 227–237.

UN, 2000: United Nations Millennium Declaration, United Nations General Assembly A/RES/55/2. Fifty-fifth session, United Nations, New York, USA. URL http://www.un.org/millennium/declaration/ares552e.pdf

UNDP, 2014: A propos du Burkina Faso. http://www.bf.undp.org/content/burkina_faso/fr/home/countryinfo/, [Online; accessed 12-August-2014].

UNFPA, 2011: State of world population 2011: People and possibilities in a world of 7 billion. UNFPA tech. rep., United Nations Population Fund, New York, USA, [http://foweb.unfpa.org/SWP2011/reports/EN-SWOP2011-FINAL.pdf].

Waha, K., C. Müller, A. Bondeau, J. P. Dietrich, P. Kurukulasuriya, J. Heinke, and H. Lotze-Campen, 2013: Adaptation to climate change through the choice of cropping system and sowing date in sub-saharan africa. *Global Environmental Change*, **23**, 130–143.

Wallach, D., D. Makowski, and J. W. Jones, 2006: *Working with Dynamic Crop Models: Evaluation, Analysis, Parameterization, and Applications*. Elsevier, Oxford, UK, 447 pp.

Waongo, M., P. Laux, S. B. Traoré, M. Sanon, and H. Kunstmann, 2014: A crop model and fuzzy rule based approach for optimizing maize planting dates in Burkina Faso, West Africa. *Journal of Applied Meteorology and Climatology*, **53**, 598–613, doi:http://dx.doi.org/10.1175/JAMC-D-13-0116.1.

Ward, M. N., 1998: Diagnosis and short-lead time prediction of summer rainfall in tropical North Africa at interannual and multidecadal timescales. *Journal of Climatology*, **11**, 3167–3191.

Webber, H., T. Gaiser, and F. Ewert, 2014: What role can crop models play in supporting climate change adaptation decisions to enhance food security in Sub-Saharan Africa? *Agricultural Systems*, **127**, 161–177, doi:10.1016/j.agsy.2013.12.006.

Wheeler, T., A. Challinor, T. Osborne, and J. Slingo, 2007: *Development of a Combined Crop and Climate Forecasting System for Seasonal to Decadal Predictions*, World Meteorological Organization, Geneva, Switzerland, chapter Climate Prediction and Agriculture: Advances and Challenges. 31–39.

Wheeler, T. R., P. Q. Craufurd, R. H. Ellis, J. R. Porter, and P. V. V. Prasad, 2000: Temperature variability and the yield of annual crops. *Agriculture, Ecosystems and Environment*, **82**, 159–167.

Wilkerson, G. G., J. W. Jones, K. J. Boote, and J. Mishoe, 1985: SOYGRO V5.0. Soybean crop growth and yield model. Technical documentation. Tech. Rep., Agr. Eng. Dep., Univ. of Florida, Gainsville, USA.

World Bank, 2000: World development indicators. Tech. Rep., World Bank, Washington DC, USA, [http://go.worldbank.org/K0TJI9FRA1].

Xiao, R., 2013: 5-Modeling and Simulation of Ant Colony's Labor Division: A Problem-Oriented Approach . *Swarm Intelligence and Bio-Inspired Computation*, X.-S. Y. C. X. H. G. Karamanoglu, ed., Elsevier, Oxford, 103 – 135.

Yang, X.-S., 2014: Chapter 4 - simulated annealing. *Nature-Inspired Optimization Algorithms*, X.-S. Yang, ed., Elsevier, Oxford, 67–75.

Zadeh, L., 1965: Fuzzy sets. *Information Control*, **8**, 338–353.

Zampaligré, N., L. H. Dossa, and E. Schlecht, 2014: Climate change and variability: perception and adaptation strategies of pastoralists and agro-pastoralists across different zones of Burkina Faso. *Regional Environmental Change*, **14**, 769–783, doi:10.1007/s10113-013-0532-5.